Development of a promising interferon gene therapy strategy by vector design

(ベクター設計に基づくインターフェロン遺伝子治療戦略の確立に関する研究)

2017

Atsushi Hamana

Contents

Preface 1

Chapter I 2

I-1 Introduction 3

I-2 Materials and Methods 4

I-3 Results 9

I-3-a. IFN-β was secreted to the culture medium from B16-BL6 cells transfected with IFN-β-expressing plasmid vectors 9

I-3-b. Transgene expression from pMx-fLuc was increased by IFN-β 11

I-3-c. Co-transfection of siIFNAR with pMx-IFN-β reduced IFN-β expression from pMx-IFN-β 12

I-3-d. Serum concentration of IFN-β was sustained in mice receiving gene delivery of pMx-IFN-β 13

I-3-e. Serum concentration of IFN-β was decreased in mice receiving co-administration of siIFNAR1 with pMx-IFN-β 14

I-3-f. Fewer tumor microvessels were observed in IFN-β-expressing plasmid DNA-treated tumor-bearing mice 15

I-3-g. Tumor growth was suppressed by gene transfer of IFN-β into tumor-bearing mice 16

I-4 Discussion 17

I-5 Conclusion 18

Chapter II 19

II-1 Introduction 20

II-2 Materials and Methods 21

II-3 Results 24

II-3-a. fLuc activity in cells containing HCV subgenomic replicons decreased after transfecting IFN-expressing plasmids 24

II-3-b. Hydrodynamic injection of the IFN-expressing plasmids in normal mice provided continuous supply of IFNs 25

II-3-c. IFN-α_2 moderately decreased HCV RNA level in the serum of chimeric mice infected with NS3- and NS5A-mutated HCV RASs 25

II-3-d. IFN-γ markedly decreased HCV RNA level in the serum of chimeric mice infected with NS3- and NS5A-mutated HCVs 27

II-3-e. IFN-λ_1 effectively decreased HCV RNA level in the serum of chimeric mice infected with NS3- and NS5A-mutated HCVs 28

II-3-f. gLuc did not affect HCV RNA level in the serum of chimeric mice infected with NS3- and NS5A-mutated HCVs 29

II-3-g. IFN treatment induced ISG expression after 42 days 30
II-3-h. Apparent damage was hardly observed in the liver sections of IFN-treated chimeric mice 30
II-4 Discussion 31
II-5 Conclusion 32
Chapter III 33
III Introduction 34
Chapter III 35
Section 1 35
III-1-1 Introduction 35
III-1-2 Materials and Methods 36
III-1-3 Results 38
III-1-3-a. Gene expression was observed in the liver but not in the brain after hydrodynamic injection into EAE mice 38
III-1-3-b. Gene transfer of pMx-IFN-β reduced the severity of EAE 39
III-1-3-c. Gene transfer of pMx-IFN-β suppressed a rise in serum IFN-γ concentration in EAE mice 40
III-1-3-d. Administration of pMx-IFN-β attenuated EB leakage into CNS of EAE mice 40
III-1-3-e. Gene transfer of pMx-IFN-β suppressed infiltration of inflammatory cells and tissue damage in the spinal cords of EAE mice 41
III-1-4 Discussion 42
III-1-5 Conclusion 43
Chapter III 44
Section 2 44
III-2-1 Introduction 44
III-2-2 Materials and Methods 44
III-2-3 Results 48
III-2-3-a. The biological activity of the IFN-β-gal-9 fusion proteins was significantly lower than that of IFN-β 48
III-2-3-b. The IFN-β-gal-9 fusion proteins effectively attenuated the activity of restimulated T cells 48
III-2-3-c. The IFN-β-gal-9 fusion proteins exerted suppressive effects on restimulated splenocytes in the presence of the anti-IFNAR antibody 50
III-2-3-d. Gene therapy using IFN-β and IFN-β-$(GS)_2$-gal-9-expressing plasmid DNA improved the clinical score for EAE symptoms 51
III-2-3-e. The IFN-γ concentration decreased following gene transfer using pMx-IFN-β-$(GS)_2$-gal-9 53
III-2-3-f. The pMx-IFN-β-$(GS)_2$-gal-9 gene transfer suppressed BBB disruption in EAE mice 53
III-2-3-g. Histological analysis 54

III-2-4 Discussion 54
III-2-5 Conclusion 55
Summary 56
Acknowledgements 58
List of Publications 59
Other Publications 59
References 60

Preface

Interferon (IFN) is a cytokine and classified into three types, namely, type I IFNs such as IFN-α and IFN-β, type II IFNs such as IFN-γ, and type III IFNs such as IFN-λs (IFN-λ_1 [interleukin {IL}-29], IFN-λ_2 [IL-28A], and IFN-λ_3 [IL-28B]) [1]. Each IFN possesses cytostatic, antiviral, and immunomodulatory effects and has been used in the treatment of patients with cancer, viral hepatitis, and multiple sclerosis (MS) for a long time. However, there are two concerns in IFN therapy, i.e. short half-life of IFN protein in the body [2] and side effects associated with biological activity of IFN.

To overcome above two concerns, gene delivery is a promising approach to achieve continuous supply of IFN based on sustained transgene expression with reduced side effects associated with IFN by modification of IFN. Gene transfer technique has attempted from late 20th [3]. Both viral vector and nonviral vector such as plasmid DNA vector have been commonly utilized as gene transfer vectors. However, viral vector has concerns regarding immune response, mutation in genome, and so on. Therefore, I utilized plasmid DNA vector for a continuous supply of modified IFNs because the use of plasmid DNA vector hardly evoke those concerns. In this thesis, I aimed to develop a promising IFN gene therapy strategy by plasmid DNA vector design for the treatment of refractory diseases.

In Chapter I, I aimed to develop a long-term expression system of IFN-β, type I IFN, using plasmid DNA vector. The long-term expression vector of IFN-γ, type II IFN, has been constructed by using CpG vector without CpG motif, which suppress transgene expression [4]. In contrast, the development of the long-term expression vector of IFN-β has not yet been achieved. Therefore, initially, I attempted to develop a novel plasmid DNA vector for long-term expression vector of IFN-β and to apply to cancer gene therapy.

In Chapter II, antiviral effect of three types of IFNs using long-term expression vector of each IFN, developed in Chapter I, against antiviral drug-resistant hepatitis C (HCV) infection was investigated. Human hepatocyte-transplanted chimeric mice were infected with antiviral drug resistant HCV and administered long-term expression vector of each IFN for comparison of antiviral effect of IFNs.

In Chapter III, I investigated whether continuous supply of IFN-β by using long-term expression vector and design of IFN-β fusion proteins was effective to treat MS. In general, repeated administration of IFN-β is required to reduce the relapse of MS and prevent MS progression. In Chapter III Section 1, the therapeutic effect of single administration of the long-term expression vector of IFN-β constructed in Chapter I into MS model mice was evaluated. In Chapter III Section 2, IFN-β fusion proteins were designed to improve the therapeutic effects and to reduce side effects of IFN-β. Therapeutic and side effects in MS model mice were compared between IFN-β and IFN-β fusion proteins.

Chapter I

Interferon-inducible Mx promoter-driven, long-term transgene expression system of interferon-β for cancer gene therapy

I-1 Introduction

IFNs are representative cytokines and are divided into three families: types I, II, and III. They have been utilized in the treatment of cancer, hepatitis, and multiple sclerosis for their antiproliferative, antiviral, and immunomodulatory effects [1]. IFN-β, a type I IFN, possesses highly potent antitumor effects and thus has been used in cancer therapy [5]. For instance, Hong *et al*. demonstrated that repetitive administrations of recombinant IFN-β protein into mice implanted with glioma cells effectively suppressed the tumor growth [6]. Because IFN-β is rapidly eliminated from the circulation after administration to patients [7], in the clinic, several injections are required per week to maintain an effective circulating concentration [2]. The half-life of IFN-β is prolonged by pegylation [8]. Therefore, the administration of pegylated IFN-β can decrease the frequency of administration to once per week. It was reported that administration of pegylated IFN-β more effectively suppressed tumor angiogenesis than administration of unmodified IFN-β in a melanoma angiogenesis model [9]. However, chemical modifications such as pegylation frequently decrease the biological activity of proteins [10]. Therefore, the balance between prolongation of half-life and reduction of biological activity is important in designing chemically modified IFN-β.

Gene delivery of IFN-β represents an attractive approach for the continuous supply of IFN-β without decreasing its biological activity. It was reported that administration of adenovirus vector encoding human IFN-β was effective to suppress the growth of glioma [11]. However, in general, the use of viral vector has the potential risk of severe adverse effects. In addition, it was reported that transgene expression of IFN-β from the adenoviral vector was transient after the gene transfer [12]. On the other hand, previous study performed in my laboratory reported that the hydrodynamic injection of plasmid DNA, a non-viral vector, encoding IFN-β effectively decreased tumor growth in a mouse model of pulmonary metastasis [13]. However, the duration of IFN-β expression achieved by this technique was too short to effectively treat chronic diseases with a single administration. My laboratory previously established that a plasmid vector containing no CpG motifs, a pCpG vector, enabled a long-term expression of IFN-γ [4]. However, in preliminary experiments, the hydrodynamic injection of this pCpG vector encoding IFN-β only caused the serum concentration of IFN-β to decline below the detection limit by 1 month.

IFN-β binds to the interferon-alpha/beta receptor (IFNAR), which consists of IFNAR1 and IFNAR2 subunits, and activates the Janus kinase/signal transducer and activator transcription (STAT) pathway to phosphorylate STAT1 and STAT2 [14]. Phosphorylated STAT1 and STAT2 dimerize and associate with interferon regulatory factor 9 to form a heterotrimeric interferon stimulated gene factor 3 complex. After nuclear localization, the interferon-stimulated gene factor 3 complex associates with a DNA sequence termed the interferon-stimulated response elements (ISRE) present in the promoter of interferon-stimulated genes (ISGs) to upregulate the expression of ISGs. It has been reported that some ISG products such as suppressors of cytokine signaling proteins and ubiquitin-specific peptidase 18 are involved in the negative regulation of gene expression of IFN [15]. Moreover, it has been reported that the transgene expression is suppressed by IFN-β through the

induction of ISGs. Therefore, I speculated that the short-term expression of IFN-β from pCpG vector might be due to the transgenes suppressing IFN-β. In fact, previous reports have demonstrated that the signal transduction of IFN-β suppressed the transgene expression of reporter proteins after gene transfer [16,17].

The Mx promoter is an IFN-responsible promoter that contains essential sequences for IFN-inducible activity: two ISRE and one IRF-binding site [18,19]. Therefore, the expression of Mx, an antiviral protein, is upregulated by type I IFN. Thus, Mx promoter-driven expression of IFN-β may circumvent IFN-β-mediated suppression of transgene expression.

In this study, I constructed a plasmid vector encoding the murine IFN-β gene under the control of the Mx promoter (pMx-IFN-β) to achieve sustained long-term expression of IFN-β. I hypothesized that the gene delivery of pMx-IFN-β would cause sustained IFN-β expression through activation of the Mx promoter. IFN-β expressed after the gene transfer of pMx-IFN-β is secreted from the cells, binds to IFNAR on transgene-expressing cells, and activates the Mx promoter to induce IFN-β expression in an autocrine manner (Figure 1). I investigated IFN-β expression profiles after the delivery of pMx-IFN-β. The contribution of IFN-β-stimulation of the Mx promoter to IFN-β expression was evaluated using small interfering RNA (siRNA) targeting IFNAR. In addition, the therapeutic effect of IFN-β was investigated using tumor-bearing mice.

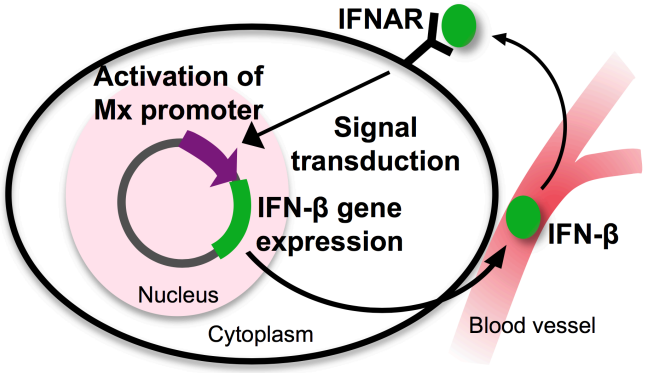

Figure 1. Schematic image of IFN-β gene expression system from pMx-IFN-β

I-2 Materials and Methods

Cell cultures and mice

A mouse melanoma cell line B16-BL6, sub-strain of B16-F10 [20], and a mouse colon carcinoma cell line colon26 were obtained from the Cancer Chemotherapy Center of the Japanese Foundation for Cancer Research (Tokyo, Japan). B16-BL6 was cultured in Dulbecco's modified Eagle's medium (DMEM) (Nissui Pharmaceutical, Tokyo, Japan) supplemented with 10% fetal bovine serum (FBS), D-glucose, and penicillin/streptomycin/L-glutamine (PSG) at 37°C and 5% CO_2. Colon26 was cultured in DMEM containing 10% FBS and PSG at 37°C and 5% CO_2. BALB/c mice (male, 6-week-old, 22 ± 3 g) were purchased from Japan SLC Inc. (Shizuoka, Japan) Mice were maintained under the rearing condition as follows: cage, 2-4 mice/cage; forage, MF (Oriental Yeast Co., ltd., Tokyo, Japan); water, water supply bottle containing tap water; bed, woody bedding (Pure chip; Shimizu Laboratory Supplies Co., Ltd., Kyoto, Japan); housing, conventional housing conditions; light/dark cycle, 12 h/12 h; temperature, 25°C. All animal experiments were performed in accordance

with the ARRIVE guidelines and all protocols for animal experiments were approved by the Animal Experimentation Committee of the Graduate School of Pharmaceutical Science, Kyoto University.

Plasmid DNA and siRNA

pCMV-IFN-β, pCpG-fLuc, and pROSA-gLuc encoding mouse IFN-β, firefly luciferase (fLuc), and *Gaussia* Luciferase (gLuc), respectively, were constructed as previously reported [4,21,22]. pROSA-mcs, an empty plasmid vector containing multi cloning site (mcs), was also constructed as previously reported [23]. A fragment of mouse IFN-β cDNA was amplified by polymerase chain reaction (PCR) from pCMV-IFN-β. The IFN-β cDNA digested by EcoO109I/NheI was inserted into the EcoO109I/NheI site of the pCpG-mcs (InvivoGene, San Diego, CA, USA) to construct pCpG-IFN-β. pMx-IFN-β, pMx-fLuc, pMx-gLuc, and pMx-mcs were constructed by replacing the enhancer and promoter regions of pCpG-IFN-β, pCpG-fLuc, pROSA-gLuc, and pROSA-mcs with the Mx promoter PCR-amplified from mouse genomic DNA. The following PCR primers were used for the amplification of the Mx promoter: 5'-AAACCTGCAGGAAGTCTAAGGGCTCT-3' and 5'-CCCAAGCTTCAAATGCCCTGCT-3'. phRL-TK was purchased from Promega (Madison, WI). Table 1 summarizes the properties of plasmid DNA used in this study. siIFNAR1, siRNA targeting IFNAR1, was obtained from Thermo Fisher Scientific (Waltham, MA, USA). siGFP, siRNA targeting green fluorescent protein (GFP), was purchased from Takara Bio Inc. (Shiga, Japan). The successful knockdown of IFNAR by siIFNAR was confirmed in previous study performed in my laboratory [17].

Table 1. Properties of plasmid DNA

Plasmid DNA	Size (kbp)	Enhancer		Promoter		cDNA
		Type	Size (bp)	Type	Size (bp)	
pCMV-IFN-β	6.0			hCMV	587	Murine interferon-beta
pCpG-IFN-β	3.6	hCMV	430	hEF1	210	Murine interferon-beta
pCpG-fLuc	4.7	hCMV	430	hEF1	210	firefly luciferase
pMx-IFN-β	3.7			mMx	710	Murine interferon-beta
pMx-fLuc	4.8			mMx	710	firefly luciferase
pMx-gLuc	3.7			mMx	710	*Gaussia* luciferase
pMx-mcs	3.2			mMx	710	None

IFN-β, interferon-β; hCMV, human cytomegalovirus; hEF1, human elongation factor 1.

***In vitro* transfection of IFN-β-expressing plasmid DNA**

B16-BL6 cells were seeded into 12-well culture plates at 1×10^5 cells/well 1 day before transfection. Cells were transfected with 0.5 μg/mL plasmid DNA or co-transfected with 0.5 μg/mL plasmid DNA and 1 μg/mL siRNA using Lipofectamine 2000 (LA; Thermo Fisher Scientific) according to the manufacturer's instructions. In brief, 1-μg nucleic acid was mixed with 3 μL LA.

Cell viability assay

B16-BL6 cells were seeded into 96-well culture plates at a density of 1×10^4 cells/well and cultured for overnight. B16-BL6 cells were transfected with pDNA (0.5 μg/mL) or co-transfected with pDNA (0.5 μg/mL) and siIFNAR1 (1 μg/mL) using LA for 4 h. As controls, B16-BL6 cells were added only with LA at the same concentrations as ones used for transfection of pDNA (LA [DNA] group) or for co-transfection of pDNA and siIFNAR1 (LA [siIFNAR1] group). After overnight incubation, cell viability was evaluated by using Cell Count Reagent SF (Nacalai Tesque, Kyoto, Japan), a WST-8 reagent. The cell viability was normalized by using the result of cells incubated with Opti-MEM (Thermo Fisher Scientific) alone.

Measurement of IFN-α

B16-BL6 cells seeded in 12-well plate at a density of 1×10^5 cells/well were transfected with 0.5 μg/mL plasmid DNA using LA. As a control group, only LA was added to cells. After 24 h incubation, conditioned media was collected. Mice received saline or pMx-mcs (3 μg/mouse) by hydrodynamic injection. Blood was collected from tail vein at 1 day after hydrodynamic injection and serum was obtained after clotting. The IFN-α

concentration in the collected conditioned media and serum was determined by using mouse IFN-α ELISA kit (mouse IFN alpha Platinum ELISA; eBioscience, San Diego, CA, USA).

Evaluation of Mx promoter activation by IFN-β

B16-BL6 cells were co-transfected with 0.05 μg/mL pMx-fLuc or pCpG-fLuc and 0.5 μg/mL phRL-TK using 1.65 μg/mL LA. After 4 h incubation, cells were seeded at 2×10^4 cells/well in 48-well culture plate and cultured overnight. Then, the culture medium was replaced with Opti-MEM containing various doses of IFN-β obtained from the conditioned medium of B16-BL6 cells transfected with pMx-IFN-β. After overnight incubation, cell lysate was prepared using lysis buffer of a luciferase assay kit (Piccagene Dual, Toyo Ink, Tokyo, Japan). Cell lysate was mixed with the luciferase assay kit (Piccagene Dual), and chemiluminescence was measured by a luminometer (Lumat LB9507; EG and G Berthold, Bad Wildbad, Germany).

Evaluation of Mx promoter activation by conditioned media of transfected cells

B16-BL6 cells were transfected as describe above. After 24 h culture, the culture media were also collected and added to B16-BL6 cells co-transfected with pMx-fLuc and phRL-TK. After 24 h incubation, cell lysate was prepared using lysis buffer and mixed with the luciferase assay kit to measure chemiluminescence.

Quantification of mRNA

Total mRNA was extracted from co-transfected cells using Sepasol-RNA I Super G (Nacalai Tesque). Reverse transcription was performed using a ReverTra Ace qPCR RT Kit (TOYOBO CO. Osaka, Japan), followed by RNaseH treatment (Ribonuclease H; Takara Bio Inc.). To determine the mRNA level of IFNAR1, real-time PCR was conducted using KAPA SYBR FAST qPCR Kit Master Mix (2×) ABI Prism (Kapa Biosystems, Boston, MA, USA). The sequence of the primers used for amplification were: beta-actin (β-actin) forward, 5'-CATCCGTAAAGACCTCTATGCCAAC-3'; reverse, 5'-ATGGAGCCACCGATCCACA-3'; IFNAR1 forward, 5'-CCCAGAGTTCACCCTCAAGA-3'; reverse, 5'-GTGGGAAGCACACATGACAC-3'. Amplified products were detected on-line via intercalation of the fluorescent dye using the StepOnePlus Real-Time PCR System (Applied Biosystems, Foster City, CA, USA). The mRNA expression of the IFNAR1 gene was normalized by using the mRNA level of β-actin.

***In vivo* gene transfer**

Mice were injected with 3 μg plasmid DNA using the hydrodynamics-based procedure [24]. In brief, plasmid DNA dissolved in saline with a volume of 10% of the mouse weight was injected into the tail vein over 5 s. In a separate set of experiments, mice received 3 μg of plasmid DNA with 10 μg of siRNA via the same procedure.

Measurement of IFN-β concentration

At the indicated time points after the transfection of pMx-IFN-β or pCpG-IFN-β, culture media was collected. At the predetermined time points after the hydrodynamic injection of pMx-IFN-β or pCpG-IFN-β, blood was collected from tail vein. The blood samples were incubated at 4°C for 2 h to clot. After clotting, the samples were centrifuged at 8000 × g for 20 min, and the supernatant serum was collected. The collected culture media and serum samples were stored at −80°C until analysis. The IFN-β concentration in the samples was measured by ELISA as previously described [16,17].

Pharmacokinetic parameters

The maximum and minimum serum concentrations of IFN-β (i.e., C_{max} and C_{min}, respectively) were read from the serum concentration-time curves of IFN-β up to 28 days after the gene transfer of IFN-β-expressing plasmid DNAs. The area under the serum concentration–time curve (AUC) and the mean residence time (MRT) of the *in vivo* experiments were calculated by the moment analysis of the time course of serum concentration of IFN-β for each animal by integration to infinite time [16].

Establishment of tumor-bearing mice and measurement of tumor growth

The dorsal hair of BALB/c mice was shaved by animal clipper prior to tumor cell inoculation. Colon26 cells suspended in Hanks' balanced salt solution (2×10^5 cells/50 μL) were subcutaneously injected into the back of mice. The mice received the hydrodynamic injection of plasmid DNA at 3 μg/mouse when the tumor volume reached 100 mm^3. After administration, the shortest and longest diameter of tumor tissue was measured every other day, and the tumor volume was calculated using the following equation: $(\text{shortest length})^2 \times (\text{longest length})/2$. Moreover, the body weight of mice was measured on day 0, 14 and 28. When the tumor volume was >3000 mm^3, mice were euthanized by cervical spine fracture dislocation.

Histological analysis

Tumor-bearing mice were undergone by hydrodynamic injection of plasmid DNA when the tumor volume reached 100 mm^3. At 14 days after the gene transfer, tumor tissue was collected and embedded in OCT compound in Tissue-Tek® O.C.T. compound, frozen in liquid nitrogen. Tumor sections (10 μm thick) were prepared by using cryostat and were fixed by 4% paraformaldehyde solution (PFA; Nacalai Tesque). TUNEL staining using an *in situ* Apoptosis Detection Kit (Takara Bio Inc.) was conducted in accordance with the manufacture's instruction. In addition, fixed tumor sections were incubated with rat anti-mouse CD31 antibody (1:500; Biolegend, San Diego, CA, USA) and then incubation with Alexa Fluor 488 Anti-Rat IgG (1:200;Thermo Fisher Scientific). Slides were prepared using a SlowFade Antifade Kit with DAPI (Thermo Fisher Scientific). The stained samples were observed under a fluorescence microscope (Biozero, BZ-X710; Keyence, Osaka, Japan).

Data analysis

Differences were statistically analyzed using Student's *t*-test for paired comparison or one-way analysis of variance (ANOVA) followed by the Student–Newman–Keuls test for multiple comparison. *P*-Values of <0.05 were considered to represent statistical significance.

I-3 Results

I-3-a. IFN-β was secreted to the culture medium from B16-BL6 cells transfected with IFN-β-expressing plasmid vectors

Figure 2 shows the IFN-β concentration in the culture media of B16-BL6 cells after transfection with pMx-IFN-β or pCpG-IFN-β. The IFN-β concentration in the culture medium of cells transfected with pMx-IFN-β was significantly higher than that of cells transfected with pCpG-IFN-β. There was no detectable cytotoxicity after the transfection (Figure 3). In addition, this transfection hardly produced IFN-α (Figure 4A).

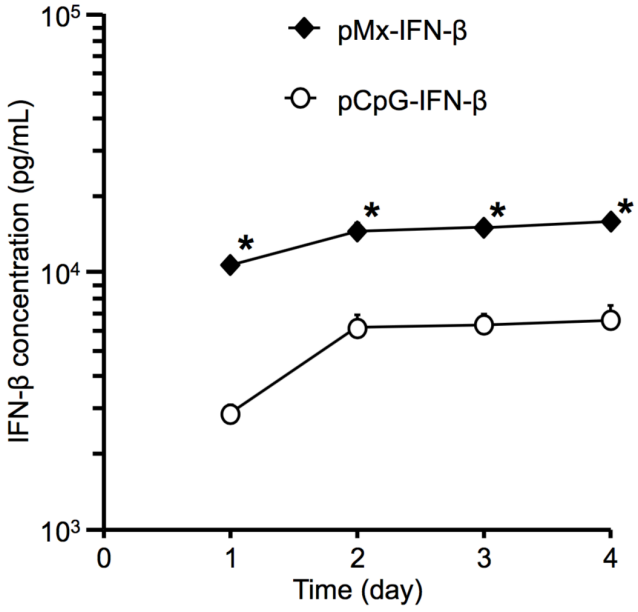

Figure 2. Expression of IFN-β from cultured B16-BL6 cells transfected with pMx-IFN-β or pCpG-IFN-β. The IFN-β concentration in the conditioned medium of B16-BL6 cells after transfection with pMx-IFN-β (closed diamond) and pCpG-IFN-β (open circle). The concentration of IFN-β in collected samples was detected by ELISA. The results are expressed as mean ± SD of four samples. *p < 0.05 compared with the pCpG-IFN-β group.

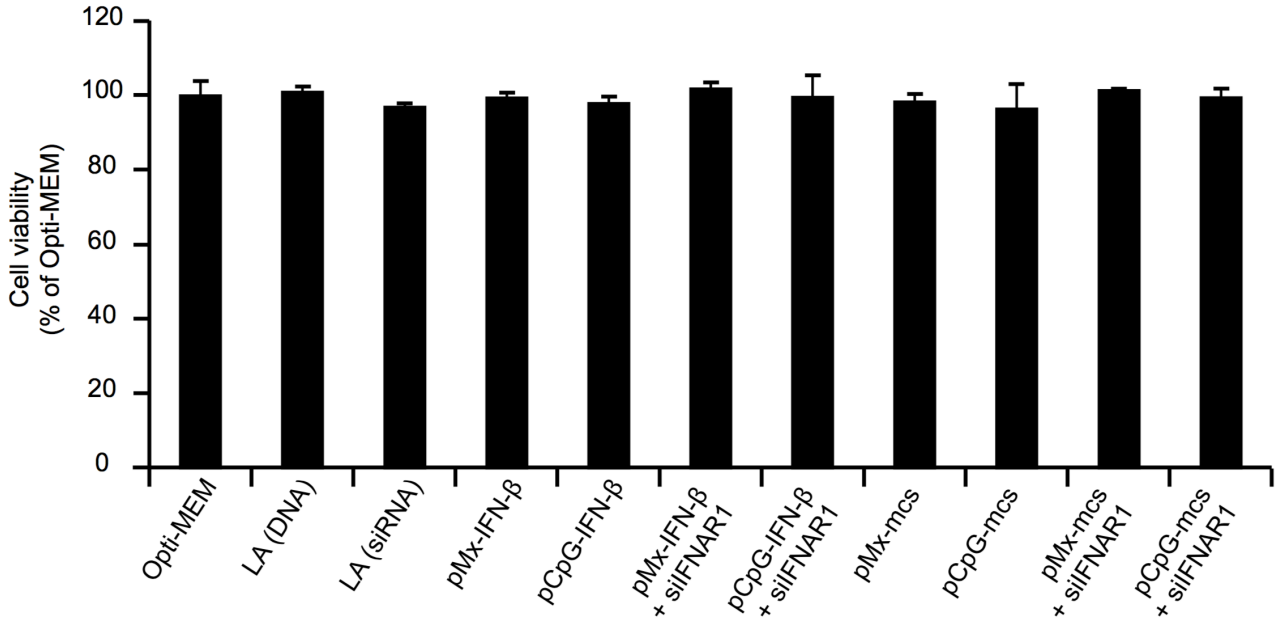

Figure 3. Cell viability after transfection of pDNA and co-transfection of pDNA and siRNA. The cell viability was evaluated at 1 day after transfection and co-transfection. LA (DNA) and LA (siIFNAR1) indicate the cell viability of B16-BL6 cells exposed to only LA at the same concentrations as one used for transfection of pDNA or for co-transfection of pDNA and siIFNAR1, respectively. The results are expressed as mean ± SD of four samples.

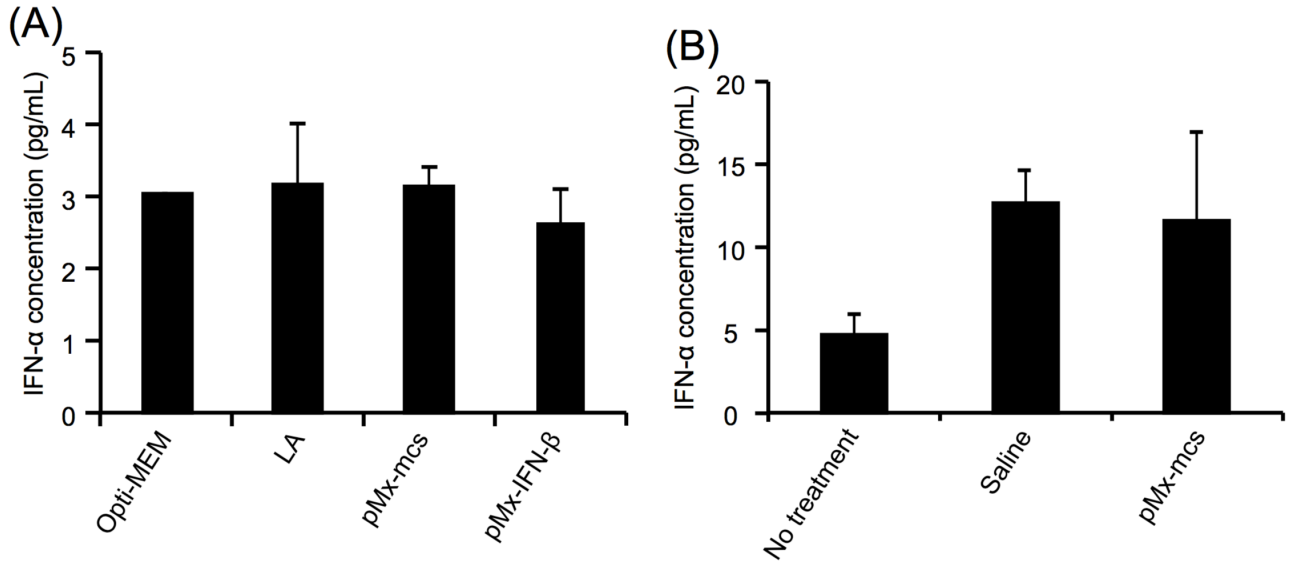

Figure 4. IFN-α concentration after *in vitro* transfection and *in vivo* gene transfer. (A) The concentration of IFN-α in the conditioned medium of B16-BL6 cells after transfection using LA with or without pDNA. (B) The serum concentration of IFN-α after hydrodynamic injection of saline or pMx-mcs. The concentration of IFN-α was measured by ELISA. The results are expressed as mean ± SD of at least three samples.

I-3-b. Transgene expression from pMx-fLuc was increased by IFN-β

Figure 5 shows the fLuc activity of B16-BL6 cells after transfection with pMx-fLuc, followed by the addition of IFN-β. IFN-β at concentrations of >10 pg/mL significantly enhanced the luciferase activity. An increase of approximately 20-fold was obtained by the addition of 100 pg/mL or more IFN-β. In contrast, luciferase activity in the cells transfected with pCpG-fLuc was hardly affected by the addition of IFN-β, irrespective of concentrations. On the other hand, condition media of the transfected cells hardly activated Mx promoter except for that of pMx-IFN-β-transfected cells, suggesting that IFN-α and other molecules that activate Mx promoter were hardly produced under the transfection condition tested (Figure 6).

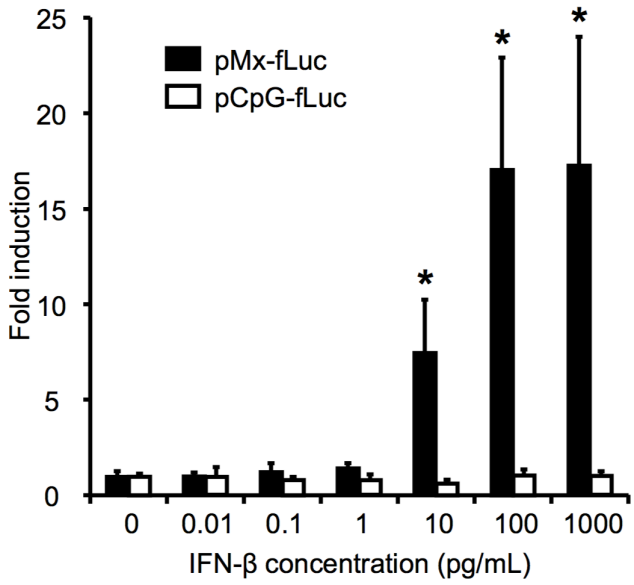

Figure 5. Induction of fLuc expression from pMx-fLuc or pCpG-fLuc by IFN-β. B16-BL6 cells were co-transfected with pMx-fLuc or pCpG-fLuc with phRL-TK. After incubation, the serial dilutions of IFN-β protein were added. The luciferase activity of cell lysates was determined after 24 h incubation. The results are expressed as mean ± SD of four mice. *$p < 0.05$ compared with 0 pg/mL.

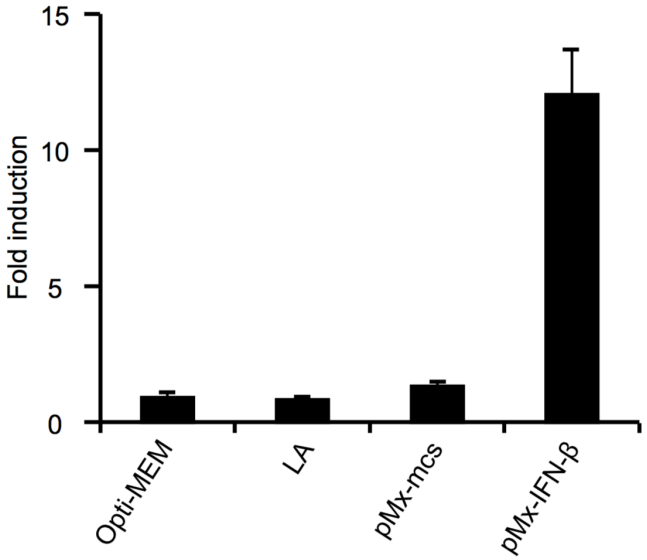

Figure 6. Mx promoter activation by conditioned media collected from transfected cells. The conditioned media collected from B16-BL6 cells transfected with or without plasmid DNA was applied to B16-BL6 cells co-transfected with pMx-fLuc with phRL-TK. The luciferase activity of cell lysates was determined after 24 h of incubation. The results are expressed as mean ± SD of four mice.

I-3-c. Co-transfection of siIFNAR with pMx-IFN-β reduced IFN-β expression from pMx-IFN-β

B16-BL6 cells were co-transfected with pMx-IFN-β and siIFNAR, siRNA targeting IFNAR, to investigate whether the binding of IFN-β to IFNAR was involved in the expression of IFN-β from pMx-IFN-β. IFNAR1 mRNA expression was decreased by co-transfection of siIFNAR1 to the same degree as the previous report [16] (Figure 7). The IFN-β concentration in the cultures of B16-BL6 cells co-transfected with pMx-IFN-β and siIFNAR1 was significantly lower than that of B16-BL6 cells co-transfected with pMx-IFN-β and siGFP at 6 or 24 h after transfection (Figure 8A). On the other hand, the IFN-β concentration in the cultures of B16-BL6 co-transfected with pCpG-IFN-β and siIFNAR1 was comparable to that of cells co-transfected with pCpG-IFN-β and siGFP (Figure 8B). There was no detectable cytotoxicity after the co-transfection (Figure 3).

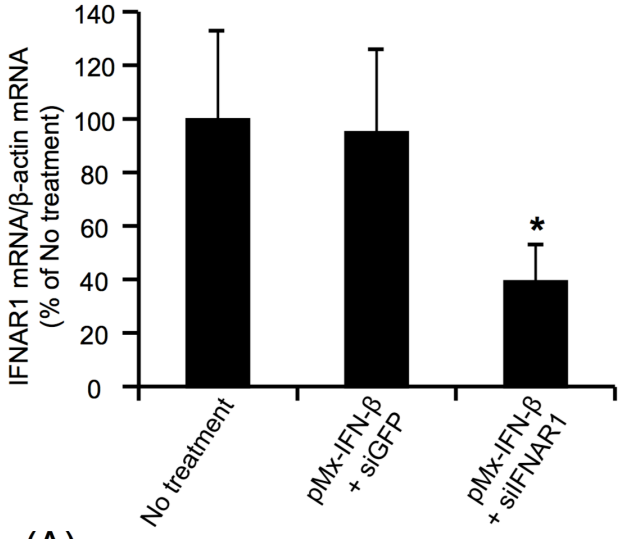

Figure 7. IFNAR1 mRNA expression in B16-BL6 cells after co-transfection of pMx-IFN-β and siRNA. The mRNA level was measured at 1 day after co-transfection of pMx-IFN-β and siRNA. The results are expressed as mean ± SD of four samples. *p < 0.05 compared with the pMx-IFN-β + siGFP group.

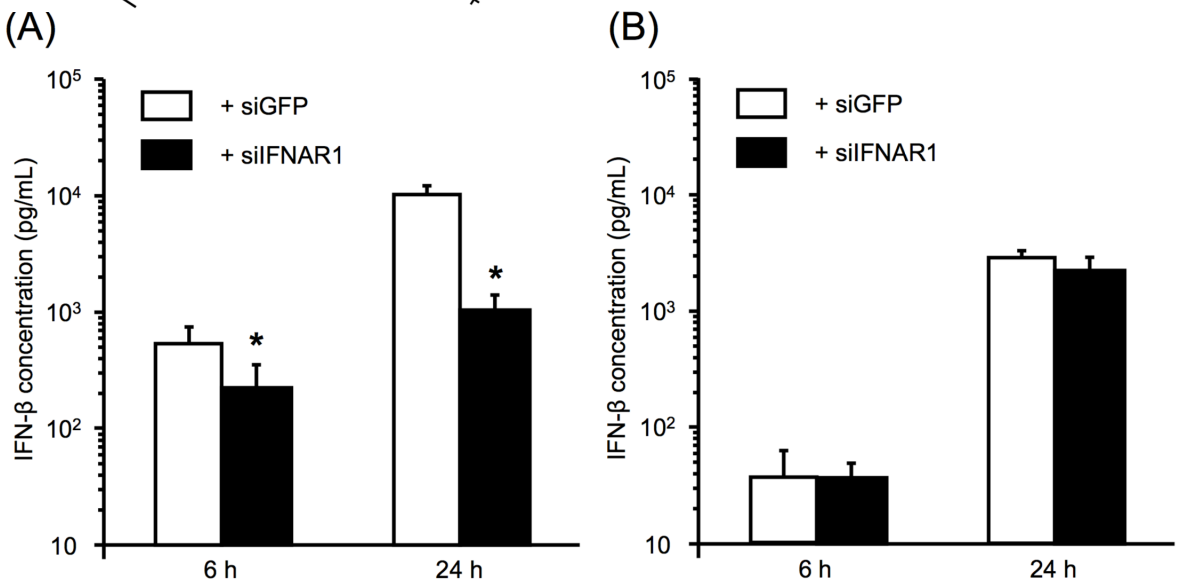

Figure 8. Effect of IFNAR knockdown using siRNA for expression of IFN-β gene *in vitro*. The concentration of IFN-β in the conditioned medium of B16-BL6 cells after co-transfection of (A) pMx-IFN-β and (B) pCpG-IFN-β with siRNA was determined by ELISA. The results are expressed as mean ± SD of four samples. *p < 0.05 compared with the siGFP-treated groups.

I-3-d. Serum concentration of IFN-β was sustained in mice receiving gene delivery of pMx-IFN-β

Figure 9 shows the serum concentration of IFN-β peaked 6 h after the hydrodynamic injection of pMx-IFN-β and gradually decreased between day 1 and 7. Thereafter, serum concentration of IFN-β was maintained at approximately 100 pg/mL. On the other hand, after the gene transfer of pCpG-IFN-β, serum concentration of IFN-β peaked at 6 h, rapidly declined until day 3, and then gradually decreased between day 3 and day 28. In addition, pCMV-IFN-β was used as a conventional plasmid vector encoding IFN-β for comparison. After the administration of pCMV-IFN-β, the serum concentration of IFN-β peaked at 6 h, and then rapidly declined to undetectable levels within 3 days post injection. On the other hand, hydrodynamic injection resulted in slight increase in serum IFN-α concentration (Figure 4B).

As described above, the C_{max} was achieved at 6 h after the administration of IFN-β-expressing plasmid DNAs, and the C_{min} values were obtained at day 28 for pMx-IFN-β and pCpG-IFN-β (Table 2). The ratio of C_{max} and C_{min} of the pMx-IFN-β-administered group was about 3-fold lower than that of the pCpG-IFN-β-administered group. AUC and MRT of serum concentration of IFN-β after the injection of IFN-β-expressing plasmid DNAs were calculated by moment analysis. AUC did not differ significantly between the pMx-IFN-β group and pCpG-IFN-β groups. However, MRT of the pMx-IFN-β-administered group was 2.4-fold higher than that of the pCpG-IFN-β-administered group.

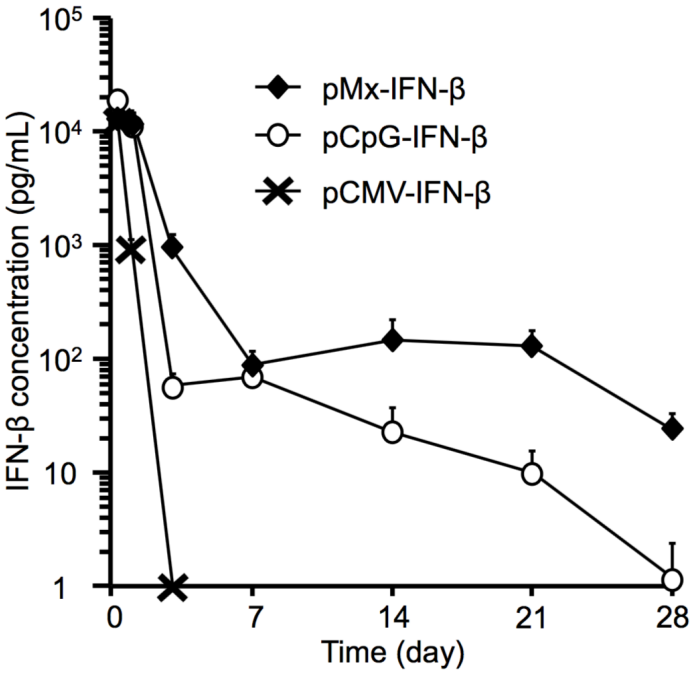

Figure 9. Expression profile of IFN-β gene after gene transfer by hydrodynamics injection. Time course of the serum concentration of IFN-β after the gene transfer of pMx-IFN-β (closed diamond), pCpG-IFN-β (open circle), and pCMV-IFN-β (cross mark) at a dose of 3 μg/mouse. The concentration of IFN-β in serum samples was analyzed by ELISA. The results are expressed as mean ± SEM of four mice.

Table 2. Pharmacokinetic parameters after hydrodynamic injection of IFN-β-expressing plasmid DNA into mice

	C_{max} (pg/mL)	C_{min} (pg/mL)	C_{max}/C_{min}	AUC (ng/mL·day)	MRT (day)
pMx-IFN-β	13100 ± 1297	24.2 ± 8.5	541	28.6 ± 4.0	2.40 ± 0.27 *
pCpG-IFN-β	17900 ± 380	1.19 ± 1.19	15000	26.1 ± 2.2	0.966 ± 0.114
pCMV-IFN-β	12600 ± 438	-	-	7.56 ± 0.61	0.370 ± 0.028

* Statistically significant ($p < 0.05$) compared with pCpG-IFN-β. The AUC and MRT are expressed as the calculated mean ± SEM of four mice.

I-3-e. Serum concentration of IFN-β was decreased in mice receiving co-administration of siIFNAR1 with pMx-IFN-β

Mice received the co-administration of IFN-β-expressing plasmid DNA with siIFNAR1 to analyze the effect of IFNAR knockdown on IFN-β expression *in vivo*. After the co-administration of pMx-IFN-β and siRNAs, there was no significant difference in the serum concentration of IFN-β at 6 h between siGFP and siIFNAR groups (Figure 10A). However, the IFN-β concentration in the serum of mice co-administered pMx-IFN-β with siIFNAR was approximately 20-fold lower than that of mice co-administered pMx-IFN-β and siGFP at 24 h after the administration. On the other hand, in mice co-administered pCpG-IFN-β with siRNAs, there was no significant difference in serum concentration of IFN-β between the siIFNAR1 and siGFP groups (Figure 10B).

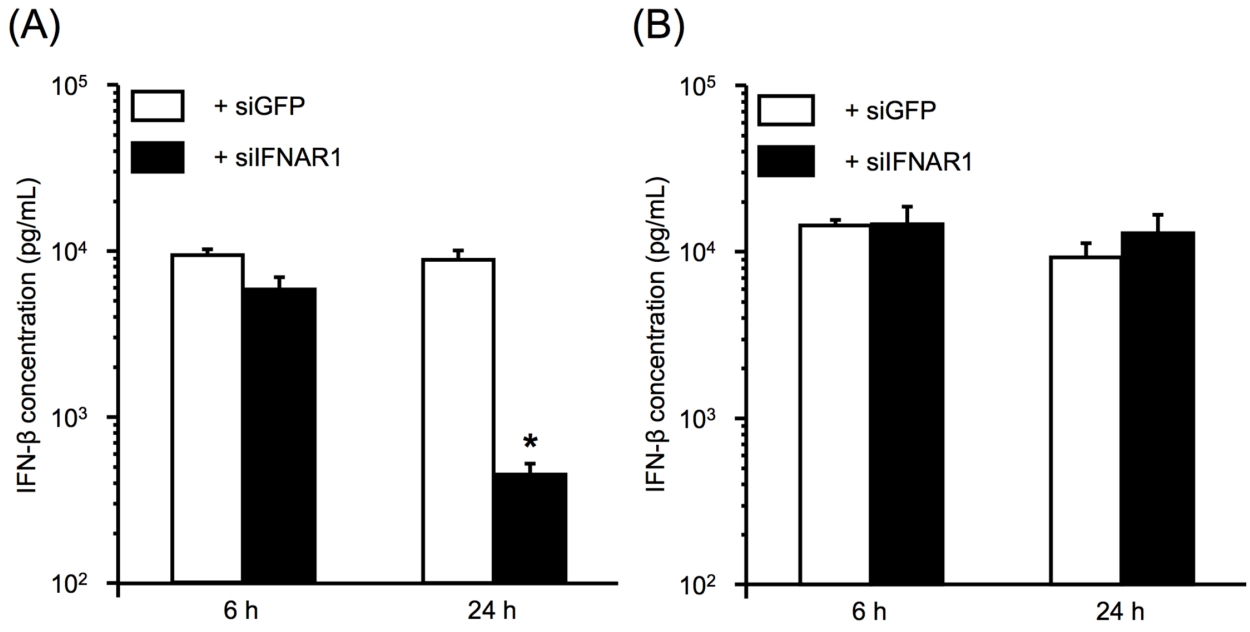

Figure 10. Effect of co-administration of plasmid DNA encoding IFN-β gene and siIFNAR on the expression of IFN-β gene in mice. Mice were co-administered (A) pMx-IFN-β and (B) pCpG-IFN-β with siRNA by hydrodynamic-based procedure at 3 μg/mouse and 10 μg/mouse, respectively. IFN-β concentration in the collected serum samples was determined by ELISA. The results are expressed as mean ± SEM of three mice. *$p < 0.05$ compared with the siGFP-administered groups.

I-3-f. Fewer tumor microvessels were observed in IFN-β-expressing plasmid DNA-treated tumor-bearing mice

To evaluate apoptotic cells and tumor microvessel in tumor tissue after gene transfer into tumor-bearing mice, TUNEL staining and CD31 immunostaining were performed with cryostat sections of tumor tissues. The plasmid DNA encoding gLuc, pMx-gLuc, was used as a control vector. Figure 11A shows some cells were positive for TUNEL staining in the tumor tissues of IFN-β-expressing plasmid DNA-treated groups. CD31 immunostaining indicated microvessel formation in the tumor tissues of the no treatment and the pMx-gLuc-treated groups (Figure 11B). On the other hand, the number of microvessels in the pMx-IFN-β-treated mice was much fewer than the no treatment and pMx-gLuc-treated groups.

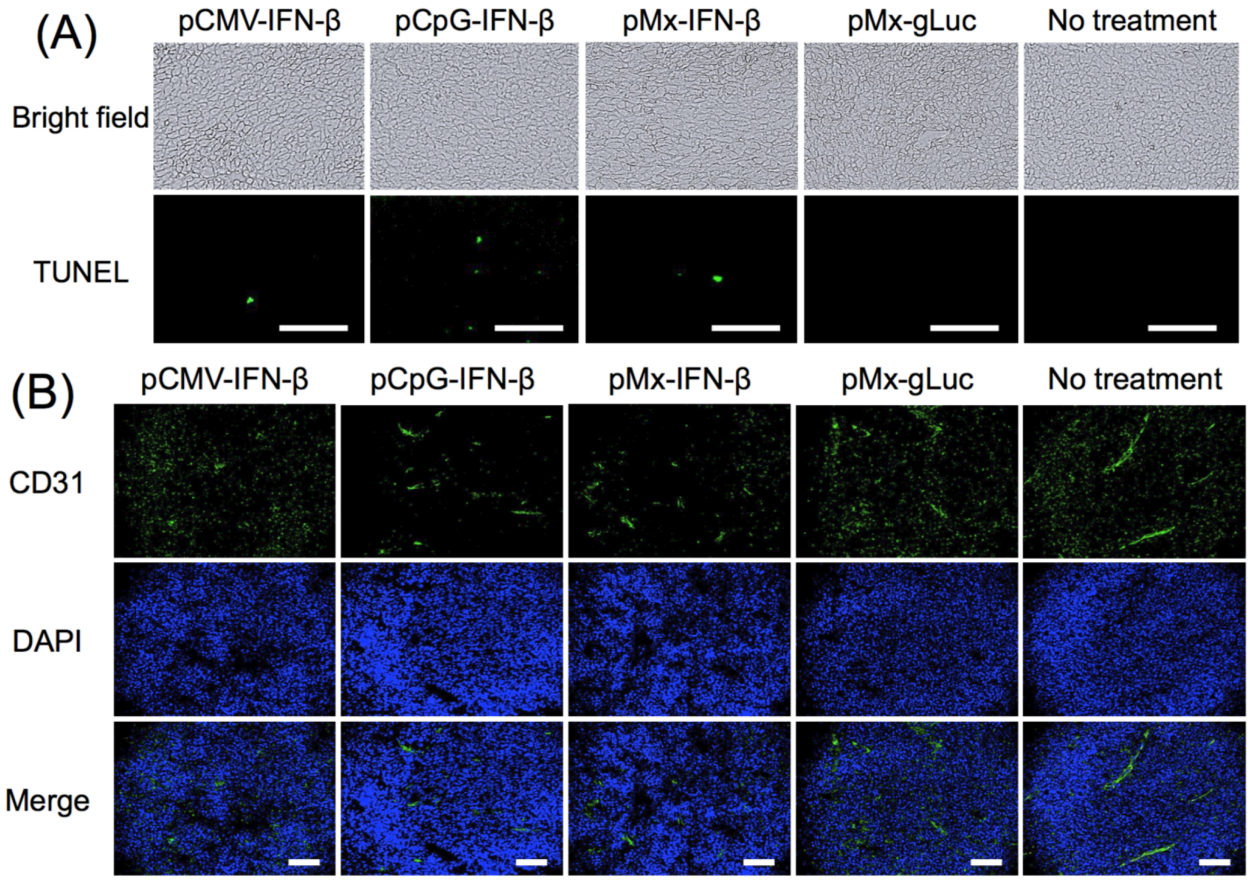

Figure 11. Apoptotic cells and tumor microvessel in tumor tissue at 14 days after gene transfer into tumor-bearing mice. Tumor-bearing mice received plasmid DNA administration by hydrodynamic injection. At day 14, tumor tissue was collected, and the tumor section was stained by (A) TUNEL and (B) anti-CD31 antibody to examine apoptotic cells and the tumor microvessel, respectively. Typical images of sections exhibiting bright field, green fluorescence ((A) TUNEL; apoptotic cells, (B) CD31; microvessel), blue fluorescence (DAPI; nucleus) and blue and green fluorescence (merged image) are shown. Scale bar = 100 μm.

I-3-g. Tumor growth was suppressed by gene transfer of IFN-β into tumor-bearing mice

The tumor volume of untreated animals and the pMx-gLuc group rapidly increased over time (Figure 12A). On the other hand, the growth of tumors in mice administered pMx-IFN-β or pCpG-IFN-β was significantly suppressed in comparison to untreated animals and the pMx-gLuc group. Although there was no significant difference in tumor volume between pMx-IFN-β and pCpG-IFN-β groups, the tumors of mice administered pMx-IFN-β tended to be smaller than that of mice administered pCpG-IFN-β. The gene transfer of pCMV-IFN-β into tumor-bearing mice moderately suppressed tumor growth. The mean survival time in the pMx-IFN-β, pCpG-IFN-β, and no treatment groups were 26.8 ± 0.8, 24.0 ± 2.3, and 18.5 ± 1.3, respectively, and mice in the pMx-IFN-β group survived for significantly longer than those in the no treatment group (Figure 12B). In addition, there was no significant difference in body weight between these groups (Figure 12C).

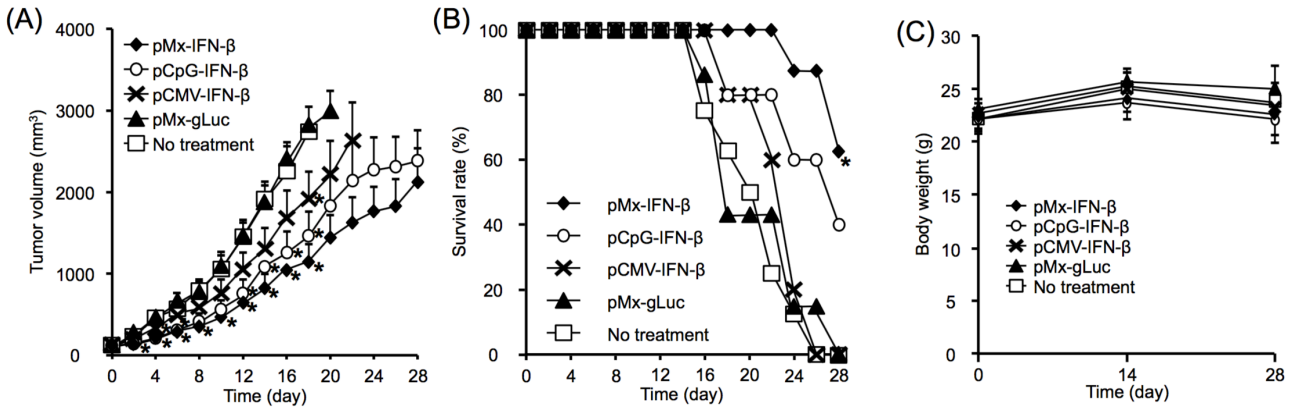

Figure 12. Anti-tumor effect of IFN-β after gene transfer into tumor-bearing mice. Mice were subcutaneously inoculated colon26 tumor cells. Gene transfer by hydrodynamic injection was conducted when the tumor volume reached approximately 100 mm^3 (day 0). (A) The tumor volume was measured by calipers every other day. (B) Survival rate of mice in each group was evaluated every day, and mice were euthanized when the tumor volume exceeded 3000 mm^3. (C) The body weight of mice was measured on days 0, 14, and 28. The results are expressed as mean ± SEM of at least five mice. *$p < 0.05$ compared with the no treatment group.

I-4 Discussion

Gene delivery represents a promising approach that allows the maintenance of high levels of circulating IFN-β for cancer therapy. CpG motifs in plasmid vectors induce inflammatory cytokine expression by stimulating Toll-like receptor-9 [25,26]. Inflammatory cytokines such as tumor necrosis factor-α (TNF-α) have been reported to inhibit transgene expression after gene transfer [27,28]. It was shown that the gene transfer of the IFN-β expressing-plasmid DNA vector containing less CpG motifs increased the serum concentration of IFN-β for only 2 days [13]. While the CpG motif-depleted plasmid vector, pCpG, induced long-term expression of IFN-γ [4]. Figure 9 indicates that the expression of IFN-β tended to decline after the hydrodynamic injection of pCpG-IFN-β into mice. IFN-β expression from pCpG-IFN-β was likely transient as a result of IFN-β-mediated transgene suppression.

In this study, I designed a system for sustained expression of IFN-β gene using the Mx promoter. A serum concentration of IFN-β of 100 pg/mL after gene transfer into mice (Figure 9) was sufficient to activate IFN-β expression from pMx-IFN-β (Figure 5). The IFN-β concentration required to activate the Mx promoter was consistent with previous reports [29,30]. In addition, using siIFNAR1 to inhibit IFN-β signal transduction, IFN-β expression from pMx-IFN-β was decreased by approximately one 20th in both *in vitro* and *in vivo* experiments. Considering the fact that an approximately 20-fold increase in fLuc expression from pMx-fLuc was induced by 100 pg/mL of IFN-β (Figure 5), these results suggest that signal transduction after the binding of IFN-β to IFNAR increased IFN-β expression from pMx-IFN-β by approximately 20-fold.

On the other hand, the fact that IFN-β gene expression was detected after the gene transfer of pMx-IFN-β with siIFNAR suggests that the Mx promoter possesses basal activity in the absence of IFN-β. The Mx promoter contains several transcription factor binding sites, including one for hepatocyte nuclear factor. Therefore, the basal activity of the Mx promoter could be attributed to the binding of these transcription factors. On the other hand, it is known that cytosolic DNA leads to the production of type I IFNs such as IFN-α, which may activate Mx promoter [31]. However, Mx promoter was hardly activated by the conditioned medium of pMx-mcs-transfected cells (Figure 6) and IFN-α was hardly detected in the conditioned medium. Therefore, IFN-α is not involved in the Mx promoter activity detected in the *in vitro* experiments. On the other hand, serum IFN-α concentration was slightly increased after hydrodynamic injection (Figure 4). As hydrodynamic injection transiently induces inflammatory cytokine production such as IL-6 and TNF-α, the slight increase in serum IFN-α concentration could be caused by the same mechanism. This result suggests that transiently induced IFN-α might be involved in the initial expression of IFN-β gene after hydrodynamic injection of pMx-IFN-β into mice.

Although no significant difference was observed between the pMx-IFN-β-treated and pCpG-IFN-β-treated groups, the administration of pMx-IFN-β tended to suppress tumor growth more effectively than pCpG-IFN-β after day 14. This tendency suggested that the serum concentration of IFN-β would be an important factor in the antitumor effect of IFN-β because the serum concentration of IFN-β in mice administered pMx-IFN-β was higher than that in mice administered pCpG-IFN-β after day 14. In addition, considering the fact that serum IFN-β

concentration was maintained at approximately 100 pg/mL in the pMx-IFN-β-administered group, approximately 100 pg/mL IFN-β might be enough serum concentration to obtain antitumor effect. Regarding to the antitumor effect of IFN-β, it was reported that IFN-β suppressed angiogenesis in tumor tissues and increased apoptosis of tumor cells [6]. Although the result of TUNEL assay for the evaluation of apoptosis showed that there was no significant difference among the pCMV-IFN-β-, pCpG-IFN-β-, and pMx-IFN-β-treated groups (Figure 11A), the CD31 immunostaining indicated that the angiogenesis in tumor tissue of the pMx-IFN-β-treated group on day 14 tended to be reduced compared with that of the pCMV-IFN-β- or pCpG-IFN-β-treated groups (Figure 11B). Considering the fact that the administration of pMx-IFN-β tended to suppress tumor growth more effectively than that of pCpG-IFN-β, the effect of IFN-β on tumor growth might be caused by the inhibition of angiogenesis. In addition, the fact that there was significant difference in MRT but not in AUC between pMx-IFN-β group and pCpG-IFN-β group implies that the persistent supply of IFN-β is also an important factor in the antitumor effect of IFN-β. The lower C_{max}/C_{min} value of the pMx-IFN-β-administered group indicated a more stable serum concentration of IFN-β than that achieved by pCpG-IFN-β. On the other hand, sustained expression of IFN-β from pMx-IFN-β might induce adverse side effects. However, the fact that body weight change was comparable among all the groups examined suggested that sustained IFN-β expression hardly cause severe adverse effects. Therefore, pMx-IFN-β is superior to pCpG-IFN-β, achieving relatively high levels of prolonged IFN-β concentration.

Optimizing the combination of enhancers/promoters driving therapeutic protein expression represents a promising approach to achieve prolonged expression of therapeutic proteins. However, as in the case of IFN-β, wherein the therapeutic proteins possess transgene suppressive effects, a sustained expression is difficult to achieve by the selection of enhancers and promoters. In this study, I demonstrated that by utilizing the biological activity of IFN-β using the Mx promoter to drive an IFN-β-expressing vector enabled sustained IFN-β expression. This approach may be applicable to other therapeutic proteins with transgene suppressing effects.

I-5 Conclusion

These results demonstrated that the Mx promoter could effectively promote long-term expression of IFN-β, which effectively suppressed tumor growth. To my knowledge, this is the first study reporting sustained IFN-β expression via gene therapy, an aim that was likely previously prevented by IFN-β's transgene suppressing effect. The Mx promoter driven expression system maintained circulating levels of IFN-β and may represent an effective treatment for chronic diseases.

Chapter II

Evaluation of antiviral effect of type I, II, and III interferons on direct-acting antiviral-resistant hepatitis C virus

II-1 Introduction

HCV infection is a common cause of chronic hepatitis, cirrhosis, and hepatocellular carcinoma and affects more than 185 million people worldwide [32]. Conventional regimen for treating chronic HCV infection includes pegylated IFN-α and ribavirin therapy, which shows limited therapeutic efficacy depending on HCV genotypes [33,34]. In the previous decade, direct-acting antivirals (DAAs), which are synthetic inhibitors of HCV nonstructural (NS) proteins, were developed and approved for treating chronic HCV infection [35]. A combination of first-generation DAAs such as telaprevir and simeprevir, NS3/4 protease inhibitors, with IFN-α and ribavirin exerts improved therapeutic effects in patients with chronic HCV infection. Moreover, treatment with next-generation DAAs such as ledipasvir and sofosbuvir, NS5A and NS5B inhibitor, respectively, allows IFN-free therapy. Results of clinical studies have reported high therapeutic efficiency of a combination ledipasvir tablet and sofosbuvir [36,37]. In particular, sofosbuvir/velpatasvir/voxileprevir regimen showed the sustained virologic response (SVR) rates >95% except for genotype 1a HCV [38,39]. However, DAA therapy is associated with concerns such as appearance of drug resistance-associated substitutions (RASs) [40,41]. Therefore, it is necessary to determine other regimens for treating infection caused by HCV RASs. According to the recent clinical study [42-44], re-treatment using DAA and IFN-based regimen was effective for the treatment of DAA failure patients. Although DAA therapy has been standard of care for HCV patients, IFN-based regimen has also contributed for the treatment of HCV for a long time. Therefore, I focused on IFN-based regimen as an optional regimen to treat DAA failure patients.

IFNs are a type of cytokines and are classified into three types, namely, type I IFNs such as IFN-α and IFN-β, type II IFNs such as IFN-γ, and type III IFNs such as IFN-λs (IFN-λ_1 [IL-29], IFN-λ_2 [IL-28A], and IFN-λ_3 [IL-28B]) [1]. All IFN types exert antiviral, immunomodulatory, and anticancer effects. However, different IFNs have different receptors and signal transduction pathways [45], which may affect their antiviral effect on HCV. Responsiveness of IFN to HCV has been evaluated. For instance, induction of IFN after infection of HCV [46,47] and the detail of antiviral activity of type I IFN against HCV [48] were investigated. However, information regarding the antiviral effect on DAA-resistant HCV was insufficient. Although previous studies have reported the antiviral effect of types I, II, and III IFNs on HCV [49,50], their effect on infection caused by DAA RASs of HCV has not been reported to date.

In the present study, I determined IFN types for effectively treating infections caused by NS3- and NS5A-mutated HCVs. NS3 and NS5A in HCV are one of the action sites of DAAs for exerting antiviral effect. Therefore, NS3- and NS5A-mutated HCVs show resistant to DAA targeting NS3 and NS5A. For this, human liver chimeric mice established by transplanting human hepatocytes into immunodeficient urokinase-type plasminogen activator (uPA/SCID) mice were infected with NS3-D168-, NS5A-L31-, and NS5A-Y93-mutated HCVs [51,52]. Previous study in my laboratory showed that transfection of chimeric mice with a human IFN-γ-expressing plasmid provided sustained supply of IFN-γ in these mice and that the expressed IFN-γ exerted a strong antiviral effect against wild-type genotype 1b HCV [52]. In the present study, I used human liver chimeric mice to evaluate

whether sustained supply of IFN-α_2, IFN-γ, and IFN-λ_1, which are typical types I, II, and III IFNs, respectively, effectively treated infection caused by NS3- and NS5A-mutated HCVs.

II-2 Materials and methods

Plasmid DNA

Plasmids pCpG-IFN-γ and pCpG-gLuc expressing human IFN-γ and gLuc, respectively, were constructed as reported previously [52] and described in Chapter I. Genes expressing human IFN-α_2 and IFN-λ_1 were synthesized by GenScript (Piscataway, NJ, USA) and FASMAC (Kanagawa, Japan), respectively. Plasmids pCpG-IFN-α_2 and pCpG-IFN-λ_1 were constructed by inserting IFN-α_2 and IFN-λ_1 gene fragments digested by KpnI/NheI and BglII/NcoI, respectively, into KpnI/NheI and BglII/NcoI sites, respectively, of plasmid pCpG-mcs. Plasmid pMx-IFN-λ_1 was constructed by replacing the enhancer and promoter regions of pCpG-IFN-λ_1 with the Mx promoter of pMx-mcs, as described in Chapter I [53].

Analysis of antiviral effect *in vitro*

LucNeo#2 cells, which are Huh-7 cells harboring self-replicating subgenomic HCV RNA replicons with a fLuc reporter [54], were kindly provided by Dr. Hijikata and Dr. Shimotohno. LucNeo#2 cells were cultured, as reported previously [55]. Briefly, LucNeo#2 cells were seeded (density, 4×10^4 cells/well) in 24-well culture plates 1 day before transfection. Next, the cells were cultured with 500 μL/well Opti-MEM containing 5 μg of the indicated plasmid and 4 μL X-tremeGENE HP DNA Transfection Reagent (Roche Applied Science, Mannheim, Germany). At 1 and 3 days after the transfection, conditioned media were collected for determining IFN concentrations. fLuc activity was measured by the procedure described in Chapter I.

Antiviral effect of IFN-λ_1 protein at a difference concentration on HCV subgenomic replicon cells

IFN-λ_1 protein was obtained from the conditioned medium, which was collected after transfection of pMx-IFN-λ_1 into B16-BL6 cells. IFN-λ_1 concentration in the culture medium was determined by ELISA method as following described. LucNeo#2 cell seeded into 24-well culture plates at 4×10^4 cells/well one day before addition of IFN-λ_1 protein. The serially diluted IFN-λ_1 protein was added to cells and fLuc activity was measured by the procedure described in Chapter I at 1 day and 3 days after addition.

Evaluation of gene expression profile *in vivo*

ICR mice (male, 4-week-old, 20 ± 2 g) were purchased from Japan SLC Inc.. Mice were maintained as described above. On day 0, ICR mice received 10 μg of plasmid DNA by hydrodynamic injection and serum samples were collected at the predetermined time points as aforementioned in Chapter I. All protocols for animal experiments were approved by the Animal Experimentation Committee of the Graduate School of Pharmaceutical Science, Kyoto University.

Animal treatment

Immunodeficient uPA$^{+/+}$/SCID$^{+/+}$ mice were generated, and human hepatocytes were transplanted, as described previously (PhoenixBio Co., Ltd., Higashi-Hiroshima, Japan) [56]. All the mice were transplanted with frozen human hepatocytes obtained from the same donor. All animal protocols were performed in accordance with the guidelines of local committees for animal experiments (Hiroshima University and Kyoto University), and all the animals received humane care. Chimeric mice showing a high replacement rate for human hepatocytes were used in this study. Eight weeks after hepatocyte transplantation, the mice were intravenously injected with 10^5 copies of HCV. Human serum samples containing high titers of NS3-D168A/G-, NS5A-L31M-, and NS5A-Y93H-mutated genotype 1b HCVs were obtained from a patient with chronic hepatitis C who did not respond to daclatasvir plus asunaprevir treatment [57]. The serum contained almost complete mutated HCV. The patient provided written informed consent for participating in the study. Study protocol conformed to the ethics guidelines mentioned in the 1975 Declaration of Helsinki and was approved by the review committee of the Hiroshima University.

Detection of drug-resistant substitutions

Amino acid sequences and population frequencies of NS3-D168, NS5A-L31, and NS5A-Y93-mutated HCV RASs were determined by performing Invader assay, as described previously [58]. Lower detectable limit for population frequency in the Invader assay was set as 1%.

***In vivo* gene transfer**

The chimeric mice were hydrodynamically injected with 250 μg plasmid as described in Chapter I [24].

Measurement of IFN concentrations, gLuc activity, and human serum albumin and alanine aminotransferase levels

Serum samples were collected from the mice at indicated times after the plasmid injection and were stored at −80°C until further analysis. IFN concentrations in the conditioned media of plasmid-transfected LucNeo#2 cells and those in the serum samples of plasmid-injected chimeric mice were determined using IFN-α_2 ELISA kit (Human IFN-α Matched Antibody Pairs; eBioscience), IFN-γ ELISA kit (Human IFN-γ ELISA Ready-SET-GO; eBioscience), and IFN-λ_1 ELISA kit (Human IL-29 [IFN-λ_1] ELISA Ready-SET-GO; eBioscience). gLuc activity was measured by the procedure described in Chapter I. Human serum albumin (HSA) concentration in the mouse serum, which correlated with repopulation index [56], was measured using Human Albumin ELISA Quantitation Kit (Bethyl Laboratories Inc., Montgomery, TX). Serum alanine aminotransferase (ALT) level was measured using a quantification kit (Transaminase CII test Wako; Wako Pure Chemical Industries, Osaka, Japan).

Detection of HCV RNA

RNA was extracted from serum and liver samples by using Sepa Gene RV-R (Sankojunyaku, Tokyo, Japan) and was reverse transcribed using a random primer (Takara Bio Inc.) and M-MLV reverse transcriptase (ReverTra Ace; TOYOBO CO.). HCV RNA was quantified by performing nested PCR in Light Cycler (Roche Diagnostic, Tokyo, Japan), as reported previously [56,59]. Lower detection limit was set as 10^2 copies/mL for nested PCR and 10^3 copies/mL for real-time PCR.

Quantification of the mRNA levels of IFN-stimulated genes

Total mRNA extraction from liver portion isolated from normal chimeric mice not infected with HCV and from chimeric mice infected with NS3- and NS5A-mutated HCVs at 42 days after the plasmid injection, reverse transcription, and real time PCR was conducted by the procedure described in Chapter I. The sequences of the primers used for amplification were as follows: β-actin forward, 5′-ACAATGAGCTGCTGGTGGCT-3′; β-actin reverse, 5′-GATGGGCACAGTGTGGGTGA-3′; myxovirus-resistance protein A (MxA) forward, 5′-GCTACACACCGTGACGGATATGG-3′; MxA reverse, 5′-CGAGCTGGATTGGAAAGCCC-3′; RNA-dependent protein kinase (PKR) forward, 5′-GCCTTTTCATCCAAATGGAATTC-3′; PKR reverse, 5′-GAAATCTGTTCTGGGCTCATG-3′; 2′,5′-oligoadenylate synthetase (OAS) forward, 5′-TCAGAAGAGAAGCCAACGTGA-3′; and OAS reverse, 5′-CGGAGACAGCGAGGGTAAAT-3′. The mRNA levels of genes encoding MxA, PKR, and OAS in chimeric mice injected with the IFN- and gLuc-expressing plasmids and infected with NS3- and NS5A-mutated HCVs were normalized using the mRNA level of the β-actin gene and were calculated using the mRNA levels of the ISGs in normal chimeric mice not infected with NS3- and NS5A-mutated HCVs.

Histological analysis

Liver samples obtained from chimeric mice injected with the IFN- or gLuc-expressing plasmids were examined by performing hematoxylin–eosin (HE) staining or immunohistochemical staining with anti-HSA antibody, as described previously [60].

Data analysis

Quantitative differences between data sets were statistically analyzed using Student's *t*-test or one-way ANOVA for paired comparison, followed by Student–Newman–Keuls test for multiple comparison. *P*-values of <0.05 were considered statistically significant.

II-3 Results

II-3-a. fLuc activity in cells containing HCV subgenomic replicons decreased after transfecting IFN-expressing plasmids

The gLuc-expressing plasmid pCpG-gLuc lacking any biological activity was used as a control vector. fLuc activity significantly decreased in LucNeo#2 cells transfected with the IFN-expressing plasmids irrespective of the IFN type expressed compared with that in cells transfected with pCpG-gLuc on days 1 and 3 after the transfection (Figure 13A). Concentrations of IFN-α_2 in the culture medium on days 1 and 3 after the transfection were approximately 1.8×10^4 and 3.0×10^4 pg/mL, respectively (Figure 13B); those of IFN-γ were approximately 6.6×10^4 and 7.7×10^4 pg/mL, respectively; and those of IFN-λ_1 were approximately 9.1×10^4 and 2.1×10^5 pg/mL, respectively. Moreover, treatment with >100 pg/mL IFN-λ_1 significantly decreased luciferase activity in HCV replicon cells in a dose-dependent manner (Figure 14).

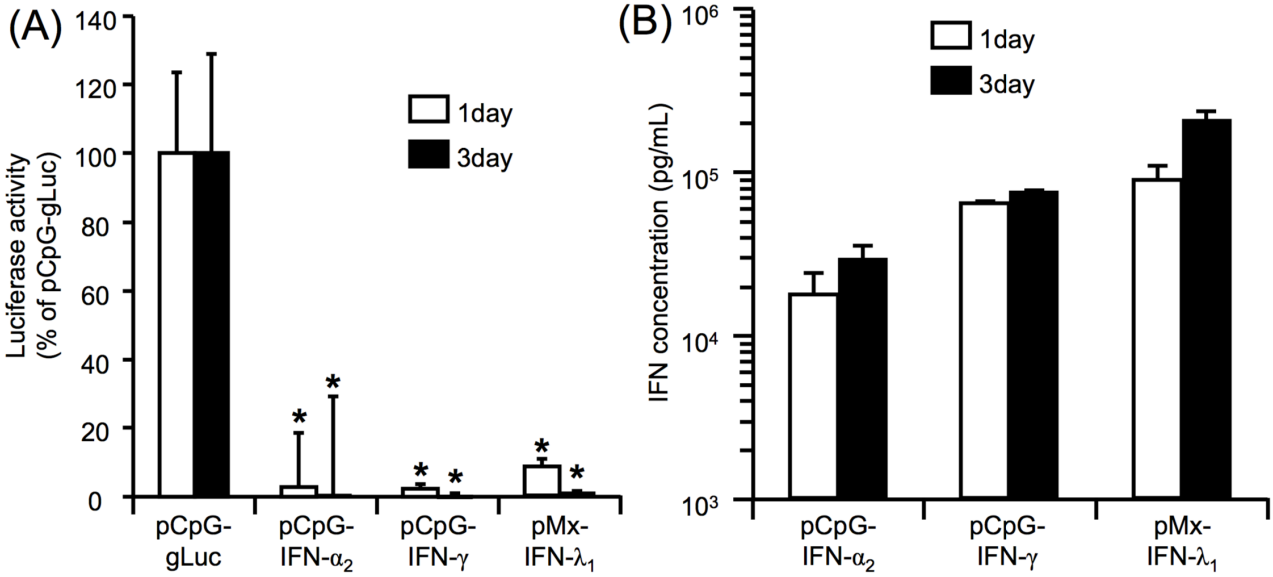

Figure 13. Antiviral activity of IFNs in cells containing HCV subgenomic replicons. (A) fLuc activity was used as an index of HCV RNA replication level on day 1 (open bar) and day 3 (closed bar) after transfecting the IFN-expressing plasmids. (B) IFN concentrations in the culture medium on days 1 and 3 after the transfection. Results are expressed as mean ± SD of four samples; *p < 0.05 compared with cells transfected with pCpG-gLuc.

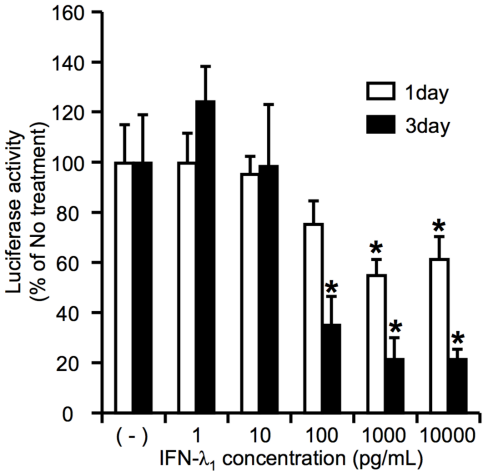

Figure 14. Antiviral activity IFN-λ_1 in HCV subgenomic replicon cells. fLuc activity as an index of HCV RNA replication level at 1 day and 3 days after IFN-λ_1 protein treatment. The results are expressed as mean ± SD of four samples. *p < 0.05 compared with the No treatment group.

II-3-b. Hydrodynamic injection of the IFN-expressing plasmids in normal mice provided continuous supply of IFNs

To determine whether hydrodynamic injection of the IFN-expressing plasmids provided continuous supply of IFNs, I assessed serum IFN concentrations in normal ICR mice after plasmid injection. Serum concentrations of IFN-α_2, IFN-γ, and IFN-λ_1 were maintained for at least 42 days after injecting pCpG-IFN-α_2, pCpG-IFN-γ, and pMx-IFN-λ_1, respectively (Figure 15A). For continuous supply of IFNs, these IFNs-expressing vectors were screened by preliminary experiment (data not shown). Moreover, gLuc activity was detected persistently for at least 42 days in the serum of pCpG-gLuc-injected mice (Figure 15B).

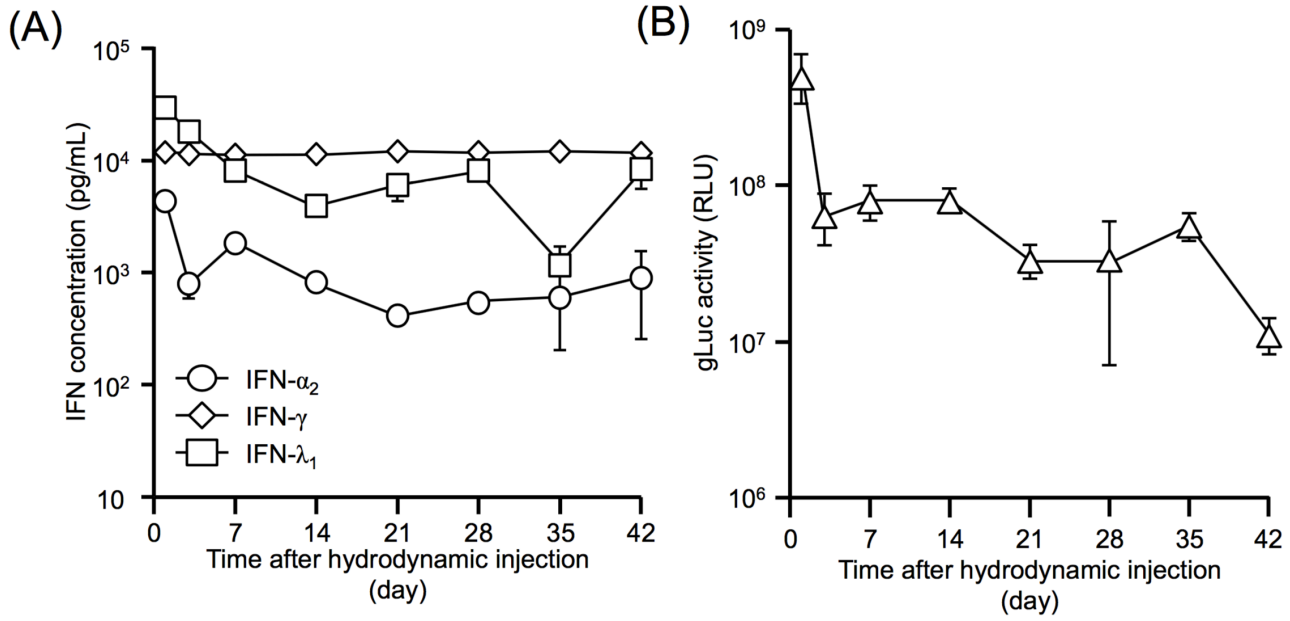

Figure 15. Expression profile of IFN-α_2, IFN-γ, IFN-λ_1, and gLuc gene after gene transfer into normal mice by hydrodynamics injection. (A) Serum concentration of IFN-α_2 (open circle), IFN-γ (open diamond), and IFN-λ_1 (open square) was determined by ELISA. (B) gLuc activity in serum was detected by luminometer. The results are expressed as mean ± SEM of four mice.

II-3-c. IFN-α_2 moderately decreased HCV RNA level in the serum of chimeric mice infected with NS3- and NS5A-mutated HCV RASs

To evaluate the antiviral activity of IFNs against HCV RASs, human hepatocyte-injected chimeric mice were inoculated with serum samples obtained from a patient with genotype 1b HCV infection who did not respond to daclatasvir plus asunaprevir therapy. Eight weeks after the inoculation, HCV RNA level in the serum of mice increased to 10^6–10^7 copies/mL. The Invader assay showed 60.4-100% of NS3-D168A/G, NS5A-L31M, and NS5A-Y93H mutated HCV in the serum of all infected mice. These NS3- and NS5A-mutated HCV-infected chimeric mice were hydrodynamically injected with pCpG-IFN-α_2. HCV RNA levels in #1, #2, and #4 chimeric mice decreased after pCpG-IFN-α_2 injection (Figure 16A), whereas those in #3 and #5 chimeric mice decreased

negligibly. Nested PCR was conducted to determine HCV RNA in the liver of pCpG-IFN-α_2-injected chimeric mice infected with NS3- and NS5A-mutated HCVs. Nested PCR detected HCV RNA in the liver of pCpG-IFN-α_2-injected chimeric mice (Figure 16B). Serum IFN-α_2 concentration in #1, #2, and #4 pCpG-IFN-α_2-injected chimeric mice peaked on day 1 after the injection and was maintained at approximately 50–500 pg/mL for 42 days (Figure 16C). In contrast, serum IFN-α_2 concentration was negligible in #3 and #5 pCpG-IFN-α_2-injected chimeric mice. Serum HSA level was negligibly affected in pCpG-IFN-α_2-injected chimeric mice (Figure 16D). In contrast, ALT activity increased transiently after pCpG-IFN-α_2 injection and decreased rapidly to its baseline level (Figure 16E).

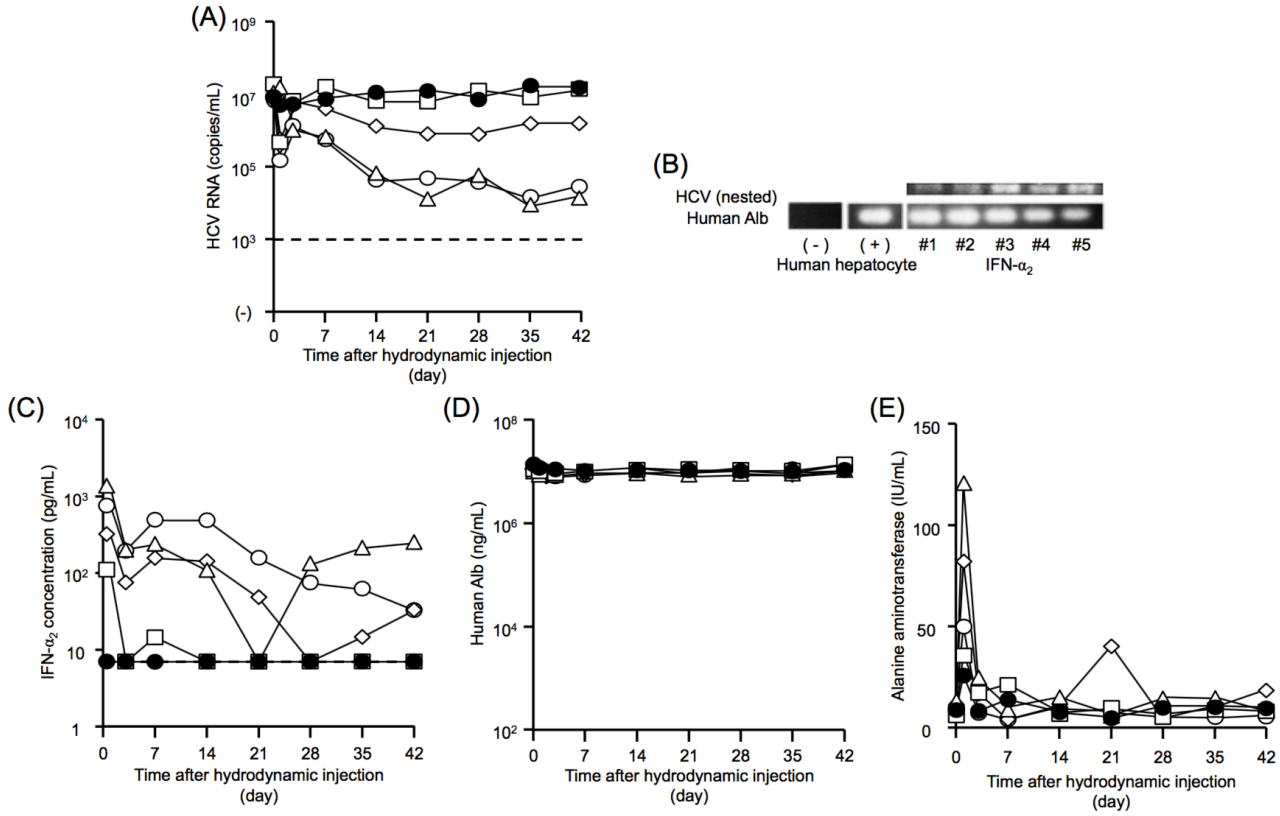

Figure 16. Effect of IFN-α_2 in chimeric mice infected with NS3- and NS5A-mutated HCVs. (A) HCV RNA copy number in the serum, (B) nested PCR results, (C) serum IFN-α_2 concentration, (D) serum HSA concentration, and (E) serum ALT level for each chimeric mouse (#1: open circle, #2: open diamond, #3: open square, #4: open triangle, and #5: closed circle) are shown. Results are expressed as mean ± SEM of five mice. Dotted line indicates detection limit.

II-3-d. IFN-γ markedly decreased HCV RNA level in the serum of chimeric mice infected with NS3- and NS5A-mutated HCVs

To examine the antiviral activity of IFN-γ against HCV RASs, chimeric mice infected with NS3- and NS5A-mutated HCVs were hydrodynamically injected with pCpG-IFN-γ. HCV RNA level decreased significantly from day 1 in pCpG-IFN-γ-injected chimeric mice and reached below the detection limit by day 14 (Figure 17A). Moreover, nested PCR did not detect HCV RNA in the liver of pCpG-IFN-γ-injected chimeric mice (Figure 17B). Serum IFN-γ concentration in pCpG-IFN-γ-injected chimeric mice was maintained at approximately 10^4 pg/mL for 42 days (Figure 17C). Moreover, serum HSA level was negligibly affected in pCpG-IFN-γ-injected chimeric mice (Figure 17D). However, ALT activity increased by day 21 after pCpG-IFN-γ injection and recovered to its baseline level (Figure 17E).

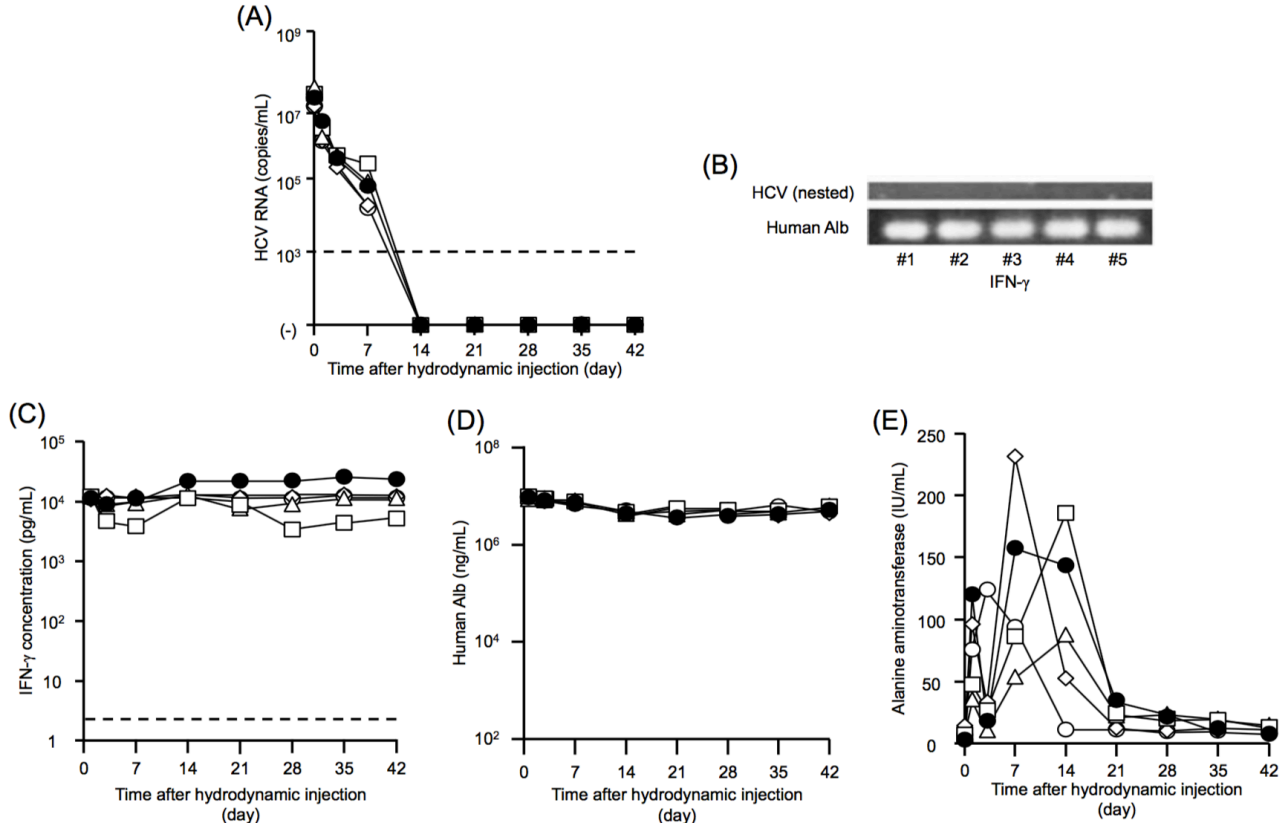

Figure 17. Effect of IFN-γ on chimeric mice infected with NS3- and NS5A-mutated HCVs. (A) HCV RNA copy number in the serum, (B) nested PCR results, (C) serum IFN-γ concentration, (D) serum HSA concentration, and (E) serum ALT level for each chimeric mouse (#1: open circle, #2: open diamond, #3: open square, #4: open triangle, and #5: closed circle) are shown. Results are expressed as mean ± SEM of five mice. Dotted line indicates detection limit.

II-3-e. IFN-λ_1 effectively decreased HCV RNA level in the serum of chimeric mice infected with NS3- and NS5A-mutated HCVs

To analyze the antiviral activity of IFN-λ_1 against HCV RASs, chimeric mice infected with NS3- and NS5A-mutated HCVs were hydrodynamically injected with pMx-IFN-λ_1. HCV RNA level decreased significantly in all pMx-IFN-λ_1-injected chimeric mice (Figure 18A). Moreover, HCV RNA level decreased below the detection limit in pMx-IFN-λ_1-injected chimeric mice, except in mouse #3. Furthermore, nested PCR did not detect HCV RNA in the livers of #1, #2, and #4 pMx-IFN-λ_1-injected chimeric mice (Figure 18B). In contrast, HCV RNA was detected in the livers of #3 and #5 pMx-IFN-λ_1-injected chimeric mice. Serum IFN-λ_1 concentration was maintained at approximately 100–250 pg/mL for 42 days after pMx-IFN-λ_1 injection in #1, #2, and #5 chimeric mice (Figure 18C). However, serum IFN-λ_1 concentration was approximately 4-fold lower in #3 and #4 pMx-IFN-λ_1-injected chimeric mice than in #1, #2, and #5 pMx-IFN-λ_1-injected chimeric mice. Serum HSA level was stable in all pMx-IFN-λ_1-injected chimeric mice (Figure 18D). However, ALT activity increased transiently after pMx-IFN-λ_1 injection and recovered to its baseline level (Figure 18E).

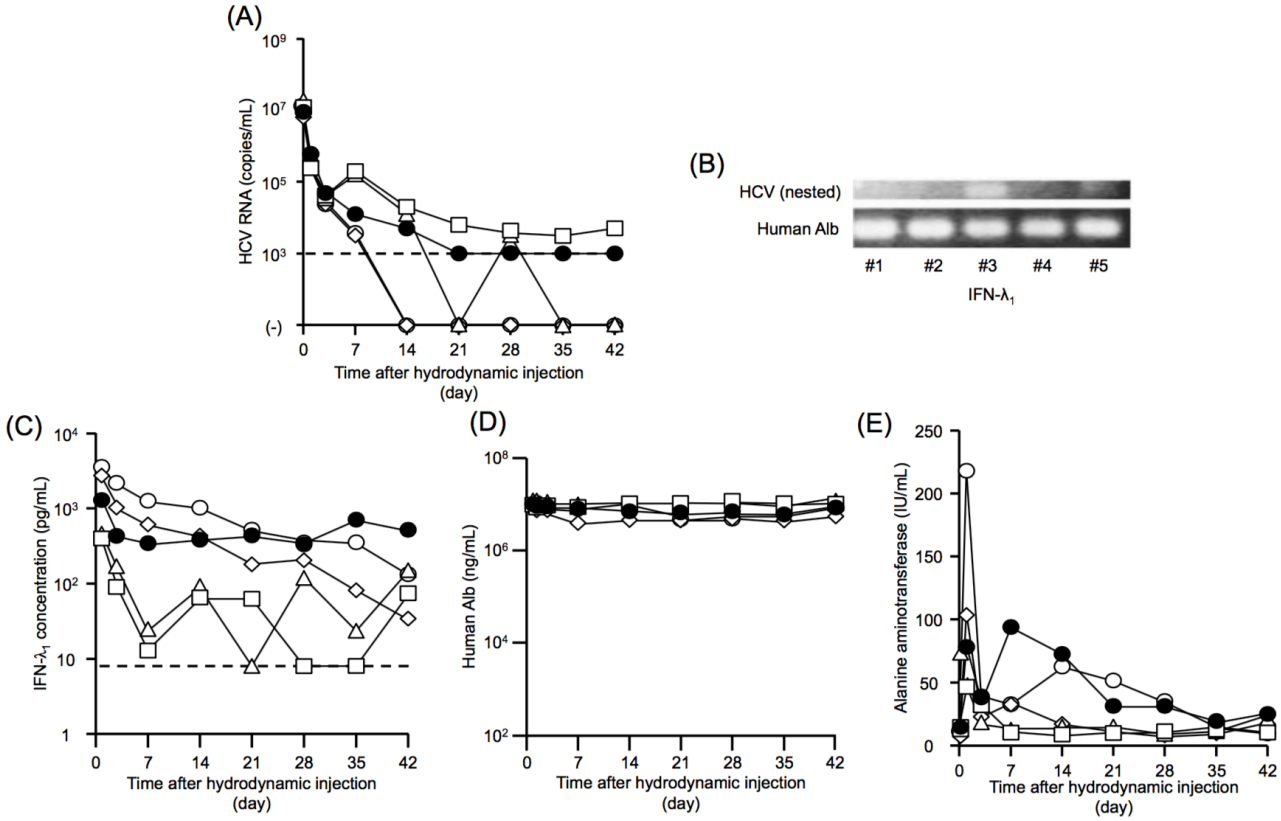

Figure 18. Effect of IFN-λ_1 on chimeric mice infected with NS3- and NS5A-mutated HCVs. (A) HCV RNA copy number in the serum, (B) nested PCR results, (C) IFN-λ_1 concentration, (C) serum HSA concentration, and (E) serum ALT level for each chimeric mouse (#1: open circle, #2: open diamond, #3: open square, #4: open triangle, and #5: closed circle) are shown. Results are expressed as mean ± SEM of five mice. Dotted line indicates detection limit.

II-3-f. gLuc did not affect HCV RNA level in the serum of chimeric mice infected with NS3- and NS5A-mutated HCVs

As a control experiment, chimeric mice infected with NS3- and NS5A-mutated HCVs were injected with pCpG-gLuc. pCpG-gLuc injection negligibly affected HCV RNA level (Figure 19A). gLuc activity in the serum samples of pCpG-gLuc-injected chimeric mice was $>10^5$ relative light unit (Figure 19B). Serum HSA level was negligibly affected in all pCpG-gLuc-injected chimeric mice (Figure 19C). Moreover, although ALT activity was transiently increased after pCpG-gLuc injection, it recovered rapidly (Figure 19D).

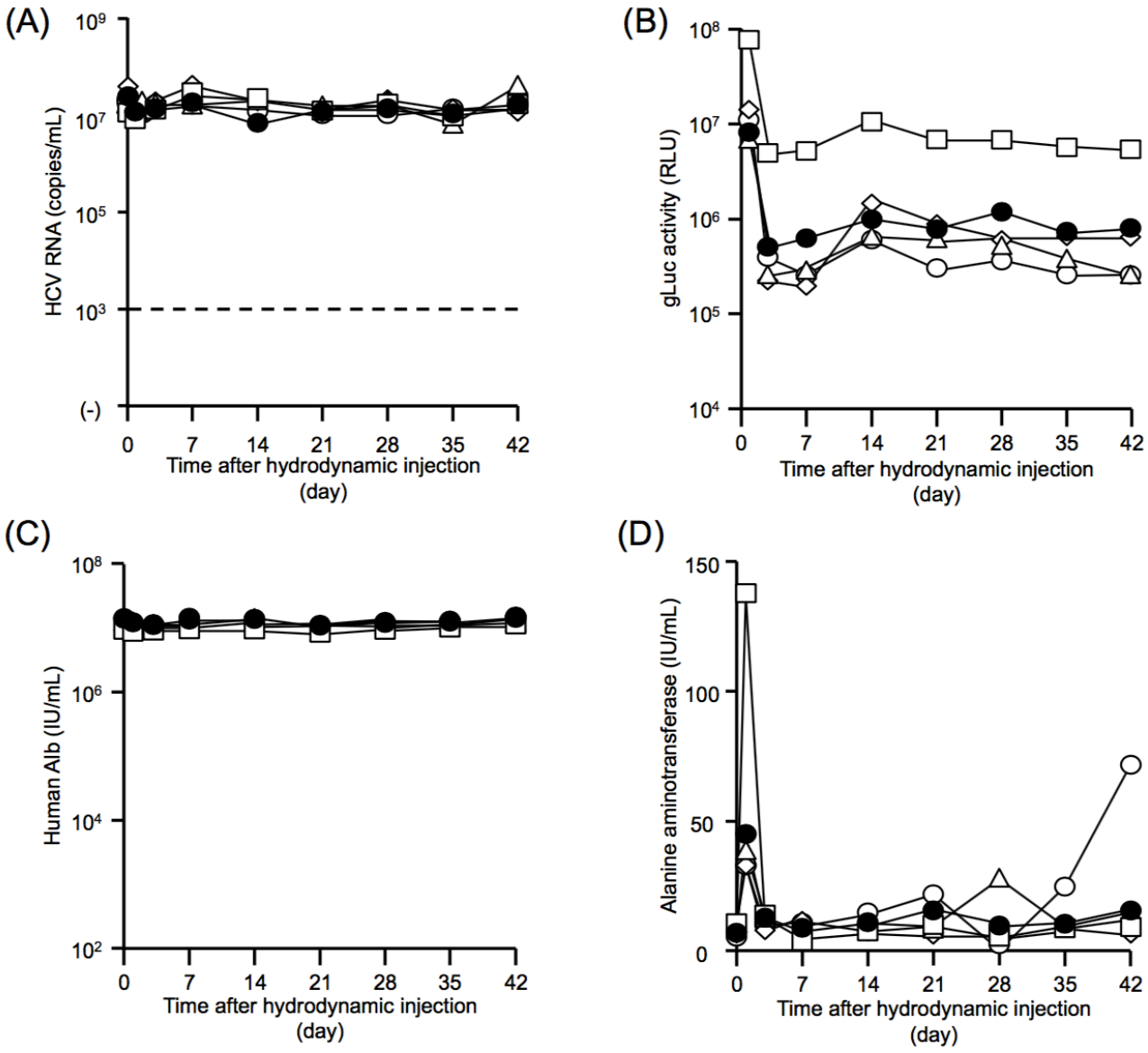

Figure 19. Effect of gLuc (control) on chimeric mice infected with NS3- and NS5A-mutated HCVs. (A) HCV RNA copy number in the serum, (B) gLuc activity in the serum, (C) serum HSA concentration, and (D) serum ALT level for each chimeric mouse (#1: open circle, #2: open diamond, #3: open square, #4: open triangle, and #5: closed circle) are shown. Results are expressed as mean ± SEM of five mice. Dotted line indicates detection limit.

II-3-g. IFN treatment induced ISG expression after 42 days

To confirm the effect of IFNs on human hepatocytes, mRNA levels of genes encoding MxA, PKR, and OAS, which are antiviral proteins belonging to the ISG family, were measured by performing real-time RT-PCR. The mRNA levels of genes encoding MxA, PKR, and OAS in normal chimeric mice, which were not infected with NS3- and NS5A-mutated HCVs, were comparable to those in pCpG-gLuc-injected chimeric mice infected with NS3- and NS5A-mutated HCVs (Figure 20). In contrast, the mRNA levels of these ISGs in chimeric mice injected with the IFN-expressing plasmids were higher than those in normal and pCpG-gLuc-injected chimeric mice; however, the difference was not significant.

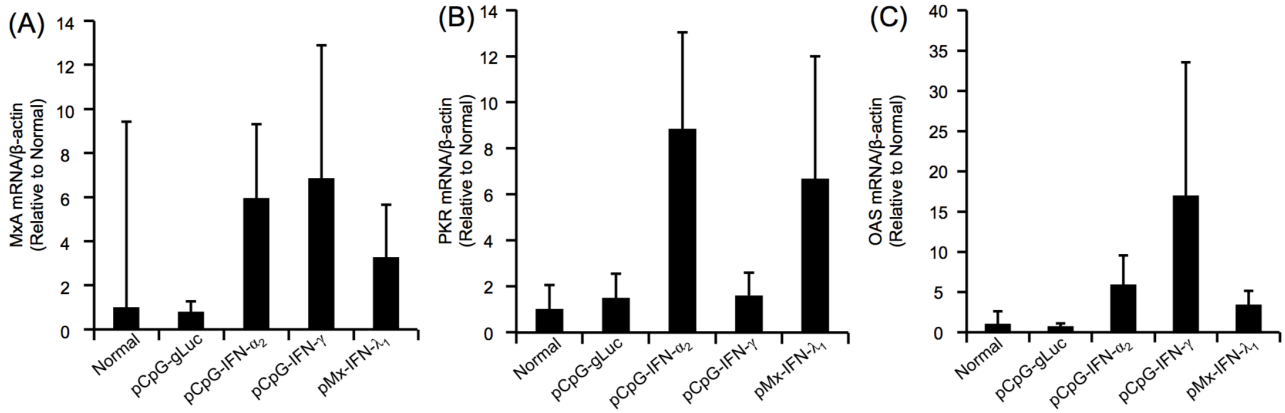

Figure 20. Quantitative analysis of the mRNA levels of ISGs after the injection of IFN- or gLuc-expressing plasmids. The mRNA levels of genes encoding (A) MxA, (B) PKR, and (C) OAS in human hepatocytes isolated from chimeric mice were determined by performing real-time RT-PCR. Results are expressed as mean ± SEM of five mice.

II-3-h. Apparent damage was hardly observed in the liver sections of IFN-treated chimeric mice

To evaluate the toxic effect of continuous IFN supply on the liver, liver samples were collected on day 42 from chimeric mice injected with the IFN- or gLuc-expressing plasmids. HE staining indicated that the livers of chimeric mice injected with the IFN-expressing plasmids showed negligible damage compared with those of mice injected with the gLuc-expressing plasmid (Figure 21). HSA-specific immunostaining was carried out to confirm the replacement of mouse hepatocyte with human hepatocyte, indicating that loss of human hepatocytes was hardly observed.

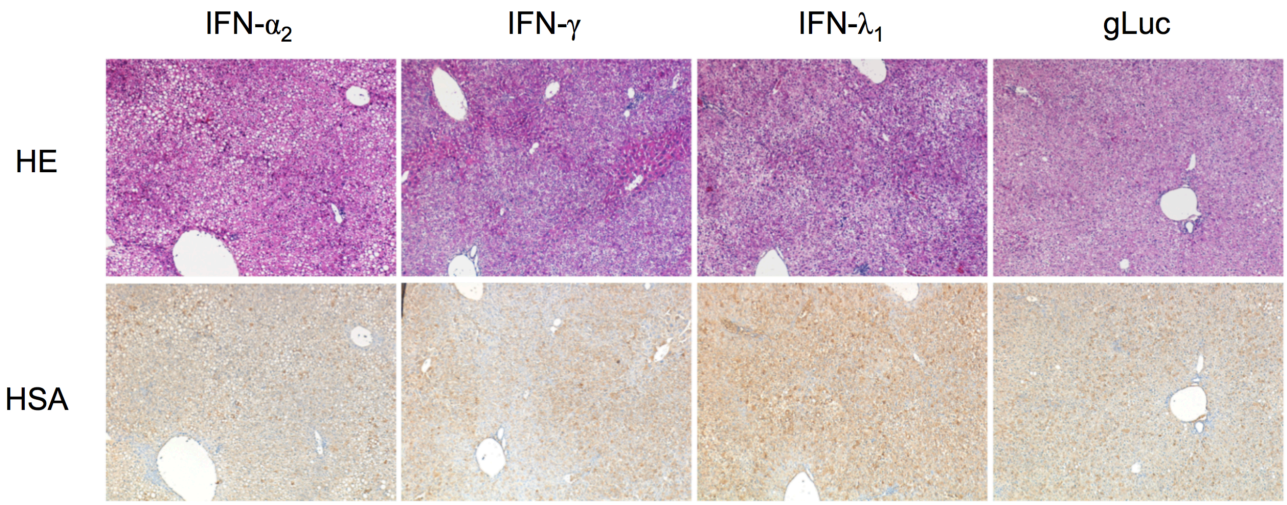

Figure 21. Histological analysis of the liver sections obtained from chimeric mice injected with IFN- or gLuc-expressing plasmids. The liver sections were analyzed by performing HE staining (upper panel) and immunostaining with anti-HSA antibody (bottom panel). Original magnification, ×100.

II-4 Discussion

My study showed that IFN-γ and IFN-λ_1 but not IFN-α_2 effectively decreased serum HCV RNA level in chimeric mice infected with NS3- and NS5A-mutated HCVs, indicating that IFN-γ and IFN-λ_1 exerted antiviral effect on daclatasvir- and asunaprevir-resistant HCVs (Figures 16–18). Although IFN-α_2, IFN-γ, and IFN-λ_1 treatment increased the mRNA levels of genes encoding antiviral proteins MxA, PKR, and OAS, IFN-α_2 treatment exerted negligible effects on NS3- and NS5A-mutated genotype 1b HCVs. IFN-α_2 exerts a poor antiviral effect on genotype 1 HCVs. Therefore, the poor antiviral effect of IFN-α_2 in NS3- and NS5A-mutated genotype 1b HCV-infected chimeric mice may be because of the presence of genotype 1b HCV. In addition, in the present study, human hepatocytes from an IL28B (rs8099917) TT genotype donor were transplanted. Using same animal models, it was previously reported that intrahepatic ISGs expressions after HCV infection were higher in IL28B TG hepatocytes than in IL28B TT hepatocytes [61]. Lack of significant induction of ISGs expressions after HCV infection in the present study might be due to IL28B TT hepatocytes.

Previous *in vitro* study performed in my laboratory showed that treatment with >1700 pg/mL IFN-γ exerted antiviral effects in HCV replicon-containing LucNeo#2 cells [52]. In contrast, evaluation of the antiviral effect of different IFN-λ_1 concentrations in the present study showed that treatment with >100 pg/mL IFN-λ_1 significantly decreased luciferase activity in HCV replicon cells (Figure 14). These results suggest that the concentration of IFN-λ_1 required for exerting antiviral effect against HCV is lower than that of IFN-γ. Serum HCV RNA levels in mice injected with the IFN-λ_1-expressing plasmid were dependent on serum IFN-λ_1 concentrations, which were moderately different among them (Figure 18C), suggesting that the antiviral effect of IFN-λ_1 on NS3- and NS5A-mutated HCVs depended on its serum concentration. Serum IFN-λ_1 concentration of approximately >100

pg/mL significantly decreased HCV RNA level, suggesting that serum IFN-λ_1 concentration of at least 100 pg/mL exerts an antiviral effect against NS3- and NS5A-mutated HCVs.

In addition, previous studies [62,43] reported that the sensitivity of IFN therapy to HCV RASs was higher than that of HCV wild type. Besides, the previous reports [63,64] showed that there is little difference in therapeutic effect of IFNs except for IFN-α between HCV genotypes. Therefore, I proposed that IFN-based therapy as an optional regimen is considerable potential for treating DAA failure patients although further research on evaluation of antiviral effect of IFNs against different DAA-resistant HCV genotypes should be performed in the future.

It is important to evaluate adverse effects. Serum ALT activity transiently increased after 3 days of injecting the different plasmids, which may be because of the hydrodynamic injection of the plasmids [65]. ALT level in chimeric mice injected with the IFN-expressing plasmids increased from day 3 onward and recovered to its baseline level, suggesting that IFN-γ- and IFN-λ_1-induced hepatic disorder was tolerable. Results of histological analysis performed on day 42 also showed no apparent damage in the livers of chimeric mice injected with the plasmids.

IFN administration is associated with side effects such as influenza-like symptoms, neuropsychiatric symptoms, and cytopenia [1]. Because types I and II IFN receptors are universally expressed in the human body, types I and II IFNs bind to and affect almost all cell types throughout the body. Therefore, treatment with types I and II IFNs is often discontinued because of systemic side effects. In contrast, distribution of type III IFN receptors, e.g., IFN-λ receptor, is limited to some cell types, including hepatocytes [66,67]. A previous clinical study assessing IFN therapy for HCV infection showed that the rate of IFN-λ-associated adverse effects was lower than that of IFN-α-associated adverse effects [68]. Therefore, use of IFN-λ_1 may be more desirable than that of IFN-γ for treating NS3- and NS5A-mutated HCV infection from the viewpoint of systemic side effects. In this study, I chose hydrodynamic gene transfer of long-term expression plasmid vector encoding IFN-λ_1 for continuous supply of IFN-λ_1 protein as a tool. For the clinical application, I think that the use of pegylated-IFN-λ_1 rather than IFN-λ_1 gene transfer is more desirable due to ease in administration.

II-5 Conclusion

Results of the present study indicate that IFN-γ and IFN-λ_1 exert antiviral effect against NS3- and NS5A-mutated HCVs. Clinically, my results suggest that IFN-λ_1 is preferable for treating infection caused by NS3- and NS5A-mutated HCVs.

Chapter III

Development of safe and effective interferon-beta gene therapy by using long-term expression vector and regulating biological activity for the treatment of patients with multiple sclerosis

III Introduction

MS is one of the refractory diseases and the most common demyelinating disease. In MS patients, the symptoms of MS frequently repeat and sequentially progress from relapse-remitting MS to secondary progressive MS. To reduce the relapse of MS and prevent MS progression, IFN-β therapy has been utilized for a long time. However, in the clinical use of IFN-β, repeated administration of IFN-β is required due to the short half-life of IFN-β in the body and side effects associated with IFN-β cause treatment interruption.

In order to verify the therapeutic effect of drugs on MS, an animal model of MS was developed in 1925 [69,70]. Experimental autoimmune encephalomyelitis (EAE) mice were established as an animal model of MS and frequently used to evaluate the therapeutic effect of candidate compound.

In Chapter III, I aimed to optimize IFN-β gene therapy strategy including continuous supply of IFN-β and improvement of side effects associated with IFN-β. Initially, in Section 1, the severity of EAE symptoms after single administration of long-term expression vector of IFN-β constructed in Chapter I into EAE mice was investigated. Next, in Section 2, I designed novel IFN-β fusion proteins to optimize biological activity of IFN-β, which was expected to be effective in improving the therapeutic effects and reducing side effects.

Chapter III

Section 1

Amelioration of experimental autoimmune encephalomyelitis in mice by interferon-beta gene therapy, using a long-term expression plasmid vector

III-1-1 Introduction

MS is the most common demyelinating disease in humans; it is characterized by spatial and temporal occurrences of inflammation and demyelination in the central nervous system (CNS). During disease progression, blood-brain barrier (BBB) function is impaired by matrix metalloproteinases (MMPs) secreted from immune cells [71], and immune cells enter into the brain parenchyma through the disrupted BBB [72]. Extended infiltration of T and B lymphocytes and macrophages into the brain parenchyma results in an immunological attack on myelin and leads to the formation of plaques of demyelination. Infiltrating T cells also induce inflammation by secreting inflammatory cytokines such as IFN-γ [73].

Patients with MS frequently experience relapse of symptoms associated with inflammation and demyelination in the CNS. When the pathology progresses, patients with MS receive steroidal anti-inflammatory medications to suppress inflammation in the CNS. In addition to reducing the severity of relapse symptoms, reducing relapse frequency is also important in the treatment of relapsing-remitting MS. IFN-β has been used as the first-line treatment. In addition, glatiramer acetate, fingolimod hydrochloride, and other medications are relatively newly approved treatments for preventing relapse of MS [74]. For instance, daily oral administration of fingolimod hydrochloride showed higher therapeutic effect than IFN-β in a clinical trial [75]. However, IFN-β is still one of important treatments of relapsing-remitting MS. In case of treatment using IFN-β, patients with MS must receive repeated injections of IFN-β protein owing to the short half-life of IFN-β, and the repetitive nature of these injections lowers the quality of life of patients with MS [2].

Gene therapy is an attractive approach for sustained supply of therapeutic proteins without requiring repetitive administration. Several studies report that IFN-β gene therapy is effective in reducing the severity of EAE, an animal model of MS [76,77]. However, it was difficult to achieve sustained IFN-β transgene expression because of the suppressing effect that the IFN-β protein itself has on transgene expression [17]. In Chapter I, I developed pMx-IFN-β, a novel plasmid DNA vector for long-term expression of IFN-β that uses the IFN-responsive Mx promoter [53]. It was shown that continuous supply of IFN-β for 1 month was achieved by using pMx-IFN-β.

In this study, I evaluated the potential effects of sustained IFN-β expression from pMx-IFN-β on MS by testing this technique in EAE mice. EAE animals are widely used as models of MS and are easily prepared by

injection of immunologic adjuvants containing CNS-derived proteins and/or peptides [69]. I assessed the therapeutic effect of a single injection of pMx-IFN-β on EAE mice by evaluation of EAE symptoms and BBB function, determination of serum cytokine concentration, and observation of CNS tissue histology.

III-1-2 Materials and Methods

Mice

C57BL/6J mice (female, 10–11-week-old, 20 ± 2 g) were purchased from Japan SLC Inc.. Mice were maintained as aforementioned in Chapter I. All protocols for animal experiments were approved by the Animal Experimentation Committee of the Graduate School of Pharmaceutical Science, Kyoto University.

EAE induction and clinical scores

Myelin oligodendrocyte glycoprotein peptide 35-55 (MOG_{35-55}, MEVGWYRSPFSRVVHLYRNGK) was synthesized by GenScript. EAE induction was performed according to the method reported by Stromnes et al [69]. Briefly, 1 week after emplacement of mice, each mouse received one subcutaneous injection of MOG_{35-55} [dissolved in phosphate-buffered saline (PBS) at a concentration of 2 mg/mL] mixed with an equal volume of incomplete Freund's Adjuvant (IFA; Becton, Dickinson & Co., Franklin Lakes, NJ, USA) containing 5 mg/mL of *Mycobacterium tuberculosis* strain H37Ra (Becton, Dickinson & Co.) at a dose of 200 μL/mouse on day 0. Pertussis Toxin (PT; List Biological Laboratories Inc., Campbell, CA, USA) was intraperitoneally administered at a dose of 200 ng/mouse on days 0 and 2. Immunized mice were clinically scored as follows. 0: no clinical symptoms; 0.5: partial limp tail; 1: limp tail; 2: partial hind leg paralysis; 3: complete hind leg paralysis; 4: complete hind leg paralysis and partial front leg paralysis; 5: moribund.

Plasmid DNA and gene transfer

pMx-IFN-β (encoding mouse IFN-β), pMx-fLuc (encoding fLuc), and pMx-gLuc (encoding gLuc) were constructed as described in Chapter I. On day 7 after EAE induction, EAE mice were given plasmid DNA by using hydrodynamic delivery procedure as described in Chapter I. In brief, 1 μg of plasmid DNA were dissolved in saline with the volume of 0.1 mL/g body weight of the receiving mouse. The injection solution containing plasmid DNA was injected into tail vein of mice within 5 seconds.

Quantification of mRNA

Total mRNA extraction from the portion of organs, reverse transcription, and real time PCR was conducted by the procedure described in Chapter I. The sequences of the primers used for amplification were as follows: β-actin forward, 5'-CATCCGTAAAGACCTCTATGCCAAC-3'; reverse, 5'-ATGGAGCCACCGATCCACA-3'; fLuc forward, 5'-GCTGGGCGTTAATCAGAGAG -3'; reverse, 5'-GTGTTCGTCTTCGTCCCAGT-3'. The

mRNA level of fLuc normalized by the mRNA level of β-actin in the pMx-fLuc-administered EAE mice was calculated by using that in the pMx-fLuc-administered normal mice.

Luciferase assay

The EAE mice received pMx-fLuc by hydrodynamic injection on day 7 post immunization. The liver and brain were isolated from the EAE mice on day 1 after gene transfer of pMx-fLuc. Organ samples were homogenized in lysis buffer [0.1 M Tris (pH 7.8), 0.05 % Triton X-100, 2 mM EDTA], and the homogenates were centrifuged at 12,000 × *g* for 10 min at 4 °C. Luciferase activity was measured by the procedure described in Chapter I.

Analysis of BBB function

Evans Blue (EB; Sigma-Aldrich, St. Louis, MO, USA) dissolved in saline (4 % wt/v) was intravenously injected into the EAE mice at a dose of 2 mL/kg on day 14 after immunization. Mice were anesthetized with pentobarbital 3 h after EB administration and euthanized by cutting the inferior vena cava. Immediately after euthanasia, a transcardial perfusion of PBS was performed. The brain and spinal cord were collected and their wet weight was measured. The organ samples were minced in *N*,*N*-dimethylformamide (Wako Pure Chemical Industries). After 24 h of incubation at room temperature, the organ samples were centrifuged at 15,000 × *g* for 30 min at 20 °C. The absorbance of the supernatants at 620 nm was measured using a Multiskan FC Microplate Photometer (Thermo Fisher Scientific).

Measurement of IFN concentration in serum

At the indicated time points after immunization, the serum samples collected from the EAE mice were stored at −80 °C until analysis as aforementioned in Chapter I. The serum IFN concentrations in the samples were measured by ELISA. IFN-β concentration in serum was determined as described in Chapter I [16,17], and IFN-γ concentration in serum was determined using an IFN-γ ELISA kit (Ready-SET-GO! Murine IFN-γ ELISA; eBioscience).

Histological analysis

The EAE mice were anesthetized by intraperitoneal injection of pentobarbital on day 35 after immunization and euthanized by cutting the inferior vena cava. Immediately after euthanasia, a transcardial perfusion of 4% PFA solution was performed. Spinal cords were collected and fixed in 4% PFA solution for 24 h. The fixed organ samples were embedded in paraffin (Paraplast, McCormick Scientific, St. Louis, MO, USA) and sliced into 3 μm thick sections. The sections of spinal cord were stained with HE and Luxol Fast Blue (LFB) to assess cellular infiltration and demyelination, respectively.

Data analysis

Quantitative differences between data sets were statistically analyzed by either the Student's *t*-test for paired comparison or one-way ANOVA, followed by Fisher's Protected Least Significant Difference (PLSD) test for multiple comparisons. *P*-values < 0.05 were interpreted as representing statistical significance.

III-1-3 Results

III-1-3-a. Gene expression was observed in the liver but not in the brain after hydrodynamic injection into EAE mice

As transgene expression could occur in the brain of the EAE mice after gene transfer because of BBB disruption, this possibility was examined by using plasmid DNA expressing fLuc, a reporter protein. No mRNA of fLuc was detected in the brain samples of all mice (Figure 22A). In addition, fLuc activity was not detected in brain samples of both the normal and EAE mice (Figure 22B). In contrast, the fLuc mRNA and fLuc activity in the liver, a major transgene-expressing organ after hydrodynamic gene transfer, was detected in both the normal and EAE mice.

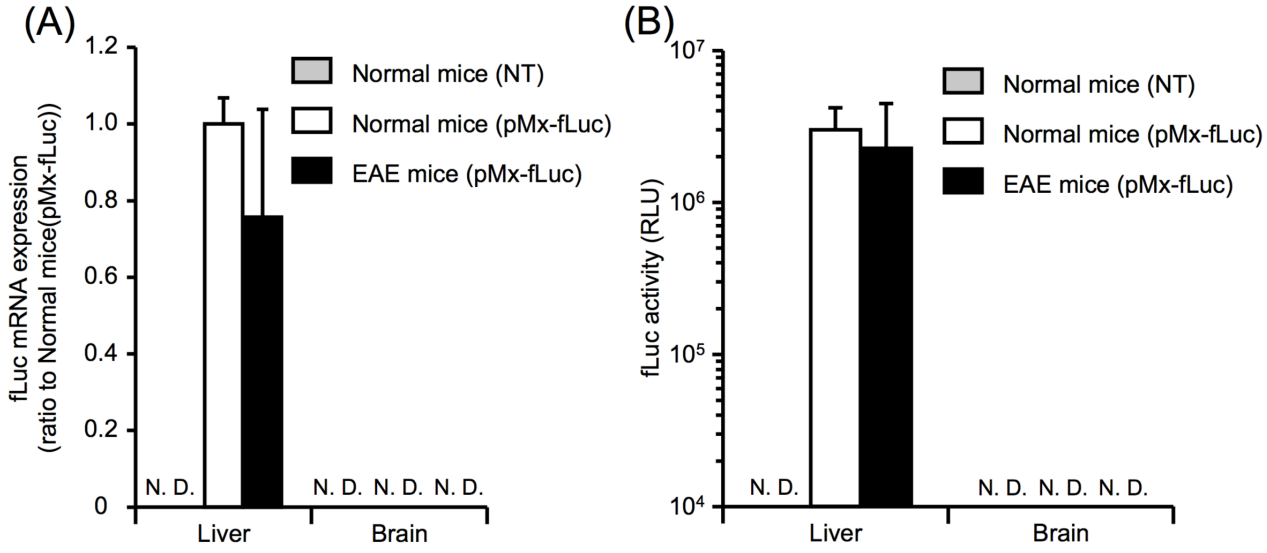

Figure 22. fLuc mRNA expression and fLuc activity in liver or brain after hydrodynamic injection of pMx-fLuc. Normal mice and EAE mice received administration of 1 μg pMx-fLuc at day 7 after EAE induction. One day after the gene transfer, (A) fLuc mRNA and (B) fLuc activity in collected liver and brain was detected by real-time RT-PCR and luciferase assay, respectively. The results are expressed as mean ± SEM of at least four mice. N.D.: Not detectable.

III-1-3-b. Gene transfer of pMx-IFN-β reduced the severity of EAE

The EAE mice received a single administration of plasmid DNA by hydrodynamic injection on day 7 after the initial immunization with MOG_{35-55}. pMx-gLuc, a plasmid vector encoding the reporter protein gLuc, was used as control vector. Concentration of serum IFN-β on day 1 after gene transfer of pMx-IFN-β (which was also day 8 after immunization) into the EAE mice was approximately 300 pg/mL (Figure 23A). IFN-β concentration in serum gradually decreased and was sustained at detectable levels for 1 month after the gene transfer. During this period, body weight was monitored as an index of side effects. No significant differences were observed in the body weights of the naïve and pMx-IFN-β mice (data not shown).

The onset day of EAE symptom, which was determined when the clinical score exceeded 1, was 15.3 ± 1.1, 12.6 ± 2.9, and 12.6 ± 4.3 days for the "no treatment", the pMx-gLuc-treated, and the pMx-IFN-β-treated groups, respectively (Figure 23B). By contrast, the clinical score of the pMx-IFN-β-treated group was significantly lower than that of the "no treatment" group on day 17 and at all subsequent time points. Moreover, the maximum scores of all the groups were used for comparison with the severity of EAE symptoms (Figure 23C). The maximum score was 2.63 ± 0.40, 3.14 ± 0.73, and 1.06 ± 0.45 for the "no treatment", the pMx-gLuc-treated, and the pMx-IFN-β-treated groups, respectively. The maximum score of the pMx-IFN-β-treated group was also significantly lower than that of the "no treatment" group.

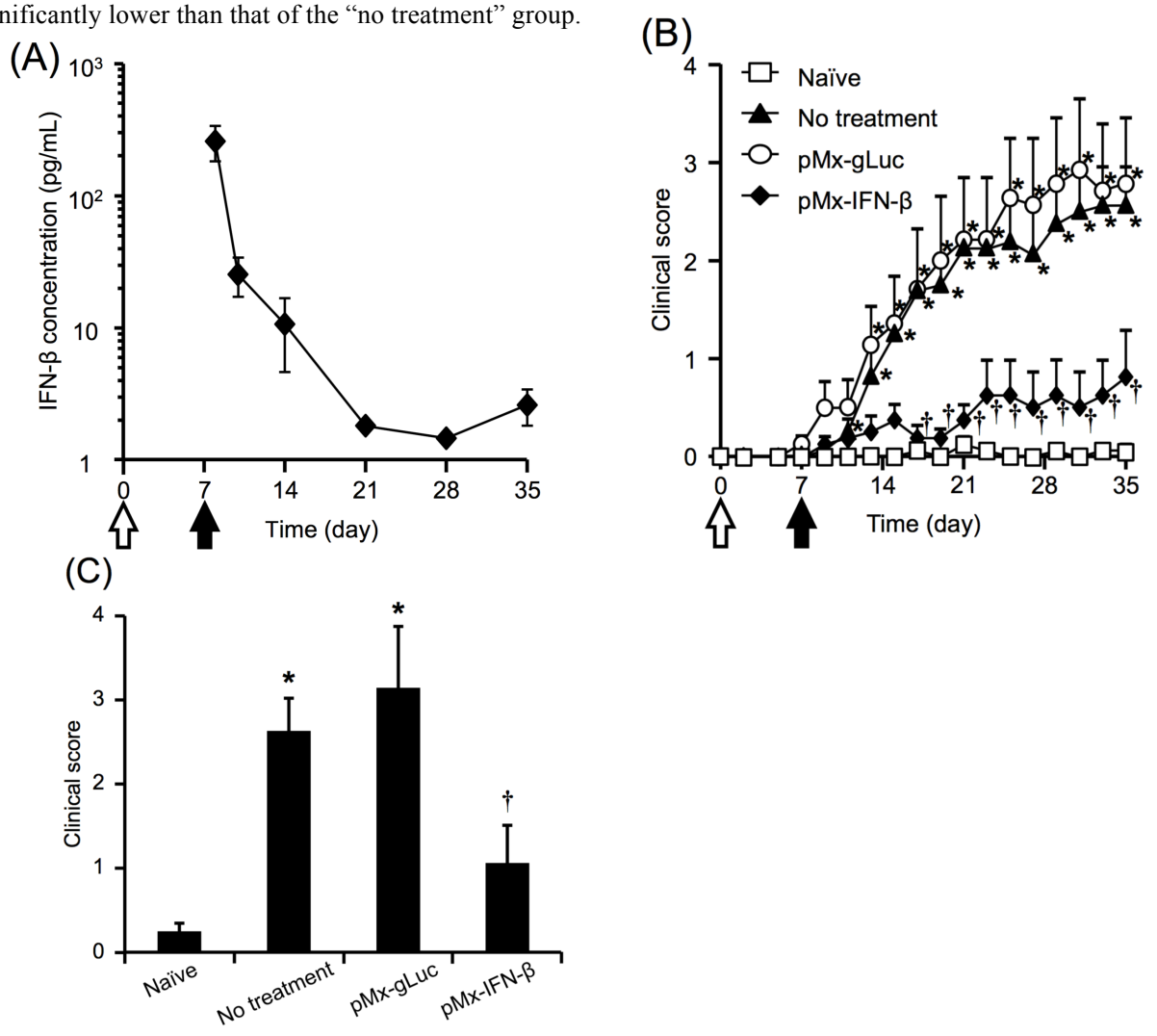

Figure 23. The severity of EAE after gene transfer into EAE mice. (A) Time course of the serum concentration of IFN-β after gene transfer of pMx-IFN-β into EAE mice. The concentration of IFN-β in serum samples was analyzed by ELISA. (B) The time course of clinical score of EAE after immunization. At day 7 after immunization, EAE mice in the pMx-gLuc group and the pMx-IFN-β group received pMx-gLuc and pMx-IFN-β at a dose of 1 μg/mouse, respectively. (C) The maximum score for all EAE mice in the Naïve group, the No treatment, the pMx-gLuc-treated group, and the pMx-IFN-β-treated group. The time points of EAE induction and gene transfer were indicated by white and black arrows, respectively. The results are expressed as mean ± SEM of eight mice. *p < 0.05 and †p < 0.05 compared with the Naïve group and the No treatment group, respectively.

III-1-3-c. Gene transfer of pMx-IFN-β suppressed a rise in serum IFN-γ concentration in EAE mice

Concentration of serum IFN-γ, a representative type 1 helper T cell (T_h1) cytokine, was determined by ELISA (Figure 24) as an indicator of activated T_h1 cells. Serum IFN-γ concentrations in the "no treatment" and pMx-gLuc groups were over 100 pg/mL. By comparison, serum IFN-γ concentrations in the pMx-IFN-β-treated mice were significantly lower than those in the "no treatment" mice.

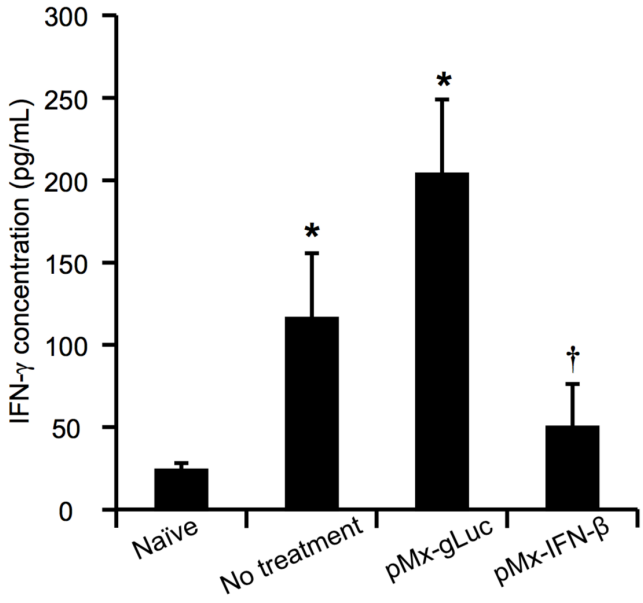

Figure 24. Serum concentration of IFN-γ at day 14 after EAE induction. Gene transfer was performed at day 7 after EAE induction and serum IFN-γ concentration was determined by ELISA at day 14 after EAE induction. The results are expressed as mean ± SEM of three mice. *p < 0.05 and †p < 0.05 compared with the Naïve group and the No treatment group, respectively.

III-1-3-d. Administration of pMx-IFN-β attenuated EB leakage into CNS of EAE mice

To examine the degree of BBB disruption, EAE mice received an intravenous injection of EB solution. Blue color was observed in the brains and spinal cords of all EAE mice in both the "no treatment" and pMx-gLuc-treated groups, which indicate that leakage of EB into the CNS occurred in these groups (Figure 25A). By comparison, blue color was hardly observed in the brains and spinal cords of the pMx-IFN-β-treated mice. EB was then extracted from the collected samples to measure EB amount in these tissues. EB amounts in samples of both the "no treatment" and pMx-gLuc-treated groups were significantly higher than those in the naïve group (Figure 25B). The amounts of EB were higher in spinal cord samples than in brain samples. In contrast, the

amounts of EB in brain samples and spinal cord samples of pMx-IFN-β-treated mice were significantly lower than those of the "no treatment" group, and were comparable with those of the naïve mice.

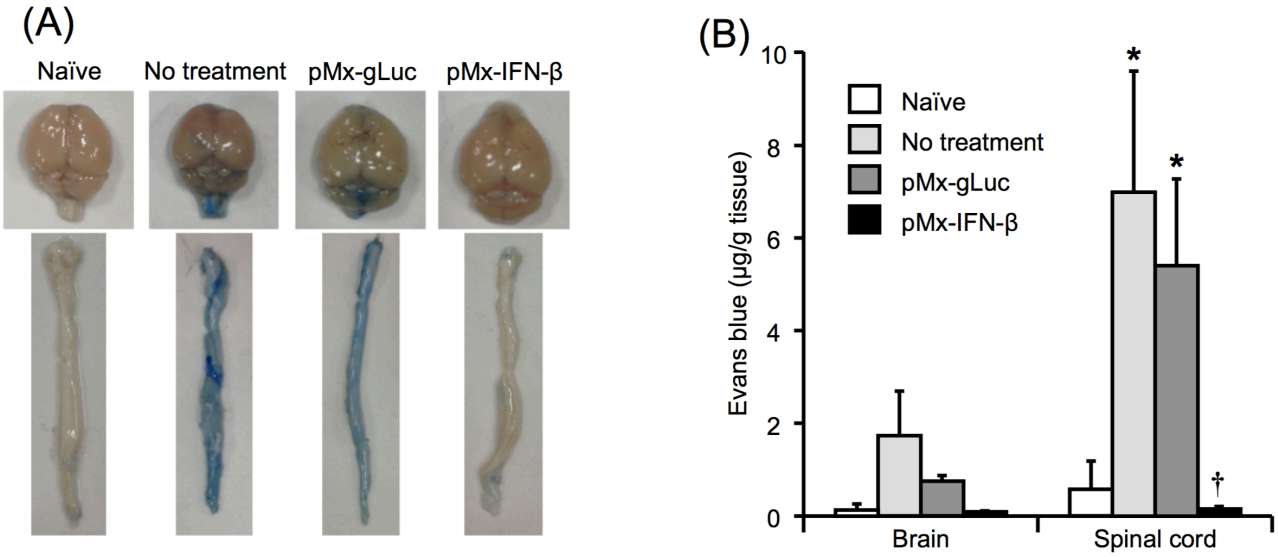

Figure 25. The effect of gene transfer on BBB permeability in EAE mice. pMx-gLuc and pMx-IFN-β was injected into EAE mice at day 7 after immunization. At day 14 after immunization, mice received intravenous EB injection and the brain and the spinal cord of EAE mice were collected at 3 h after EB injection. (A) Representative images of brain and spinal cord of mice in each group. Blue color indicates leakage of EB into brain and spinal cord through BBB. (B) Amount of EB in brain and spinal cord of mice in each group. The results are expressed as mean ± SEM of at least three samples. *$p < 0.05$ and †$p < 0.05$ compared with the Naïve group and the No treatment group, respectively.

III-1-3-e. Gene transfer of pMx-IFN-β suppressed infiltration of inflammatory cells and tissue damage in the spinal cords of EAE mice

Sections of spinal cords were subjected to HE and LFB staining to evaluate inflammatory infiltrates and tissue damage (Figure 26). The results of HE and LFB staining show that infiltration of inflammatory cells occurred in the spinal cords of mice in both the "no treatment" and pMx-gLuc-treated groups. By comparison, infiltration of cells was hardly observed in the spinal cords of mice in the pMx-IFN-β-treated group.

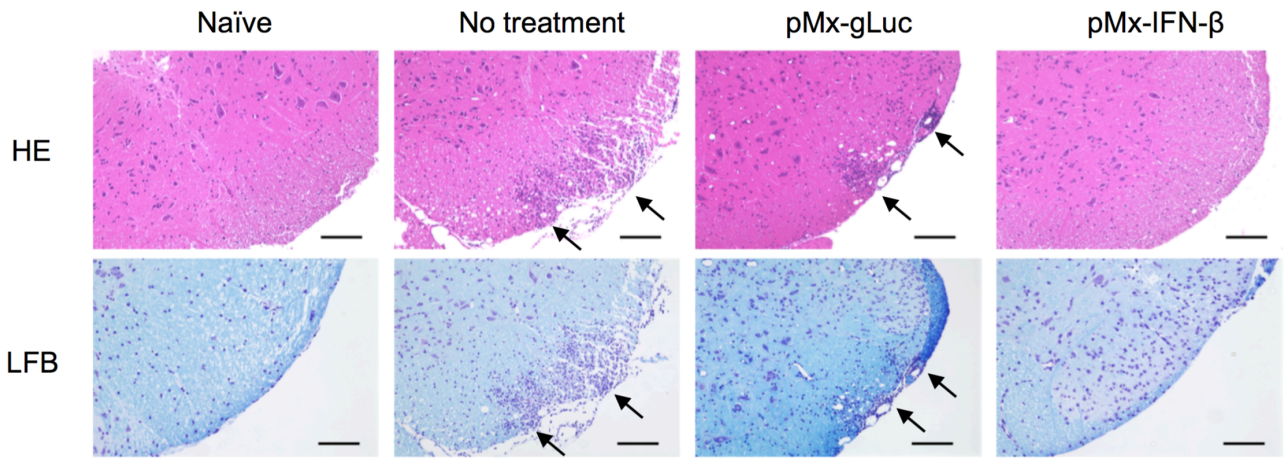

Figure 26. Histological analysis of the spinal cord of EAE mice. At day 35 after immunization, the spinal cord was collected from Naïve mice or EAE mice of No treatment group, pMx-gLuc-treated group, or pMx-IFN-β-treated group. HE (upper panel) and LFB (bottom panel) staining were performed to evaluate the infiltrated cells and demyelination, respectively. Arrows indicated the areas with the infiltrated cells. Scale bar = 100 μm

III-1-4 Discussion

Several studies have reported that repeated administration of IFN-β protein is required to achieve therapeutic effects in EAE animals [76,78]. In the present study, therapeutic effects in EAE mice were achieved via one-time administration of the pMx-IFN-β plasmid. This indicates that single administration of a long-term expression vector of IFN-β is more useful than repeated injections of IFN-β protein.

In this study, pMx-IFN-β was administered by hydrodynamic injection into EAE mice to examine the long-term therapeutic effects of IFN-β gene therapy. Although it is well-known that the liver is a major transgene-expressing organ following hydrodynamic injection of naked plasmid DNA, other organs also expresses transgenes at a low level after the injection [79]. Therefore, there was a possibility that the brains of EAE mice were transfected with plasmid DNA after the hydrodynamic injection, because the BBB is disrupted in EAE mice. Figure 22A and 22B indicates that the therapeutic effects obtained by IFN-β gene transfer into EAE mice were not caused by IFN-β expressed in the brain, but by IFN-β expressed in the liver.

It has been reported that pathogenic T cells invade from blood to parenchyma through a disrupted BBB, especially at the fifth lumbar region of the spinal cord in EAE mice [72]. In addition, it has been reported that MMP-9 secreted from pathogenic T cells impairs the BBB in EAE model mice [71]. By contrast, it has been reported that IFN-β suppresses pathogenic T cells such as IFN-γ-producing T_h1 cells [80]. The fact that serum IFN-γ concentrations in the pMx-IFN-β-treated group were significantly lower than those in the "no treatment" group indicates that gene transfer of pMx-IFN-β into these EAE mice suppressed their pathogenic T cells. Axtell et al. reported that IFN-β mainly suppressed the function of T_h1 cells and improved the symptoms of EAE mice [81,82]. Therefore, it can be hypothesized that IFN-β protein expressed after the gene transfer of pMx-IFN-β into EAE mice could improve the clinical score of EAE mice by the suppression of pathogenic T_h1 cells. Regarding

the question of what causes the prevention of BBB disruption in EAE mice when they receive IFN-β gene transfer, the suppressive effect of IFN-β on T_h1 cells (which secrete MMP-9) may be the answer. Moreover, if pMx-IFN-β gene transfer prevents BBB disruption, this might also reduce the severity of inflammatory cell invasion into the spinal cord (Figure 26). It has been reported that BBB function recovered approximately 1 month later after EAE induction without any therapeutic treatment [83]. I also confirmed that BBB function recovered at 35 days after EAE induction even in the "no treatment" group (data not shown). However, it is important to suppress BBB disruption in the acute phase of EAE by using IFN-β to prevent the infiltration of inflammatory cells.

Although serum IFN-β concentrations were detected 1 month after gene transfer of pMx-IFN-β (Figure 23), expression levels of IFN-β in EAE mice were lower than what was seen in normal mice, which was examined in Chapter I [53]. It has been reported that proinflammatory cytokines are produced in EAE mice after immunization [84], and among the proinflammatory cytokines, IFN-γ and TNF-α, inhibit transgene expression [85]. Therefore, low levels of IFN-β expression after gene transfer of pMx-IFN-β into EAE mice could be due to the suppression of transgene expression by proinflammatory cytokines. In general, IFN-β was utilized in the remission phase for preventing the relapse of MS symptoms. In Chapter I, I showed that transgene expression of IFN-β after gene transfer of pMx-IFN-β into normal mice, which could be assumed as mice in the remission phase of MS, was sustained and serum IFN-β concentration was maintained at approximately 100 pg/mL at least for 1 month [53]. Therefore, if gene transfer of pMx-IFN-β was performed before EAE induction, the onset of EAE could be prevented. Considering the long-term therapeutic effects achieved with IFN-β gene therapy, pMx-IFN-β is still a desirable vector for sustained supply of IFN-β to prevent relapse of MS symptoms.

III-1-5 Conclusion

Gene transfer of pMx-IFN-β, accomplished via a single low-dose injection, enabled long-term expression of IFN-β in EAE mice and effectively reduced the severity of their EAE symptoms for a period of 1 month. In conclusion, IFN-β gene therapy using the pMx-IFN-β plasmid vector is a promising method for long-term symptom prevention therapy for patients with MS.

Chapter III

Section 2

Safe and effective interferon-beta gene therapy for multiple sclerosis by designing interferon-beta-galectin-9 fusion proteins

III-2-1 Introduction

As described in Chapter III Section 1, MS is one of the orphan diseases and the most common demyelinating disease. In patients with MS, spatial and temporal demyelination and inflammation occur in the CNS. A previous report has suggested that autoimmune responses, infection, and environmental factors were related to the onset of MS [86]. In particular, an earlier study has demonstrated that autoimmune neuronal damage plays an important role in the onset of MS [87]. Moreover, it was shown that demyelination and inflammation in the CNS were associated with activated $CD4^+$ T cells. Sequentially, it was revealed that the production of inflammatory cytokines such as IFN-γ from differentiated T_h1 cells evokes demyelination and axonopathy [80,89]. On the other hand, T cell immunoglobulins and mucin domain-3 (Tim-3) are specifically expressed on the surface of T_h1 cells and are related to immune regulation [89]. Moreover, galectin-9 (gal-9) was identified as the ligand of Tim-3, and the binding of gal-9 to Tim-3 results in the suppression of T_h1 cellular functions [90,91]. Therefore, it has been proposed that gal-9 may relate to the onset and the progression of MS, and may be applicable to MS therapy [92,93].

In Chapter III Section 1, it was demonstrated that IFN-β gene therapy, by using a long-term expression plasmid vector containing IFN-β, effectively ameliorated disease symptoms in EAE mice [94]. However, concerns exist regarding the side effects of IFN-β. Therefore, in this section, I designed novel IFN-β-gal-9 fusion proteins to improve the therapeutic effects and reduce side effects, by two hypothetical mechanisms: 1) IFN-β-gal-9 fusion proteins might exert improved therapeutic effects through an additive suppressive effect of both IFN-β and gal-9, through the fusion protein on T_h1 cells; 2) a fusion of gal-9 and IFN-β might reduce the side effects of IFN-β by reducing the bioactivity of IFN-β on non-target cells. Since IFN-β was fused to gal-9, I expected that IFN-β was unlikely to work on non-target cells, compared to target T cells expressing Tim-3. In the present study, I designed IFN-β-gal-9 fusion proteins, containing a linker of different lengths, and evaluated the effects of these IFN-β-gal-9 fusion proteins in EAE mice.

III-2-2 Materials and Methods

Plasmid DNA

pMx-IFN-β, pMx-fLuc, and pMx-gLuc encoding the mouse IFN-β, fLuc, and gLuc, respectively, were constructed as described in Chapter I. The insert containing the mouse gal-9 cDNA was amplified from mouse

genomic DNA by PCR using the following primers: IFN-β-gal-9 forward primer (Fw): 5′-CCCCTTAAGGCTCTCTTCAGTGCCCAGTC-3′ and IFN-β-gal-9 reverse primer (Rv): 5′-CTAGCTAGCCTATGTCTGCACGTGGGTCATGACCCACGTGCAGACATAGGCTAGCTAG-3′, IFN-β-$(GS)_1$-gal-9 Fw: 5′-CCCCTTAAGGGCGGCGGCGGCTCCGCTCTCTTCAGTGCCCAGTC-3′ and IFN-β-$(GS)_1$-gal-9 Rv: 5′-CTAGCTAGCCTATGTCTGCACGTGGGTCATGACCCACGTGCAGACATAGGCTAGCTAG-3′, IFN-β-$(GS)_2$-gal-9 Fw: 5′-CCCCTTAAGGGCGGCGGCGGCTCCGGCGGCGGCGGCTCCGCTCTCTTCAGTGCCCAGTC-3′ and IFN-β-$(GS)_2$-gal-9 Rv: 5′-CTAGCTAGCCTATGTCTGCACGTGGGTCATGACCCACGTGCAGACATAGGCTAGCTAG-3′, IFN-β-$(GS)_3$-gal-9 Fw: 5′-CCCCTTAAGGGCGGCGGCGGCTCCGGCGGCGGCGGCTCCGGCGGCGGCGGCTCCGCTCTCTTCAG TGCCCAGTC-3′ and IFN-β-$(GS)_3$-gal-9 Rv: 5′-CTAGCTAGCCTATGTCTGCACGTGGGTCATGACCCACGTGCAGACATAGGCTAGCTAG-3′. The gal-9 cDNA, digested using AflII/NheI, was inserted into the AflII/NheI site of pMx-IFN-β to construct pMx-IFN-β-gal-9, pMx-IFN-β-$(GS)_1$-gal-9, pMx-IFN-β-$(GS)_2$-gal-9, and pMx-IFN-β-$(GS)_3$-gal-9 (Figure 27). The phRL-TK vector, encoding Renilla luciferase (rLuc), was purchased from Promega.

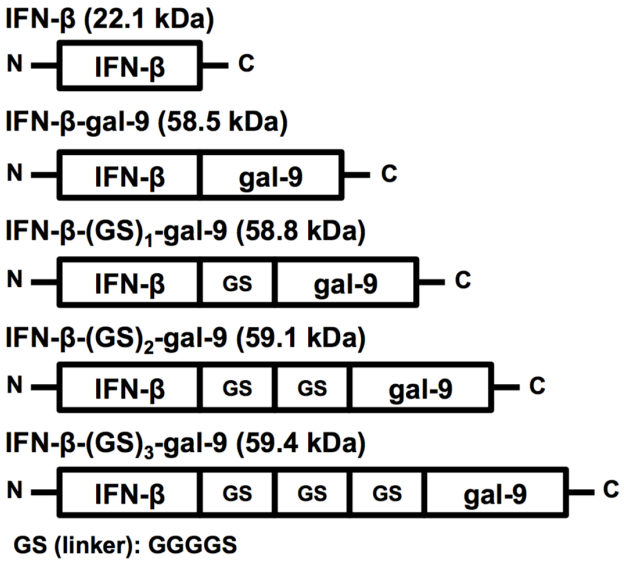

Figure 27. Schematic representation of the IFN-β and IFN-β-gal-9 fusion proteins.

Isolation of the IFN-β and IFN-β-gal-9 fusion proteins

B16-BL6 cells were cultured as aforementioned in Chapter I. B16-BL6 cells were seeded into 12-well culture plates at a density of 1×10^5 cells/well one day before transfection. To isolate the IFN-β, IFN-β-gal-9, IFN-β-$(GS)_1$-gal-9, IFN-β-$(GS)_2$-gal-9, and IFN-β-$(GS)_3$-gal-9 proteins, B16-BL6 cells were transfected with 0.5 μg/mL of pMx-IFN-β, pMx-IFN-β-gal-9, pMx-IFN-β-$(GS)_1$-gal-9, pMx-IFN-β-$(GS)_2$-gal-9, and pMx-IFN-β-$(GS)_3$-gal-9 plasmids, respectively, by using LA as described in Chapter I. On 1 day after transfection,

the culture media containing the corresponding IFN-β and IFN-β-gal-9 fusion proteins were collected and stored at −80 °C until use.

Measurement of IFN concentration

Culture media and the serum samples were collected at the indicated time points as described in Chapter I. The samples were stored at −80 °C until analysis. The IFN concentrations in the samples were measured using the ELISA method as described in Chapter III, Section 1.

Western blotting

The IFN-β, IFN-β-gal-9, IFN-β-$(GS)_1$-gal-9, IFN-β-$(GS)_2$-gal-9, and IFN-β-$(GS)_3$-gal-9 proteins were reduced using 1 M dithiothreitol and heated at 95 °C for 3 min. Reduced samples were subjected to electrophoresis on a 10% sodium dodecyl sulfate polyacrylamide gel and transferred to a polyvinylidene fluoride transfer membrane. The membrane was blocked with Blocking One solution (Nacalai Tesque) for 30 min. Next, the membrane was probed with rat anti-mouse IFN-β monoclonal antibody (1:1000; Abcam Cambridge, MA, USA), followed by goat anti-rat IgG polyclonal antibody conjugated with horseradish peroxidase (1:10000; R&D System, Minneapolis, MN, USA). The membrane was soaked with Immobilon Western Chemiluminescent HRP Substrate (Merck Millipore, Billerica, MA, USA), and chemiluminescence was detected using a LAS3000 instrument (Fujifilm, Tokyo, Japan).

Evaluation of IFN-β bioactivity for IFN-β-gal-9 fusion proteins

B16-BL6 cells were co-transfected with 0.05 μg/mL pMx-fLuc and 0.5 μg/mL phRL-TK using 1.65 μg/mL LA. After 4-h incubation, cells were seeded at 2×10^4 cells/well in 48-well culture plates. After the overnight incubation, the culture medium was replaced with Opti-MEM (Thermo Fisher Scientific), containing various concentrations of IFN-β or IFN-β-gal-9 fusion proteins and incubated overnight. Next, cell lysates were prepared using the lysis buffer supplied in a luciferase assay kit (Piccagene Dual). The cell lysate was mixed with the luciferase assay kit (Piccagene Dual), and chemiluminescence was measured using a luminometer (Lumat LB9507; EG and G Berthold). The fold induction was calculated using the ratio of the fLuc activity in IFN-β and IFN-β-gal-9 fusion protein treated-samples, normalized to the rLuc activity in untreated samples.

Establishment of EAE mice

C57BL/6J mice (female, 10–11-week-old, 20 ± 2 g) were purchased from Japan SLC Inc. and bred for 1 week at the same condition as described in Chapter I. Next, EAE induction was performed as described in Chapter III Section 1. Following the EAE induction, immunized mice were clinically scored as described in Chapter III Section 1. All protocols for animal experiments were approved by the Animal Experimentation Committee of the Graduate School of Pharmaceutical Science, Kyoto University.

Evaluation of the activity of re-stimulated T cells in the spleen

The spleen was harvested from EAE mice at 10 days after EAE induction, as previously described [69]. Then, splenocytes were isolated from the spleen and cultured in Roswell Park Memorial Institute 1640 medium (Nissui Pharmaceutical), supplemented with 10% FBS, PSG, and monothioglycerol at 37 ºC and 5% CO_2. After a 2 h incubation, the cells in supernatant were collected and seeded at 5×10^5 cells/well in 96-well culture plates. Immediately after splenocytes seeding, MOG_{35-55} at a concentration of 10 μg/mL, and a serial concentration of IFN-β or IFN-β-gal-9 fusion proteins was added to each well. In addition, an IFNAR antibody (1:600; Leinco Technologies Inc, St Louis, MO, USA) was added to the culture media for the inhibition of IFN-β bioactivity. After a 3-day incubation, the concentration of IFN-γ in the conditioned media was determined by ELISA and cell proliferation was evaluated by the WST-8 assay as described in Chapter I.

Gene transfer into EAE mice

Seven days after EAE induction, EAE mice received a 5-s injection into the tail vein with 1 μg of plasmid DNA dissolved in saline by the hydrodynamic delivery procedure as described in Chapter I.

White blood cell count

The blood samples obtained from EAE mice after gene transfer were treated with a 5% EDTA solution to inhibit coagulation. The white blood cells (WBC) from the blood samples were stained using Turk's solution (Nacalai Tesque) and counted under the microscope using a hemocytometer.

CNS analysis

BBB function was analyzed by intravenously injecting EB (Sigma-Aldrich) at 14 days after the induction of EAE, as described in Chapter III Section 1. Moreover, HE and LFB staining of the spinal cord sections isolated from EAE mice was performed at 35 days after EAE induction, as described in Chapter III Section 1.

Data analysis

Quantitative differences between data sets were statistically analyzed, using either the Student's *t*-test for paired comparisons, or a one-way ANOVA, followed by Fisher's PLSD test for multiple comparisons. *P*-values < 0.05 were interpreted as statistically significant.

III-2-3 Results

III-2-3-a. The biological activity of the IFN-β-gal-9 fusion proteins was significantly lower than that of IFN-β

Western blotting was performed to confirm the molecular weight of IFN-β and of the IFN-β-gal-9 fusion proteins (Figure 28A). Lane #1 shows a 15-20 kDa band, which corresponds to IFN-β. Lanes #2-5 show bands of approximately 60 kDa, which match the expected molecular weight of the IFN-β-gal-9 fusion proteins.

To evaluate the biological activity of IFN-β-gal-9 fusion proteins relative to IFN-β, a reporter assay, measuring luciferase activity, was conducted (Figure 28B). The fold inductions of IFN-β-gal-9 proteins were significantly lower than that of IFN-β at all concentrations examined, which indicates that the IFN biological activity of IFN-β-gal-9 fusion proteins was lower than that of IFN-β.

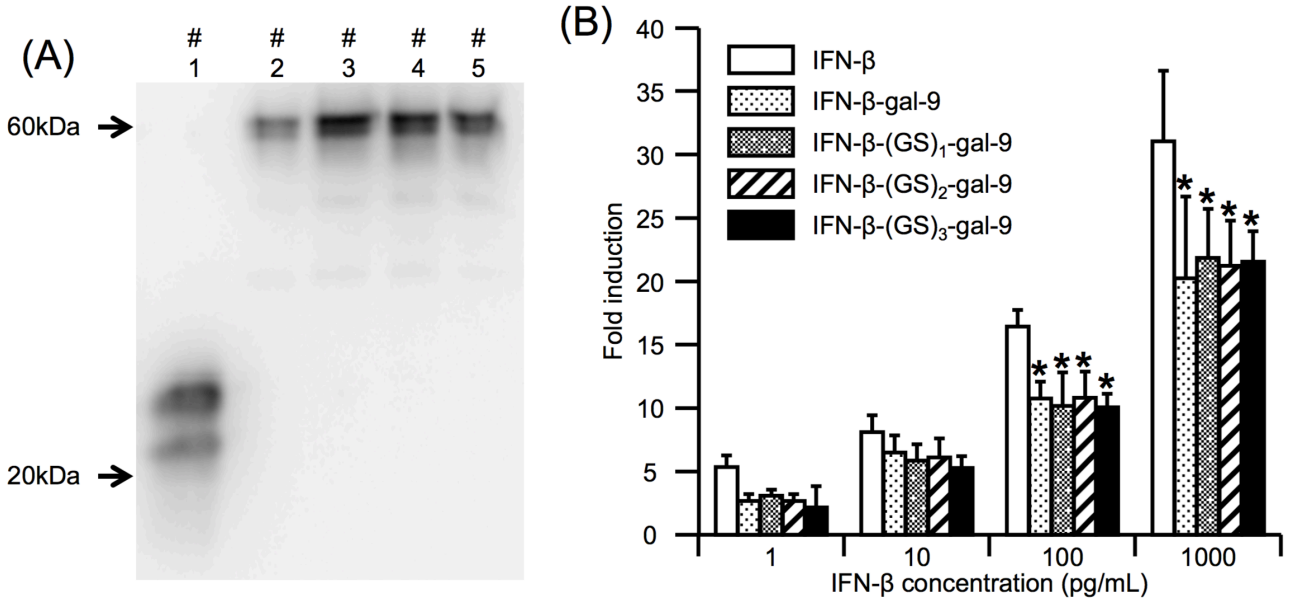

Figure 28. Expression and biological activity of the IFN-β and IFN-β-gal-9 fusion proteins. (A) Western blotting analysis of the IFN-β and IFN-β-gal-9 fusion proteins, to confirm the molecular weight of the constructs (lane #1: IFN-β, lane #2: IFN-β-gal-9, lane #3: IFN-β-(GS)1-gal-9, lane #4: IFN-β-(GS)2-gal-9, lane #5: IFN-β-(GS)3-gal-9). (B) Induction of fLuc expression in pMx-fLuc-transfected B16-BL6 cells after treatment with the IFN-β and IFN-β-gal-9 fusion proteins. The results are expressed as the mean ± SD of four samples. *$p < 0.05$ compared with IFN-β.

III-2-3-b. The IFN-β-gal-9 fusion proteins effectively attenuated the activity of restimulated T cells

T cells stimulated by MOG_{35-55} are involved in the onset of EAE symptoms, following EAE induction. Therefore, I examined the biological effect of IFN-β and IFN-β-gal-9 fusion proteins on restimulated T cells, collected from splenocytes isolated from EAE mice. Cell proliferation in the presence of IFN-β and IFN-β-gal-9 fusion proteins in restimulated splenocytes was evaluated using the WST-8 assay (Figure 29A). Treatment with a concentration of IFN-β and IFN-β-gal-9 fusion proteins above 1000 pg/mL significantly reduced cell proliferation compared to the control group. Cell proliferation in the IFN-β-$(GS)_1$-gal-9 and the IFN-β-$(GS)_2$-gal-9 groups at

concentrations of 1000 pg/mL and 2000 pg/mL was significantly lower than that of the IFN-β group. In contrast, there was no significant difference between the IFN-β group and the IFN-β-gal-9 group.

The IFN-γ concentration in conditioned media was determined for evaluating the activation of T cells after the addition of IFN-β and IFN-β-gal-9 fusion proteins to restimulated T cells (Figure 29B). The IFN-γ concentration in the IFN-β and the IFN-β-gal-9 fusion protein groups at concentrations of 1000 pg/mL and 2000 pg/mL significantly declined compared to that in the control group. In particular, IFN-β-$(GS)_2$-gal-9 showed stronger suppressive effects on restimulated splenocytes at all concentrations, when compared to IFN-β and other IFN-β-gal-9 fusion proteins.

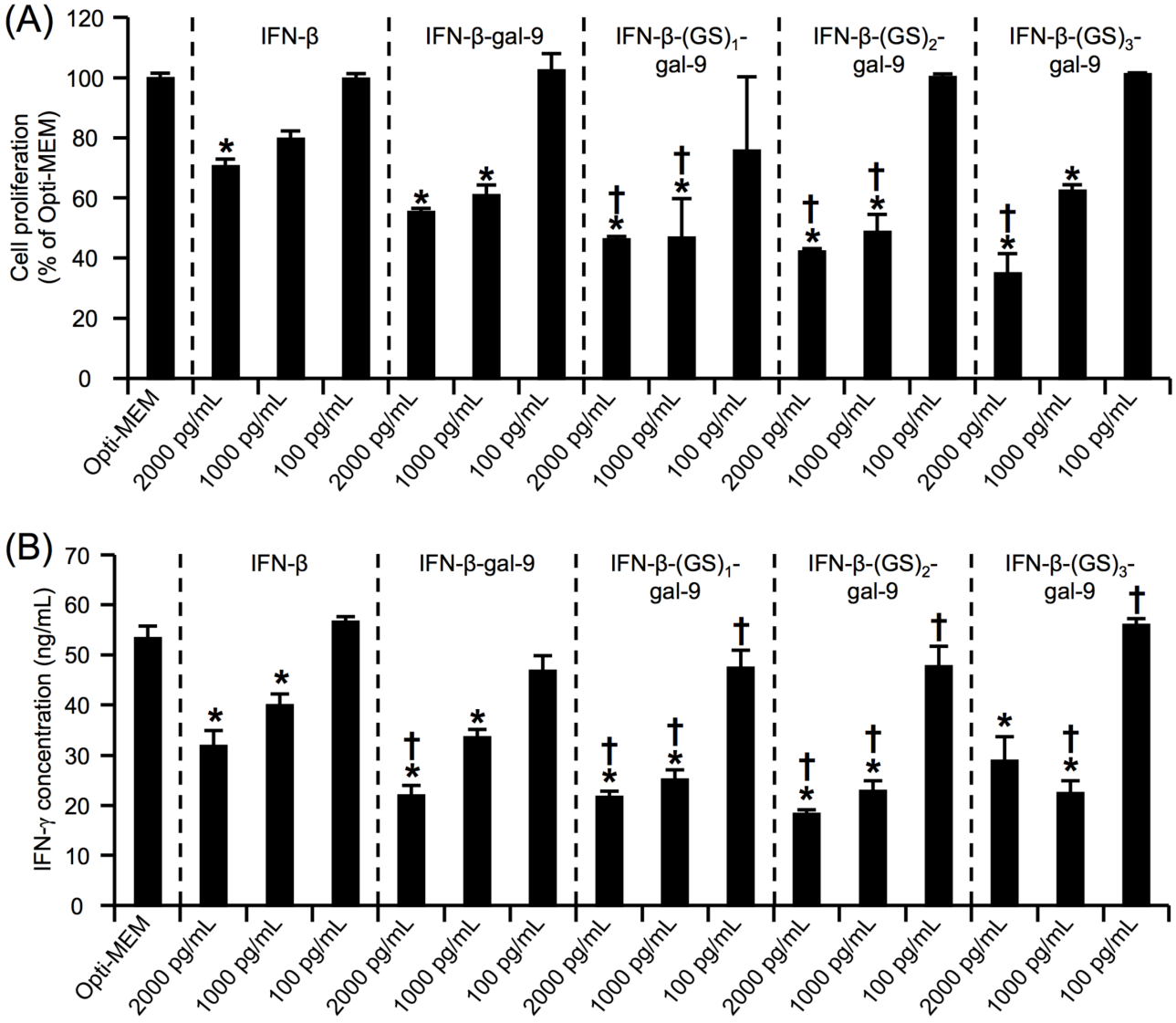

Figure 29. Suppressive effects of the IFN-β and IFN-β-gal-9 fusion proteins on restimulated T cells. IFN-β and IFN-β-gal-9 fusion proteins were added to restimulated T cells. After a 3-day incubation, cell proliferation and the IFN-γ concentration in the conditioned media were measured using (A) the WST-8 assay and (B) ELISA, respectively. The results are expressed as the mean ± SEM of four samples. *$p < 0.05$ and †$p < 0.05$ compared with Opti-MEM and IFN-β at the same concentration, respectively.

III-2-3-c. The IFN-β-gal-9 fusion proteins exerted suppressive effects on restimulated splenocytes in the presence of the anti-IFNAR antibody

The effect of gal-9 in the IFN-β-gal-9 fusion proteins on restimulated T cells was examined by using anti-IFNAR antibody, which inhibits the IFNAR function and IFN signaling. In these experiments, anti-IFNAR antibody was added to the culture media of restimulated T cells containing 1000 pg/mL IFN-β or IFN-β-gal-9 fusion proteins. Treatment with IFN-β and IFN-β-gal-9 fusion proteins in the presence of the anti-IFNAR antibody led to a considerable recovery in cell proliferation, when compared to that in cells treated with a control antibody (Figure 30A). In the presence of the anti-IFNAR antibody, cell proliferation in the IFN-β-$(GS)_2$-gal-9 group significantly declined, compared to that in the IFN-β group. Moreover, the IFN-γ concentration in cells treated with IFN-β and IFN-β-gal-9 fusion proteins in the presence of the anti-IFNAR antibody was higher than that in cells treated with IFN-β or IFN-β-gal-9 fusion proteins and a control antibody (Figure 30B). In addition, the IFN-γ concentration in cells treated with the IFN-β-$(GS)_2$-gal-9 and the anti-IFNAR antibody tended to be lower than that in cells treated with IFN-β and the anti-IFNAR antibody. Since the suppressive effect of IFN-β-$(GS)_2$-gal-9 on T cells was strongest among IFN-β-gal-9 fusion proteins, IFN-β-$(GS)_2$-gal-9 was further used for evaluating the therapeutic effect of IFN-β-gal-9 fusion proteins in EAE mice.

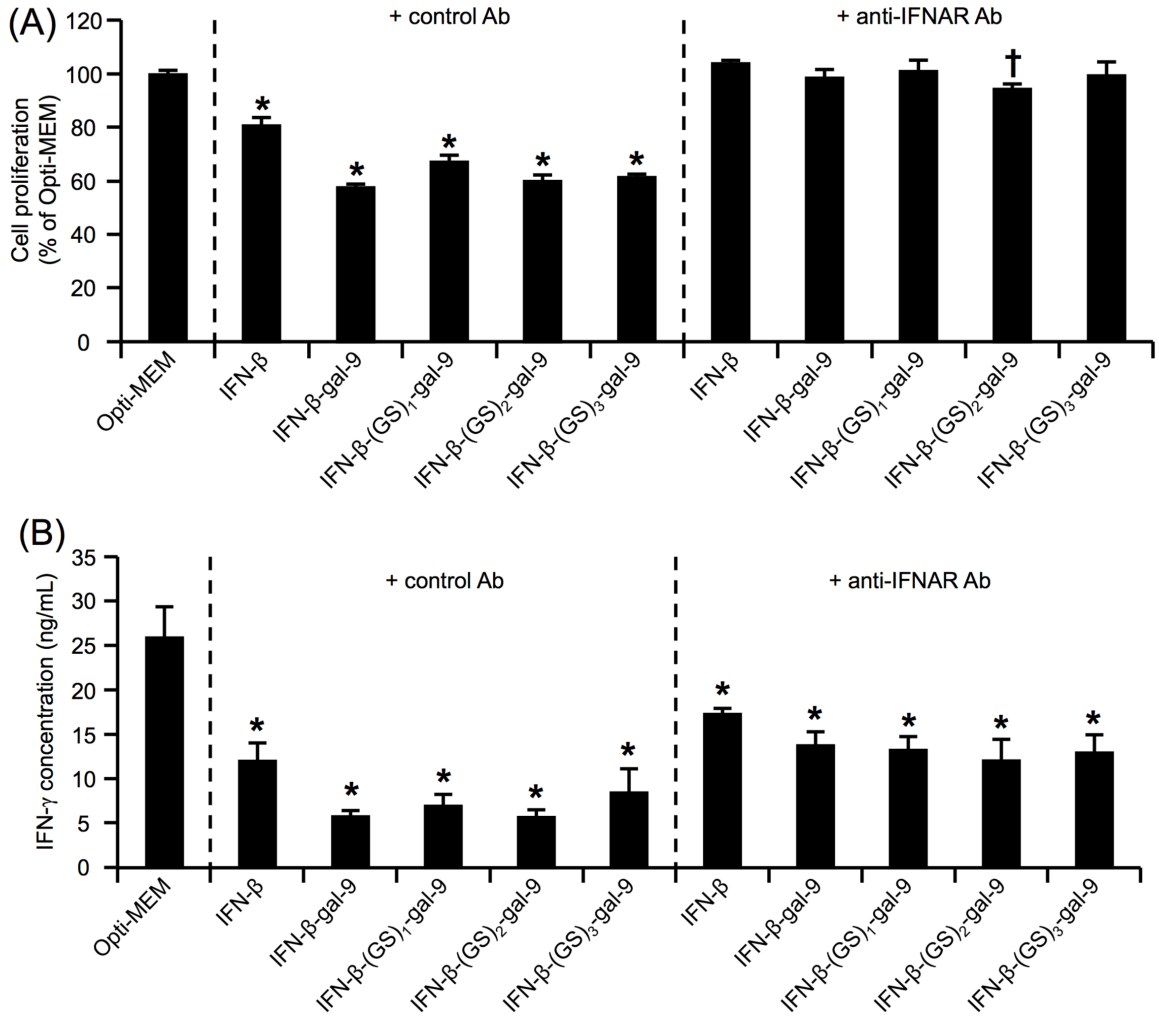

Figure 30. Evaluation of the suppressive effects of the IFN-β and IFN-β-gal-9 fusion proteins in the presence of the anti-IFNAR antibody. IFN-β and IFN-β-gal-9 fusion proteins and a control antibody or the anti-IFNAR antibody were added to restimulated T cells. After a 3-day incubation, cell proliferation and the IFN-γ concentration in the conditioned media was measured using (A) the WST-8 assay and (B) ELISA, respectively. The results are expressed as the mean ± SEM of four samples. *$p < 0.05$ and †$p < 0.05$ compared with Opti-MEM and IFN-β, respectively.

III-2-3-d. Gene therapy using IFN-β and IFN-β-$(GS)_2$-gal-9-expressing plasmid DNA improved the clinical score for EAE symptoms

The gene transfer of pMx-IFN-β and pMx-IFN-β-$(GS)_2$-gal-9 into EAE mice was performed on day 7 following EAE induction. The IFN-β and IFN-β-$(GS)_2$-gal-9 concentrations in the serum were approximately 1000 pg/mL at day 1 after the gene transfer (Figure 31A). Afterwards, the IFN-β and IFN-β-$(GS)_2$-gal-9 concentrations in the serum decreased, but the proteins were detected for at least 1 month after the gene transfer.

The clinical score after EAE induction was evaluated at the indicated time points (Figure 31B). The clinical score of the group treated with pMx-gLuc, which was used as a control plasmid, rapidly increased from approximately 10 days after EAE induction. In contrast, the clinical scores of the pMx-IFN-β and pMx-IFN-β-$(GS)_2$-gal-9-treated groups gradually increased and were significantly lower than that of the pMx-gLuc-treated group. In addition, the clinical score of the pMx-IFN-β-$(GS)_2$-gal-9-treated group tended to be lower than that of the pMx-IFN-β-treated group, although the difference was not statistically significant. The mean maximum score in the pMx-gLuc-treated group was 3.9 ± 0.4 (Figure 31C), whereas the mean maximum scores in the pMx-IFN-β and pMx-IFN-β-$(GS)_2$-gal-9-treated group were 2.0 ± 0.5 and 1.4 ± 0.4, respectively. The mean maximum score of the pMx-gLuc-treated group was significantly higher than those in the pMx-IFN-β and pMx-IFN-β-$(GS)_2$-gal-9-treated groups.

The WBC count was assessed as an index of the side effects of IFN-β (Figure 31D). The WBC count in the pMx-gLuc-treated group was approximately $5.8 \times 10^3/mm^3$ at 1 day after gene transfer and gradually decreased to approximately $2.1 \times 10^3/mm^3$ over 1 month. The profile of the WBC count in the pMx-IFN-β-$(GS)_2$-gal-9-treated group was comparable to that of the pMx-gLuc-treated group. On the other hand, the WBC count in the pMx-IFN-β-treated group was significantly lower than that of the pMx-gLuc-treated group and that of the pMx-IFN-β-$(GS)_2$-gal-9-treated group.

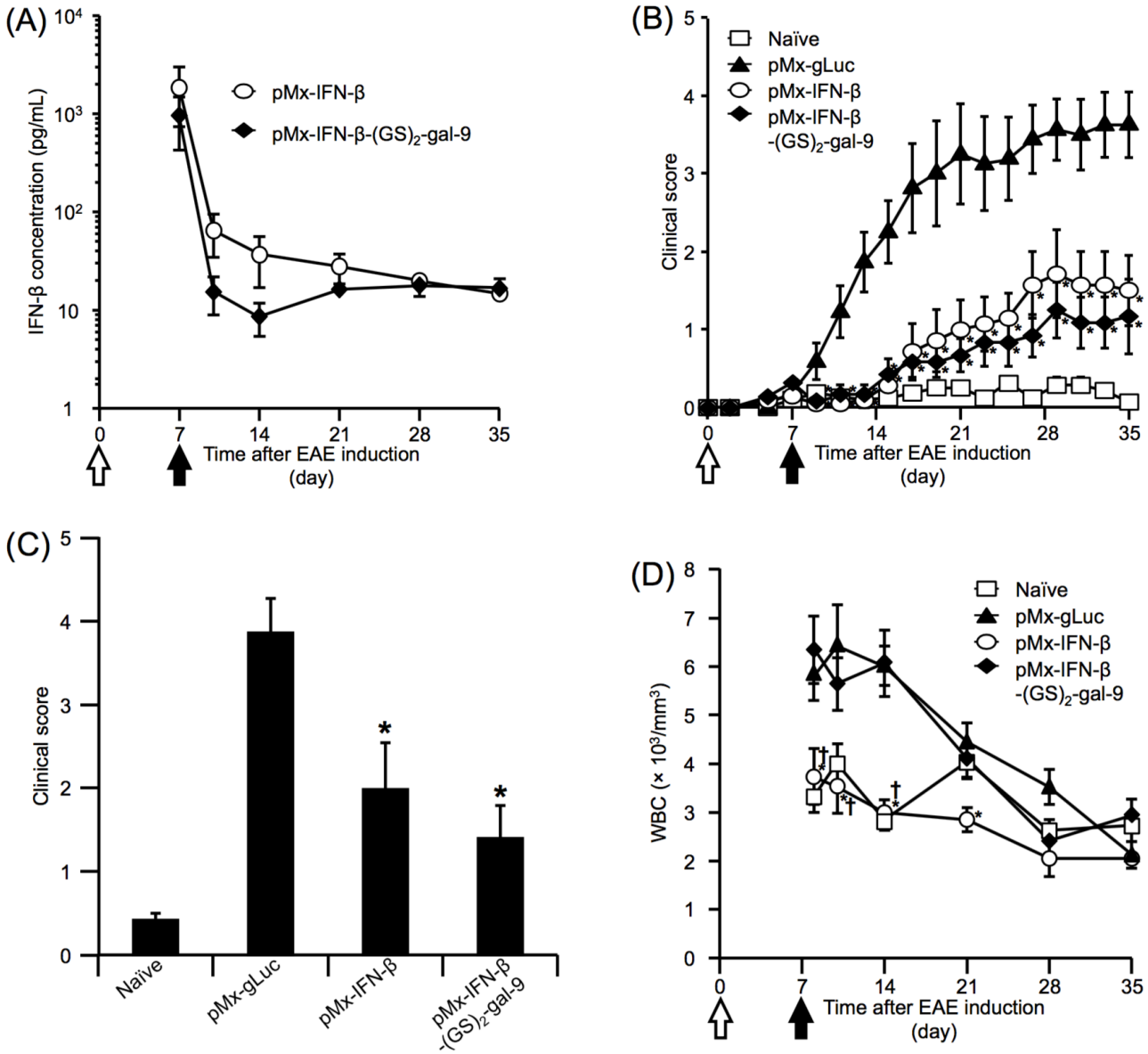

Figure 31. Severity of EAE after gene transfer into EAE mice. (A) Time course of the serum concentration of IFN-β after gene transfer of pMx-IFN-β into EAE mice. The concentration of IFNβ in serum samples was analyzed by ELISA. (B) Time course of clinical score of EAE after EAE induction. At day 7 after EAE induction, EAE mice in the pMx-gLuc and the pMx-IFN-β groups received pMx-gLuc and pMx-IFN-β at a dose of 1 μg/mouse, respectively. (C) The maximum score for all EAE mice in the Naïve, the No treatment, the pMx-gLuc-treated, and the pMx-IFN-β-treated groups. The time points for the EAE induction and gene transfer were indicated by white and black arrows, respectively. (D) WBC in blood samples collected from EAE mice stained by Turk's solution and counted at the indicated time points. The results are expressed as mean ± SEM of eight mice. *$p < 0.05$ and †$p < 0.05$ compared with the pMx-gLuc group and IFN-β, respectively.

III-2-3-e. The IFN-γ concentration decreased following gene transfer using pMx-IFN-β-$(GS)_2$-gal-9

The serum IFN-γ concentration was measured at 14 days after EAE induction. The IFN-γ concentration in the pMx-gLuc-treated group was approximately 110 pg/mL (Figure 32). By comparison, the IFN-γ concentration in both the pMx-IFN-β-treated and the pMx-IFN-β-$(GS)_2$-gal-9-treated groups was approximately 45 pg/mL, and was significantly lower than that of the pMx-gLuc treated group.

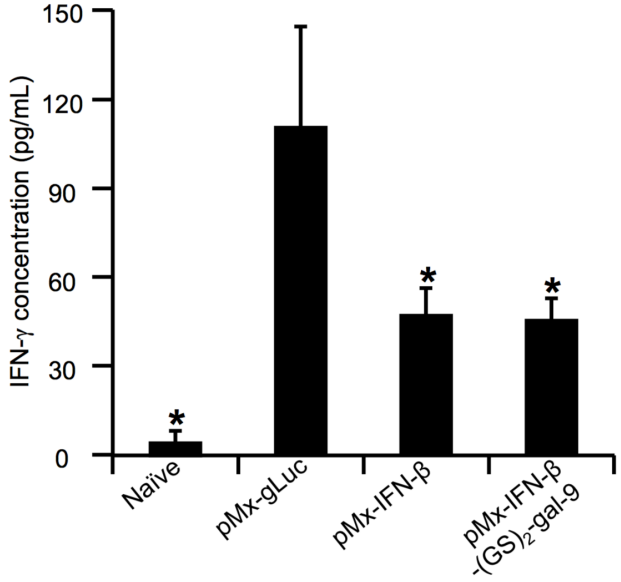

Figure 32. Serum concentration of IFN-γ at day 14 after EAE induction. The gene transfer was performed at day 7 after EAE induction and the serum IFN-γ concentration was determined by ELISA at day 14 after EAE induction. The results are expressed as mean ± SEM of three mice. *$p < 0.05$ compared with the pMx-gLuc group.

III-2-3-f. The pMx-IFN-β-$(GS)_2$-gal-9 gene transfer suppressed BBB disruption in EAE mice

The BBB function was evaluated by intravenously injecting EB into EAE mice at 14 days after EAE induction. The blue dye was observed in the brain and spinal cord samples, in the pMx-gLuc-treated group (Figure 33A). In contrast, the blue dye was hardly observed in other groups. In addition, the amount of EB extracted from the spinal cord samples in the pMx-IFN-β-treated and pMx-IFN-β-$(GS)_2$-gal-9-treated groups was significantly lower compared to that extracted from the pMx-gLuc-treated group (Figure 33B).

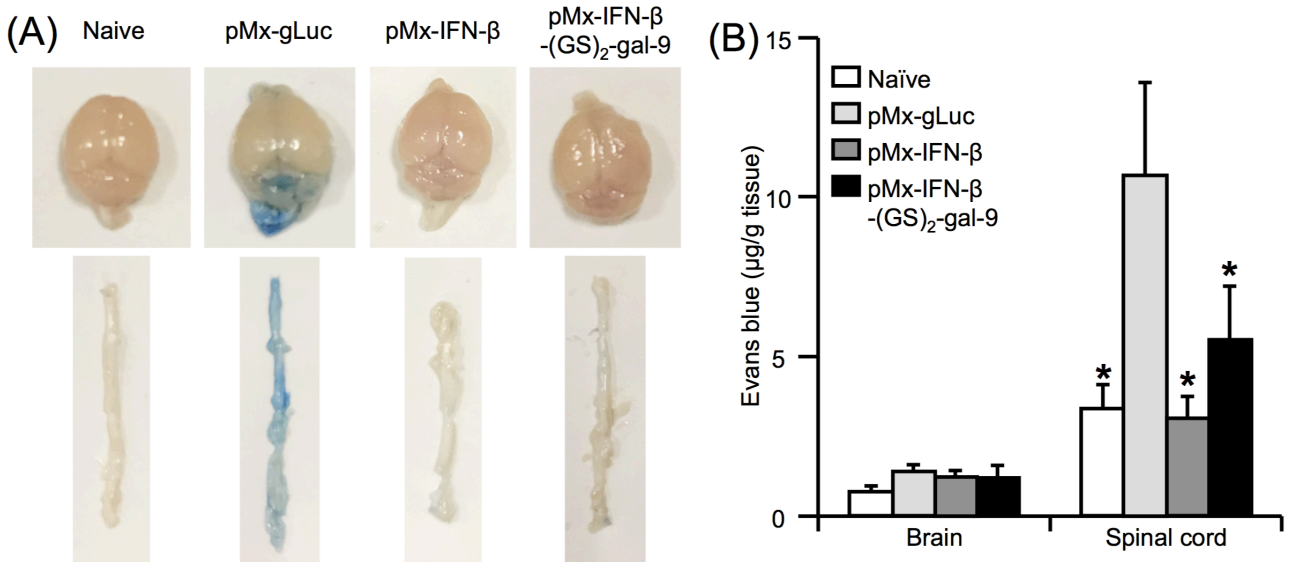

Figure 33. The effect of gene transfer on BBB permeability in EAE mice. pMx-gLuc and pMx-IFN-β was injected into EAE mice at day 7 after EAE induction. At day 14 after immunization, mice received an intravenous EB injection and the brain and spinal cord of EAE mice were collected 3 h after the EB injection. (A) Representative images of brain and spinal cord of mice in each group. The blue color indicates the leakage of EB into the brain and spinal cord through BBB. (B) The amount of extracted EB from the brain and spinal cord of mice in each group. The results are expressed as mean ± SEM of at least three samples. *p < 0.05 compared with the pMx-gLuc group.

III-2-3-g. Histological analysis

HE staining and LFB staining were conducted for the histological analysis of CNS in EAE mice after gene transfer using IFN-β and IFN-β-$(GS)_2$-gal-9-expressing plasmid DNA (Figure 34). Infiltrating inflammatory cells were observed in the HE-stained spinal cord of pMx-gLuc-treated EAE mice. In contrast, cell infiltration was hardly observed in the spinal cord samples from pMx-IFN-β and pMx-IFN-β-$(GS)_2$-gal-9-treated EAE mice.

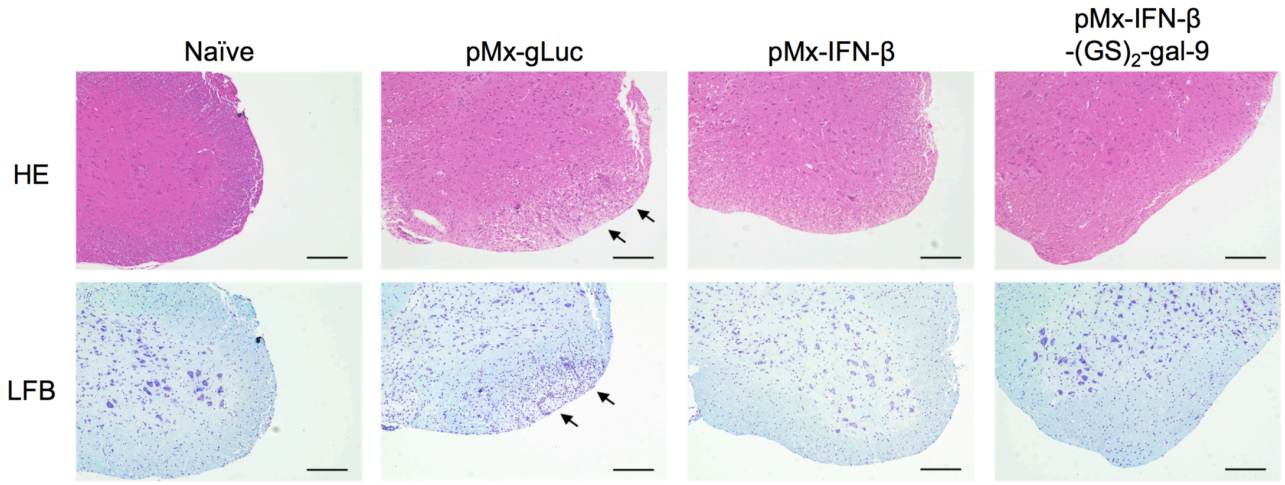

Figure 34. Histological analysis of the spinal cord of EAE mice. At day 35 after EAE induction, the spinal cord was collected from Naïve mice or EAE mice in the No treatment, pMx-gLuc-treated, or pMx-IFN-β-treated groups. HE (upper panel) and LFB (bottom panel) staining were performed to evaluate infiltrated cells and demyelination, respectively. Arrows indicated areas containing infiltrated cells. Scale bar = 100 μm

III-2-4 Discussion

In *in vitro* experiments using restimulated T cells, the cell proliferation rate and IFN-γ concentration in the culture media showed that IFN-β-gal-9 fusion proteins were superior to IFN-β alone (Figure 29A, 29B). In addition, when the biological activity of IFN-β was inhibited using an anti-IFNAR antibody to evaluate the effect of gal-9 in the IFN-β-gal-9 fusion proteins, the IFN-β-gal-9 fusion proteins slightly suppressed the activity of restimulated T cells (Figure 30A, 30B). These results indicate that a fusion of gal-9 and IFN-β effectively suppresses the function of restimulated T cells, when compared to IFN-β. On the other hand, the effect of gal-9 on EAE mice was evaluated by repetitive intraperitoneal injections of 100 μg gal-9 protein [90]. In that study, the

degree of the improvement in the clinical score by the administration was approximately 0.5, which is lower than that achieved by IFN-β-$(GS)_2$-gal-9 gene transfer. Considering that the serum concentration of gal-9 in the preceding study estimated from the administration dose would be highly likely to be higher than the serum concentration in the IFN-β-$(GS)_2$-gal-9 gene transfer group estimated from the IFN-β concentration (Figure 31A), IFN-β-$(GS)_2$-gal-9 fusion protein may have higher therapeutic effect on EAE mice than gal-9 protein.

In general, the biological activity of fusion proteins is easy to modulate, compared to unmodified proteins. For instance, the biological activity of the human IFN-α fused to human albumin was lower than that of unmodified IFN-α [95]. In fact, the biological activity of IFN-β was attenuated by its fusion to gal-9 (Figure 28B), whereas my *in vitro* experiments demonstrated that a fusion of gal-9 to IFN-β compensated or rather improved its suppressive effect on T cells. The reason for this suppressive effect mediated by IFN-β-gal-9 fusion proteins may be linked to their inhibitory signaling through the Tim-3/gal-9 pathway. Previous studies have shown that Tim-3 is specifically expressed on T_h1 shifted $CD4^+$ T cells [89,96]. Following the binding of gal-9 to Tim-3 on T_h1 cells, T_h1 cell function was suppressed through the inhibition of the Tim-3/gal-9 signaling pathway [97]. Therefore, it was suggested that the IFN-β-gal-9 fusion proteins suppressed T_h1 cell function through immunosuppression by IFN-β and through suppressive signaling after the binding of gal-9 to Tim-3 on the T_h1 cell surface.

Based on my *in vivo* evaluation, the IFN-β and IFN-β-$(GS)_2$-gal-9 concentrations in the serum were maintained after the gene transfer of the long-term expression vectors containing IFN-β and IFN-β-$(GS)_2$-gal-9, and pMx-IFN-β and pMx-IFN-β-$(GS)_2$-gal-9, respectively, into EAE mice, indicating that gene therapy using the Mx vector was useful for the long-term treatment of MS. Moreover, the gene transfer of plasmid DNA encoding IFN-β-$(GS)_2$-gal-9 into EAE mice was equal to or better than that involving plasmid DNA encoding IFN-β, demonstrating that IFN-β-$(GS)_2$-gal-9 may potentially be used in the treatment of MS.

In the clinical use of IFN-β, cytopenia is one of the severe side effects that cause treatment interruption [98]. Therefore, the prevention of cytopenia is important for the safe and sustained treatment of MS. The WBC count was markedly reduced following the gene transfer of the IFN-β-expressing plasmid DNA into EAE mice, suggesting the presence of cytopenia (Figure 31D). In contrast, barely any decrease in the WBC count was associated with the gene transfer of the IFN-β-$(GS)_2$-gal-9-expressing plasmid, probably since the biological activity of IFN-β-$(GS)_2$-gal-9 was lower than that of IFN-β. By contrast, the therapeutic effects of IFN-β and IFN-β-$(GS)_2$-gal-9 were comparable, indicating that IFN-β-$(GS)_2$-gal-9 was more desirable than IFN-β for the treatment of MS.

III-2-5 Conclusion

IFN-β-$(GS)_2$-gal-9 effectively improved the suppressive effect against restimulated splenocytes *in vitro* and attenuated the severity of EAE symptoms *in vivo*. In conclusion, gene therapy using IFN-β-$(GS)_2$-gal-9 is a promising avenue for the effective treatment of MS, without triggering cytopenia.

Summary

The aim of this study was to develop long-term expression system of IFN-β by design of a novel plasmid DNA vector and to reduce side effects associated with IFN-β by design of IFN-β fusion proteins for the treatment of patients with refractory diseases. The main findings from each chapter are summarized as follows.

I. Interferon-inducible Mx promoter-driven, long-term transgene expression system of interferon-β for cancer gene therapy

In Chapter I, I used the IFN-inducible Mx promoter to promote IFN-β expression. The pMx-IFN-β plasmid was constructed to achieve the long-term IFN-β expression. In cultured cells transfected with the Mx promoter-driven reporter protein plasmid, IFN-β induced concentration-dependent expression of the reporter protein. After the hydrodynamic injection of pMx-IFN-β into mice, the serum concentration of IFN-β was maintained at 100 pg/mL or higher for more than 1 month. IFN-β expression was significantly suppressed by the co-injection of siRNA targeting the IFNAR, suggesting that IFN-β binding to IFNAR increased IFN-β expression. Moreover, the hydrodynamic injection of pMx-IFN-β significantly suppressed the growth of colon26 tumors in mice. In contrast, a conventional promoter-driven plasmid was less effective than pMx-IFN-β in all the experiments. Taken together, these results indicate that the interferon-inducible Mx promoter-driven expression system effectively achieves long-term expression of IFN-β and represents a potential tool for cancer gene therapy.

II. Evaluation of antiviral effect of type I, II, and III interferons on direct-acting antiviral-resistant hepatitis C virus

In Chapter II, I evaluated the *in vivo* antiviral effect of three classes of IFNs, namely, types I, II, and III IFNs, on DAA-resistant HCVs. IFN-α_2, IFN-γ, and IFN-λ_1 were selected as typical types I, II, and III IFNs, respectively. Human hepatocyte-transplanted chimeric mice were infected with NS3-D168, NS5A-L31-, and NS5A-Y93-mutated HCVs, and the antiviral effect of IFN-α_2, IFN-γ, and IFN-λ_1 on these HCV RASs was examined. Chimeric mice infected with NS3- and NS5A-mutated HCVs were hydrodynamically injected with IFN-expressing plasmids to evaluate the antiviral effect of IFNs. Serum concentrations of IFNs were maintained for at least 42 days. It was found that serum HCV level significantly decreased and serum and hepatic HCV levels reached below detection limit in chimeric mice injected with IFN-γ- and IFN-λ_1-expressing plasmids. The antiviral effect of IFN-α_2 on DAA-resistant HCVs was weaker than that of IFN-γ and IFN-λ_1. Serum ALT levels showed a small and transient increase in mice injected with the IFN-γ-expressing plasmid but not in mice injected with the IFN-λ_1-expressing plasmid. However, no apparent histological damage was observed in the liver sections of mice injected with the IFN-γ-expressing plasmid. These results indicate that IFN-γ and IFN-λ_1 are an attractive therapeutic option for treating infection caused by NS3- and NS5A-mutated HCV.

III. Development of safe and effective interferon-beta gene therapy by using long-term expression vector and regulating biological activity for the treatment of patients with multiple sclerosis

III-1. Amelioration of experimental autoimmune encephalomyelitis in mice by interferon-beta gene therapy, using a long-term expression plasmid vector

In Chapter III Section 1, I examined whether gene transfer of pMx-IFN-β could be effective for the treatment of MS in EAE mice. Seven days after injection of the EAE-inducing peptide, the EAE mice received hydrodynamic injections pMx-IFN-β. The severity of EAE symptoms in the pMx-IFN-β-treated mice was significantly lower for 1 month than that observed in the untreated-mice. An evaluation of BBB function, using EB, showed that injection of pMx-IFN-β suppressed the BBB disruptions normally observed in EAE mice, while BBB disruptions remained evident in the untreated EAE mice. Histological analysis showed fewer invasive inflammatory cells in the spinal cords of the pMx-IFN-β-treated mice than in the spinal cords of the other mice. Serum IFN-γ concentrations in the pMx-IFN-β-treated mice were significantly lower than that in the untreated mice, indicating that IFN-β gene transfer suppressed the production of IFN-γ from pathogenic T cells. These results indicate that IFN-β transgene expression by single administration of the pMx-IFN-β can be an effective long-term treatment for MS.

III-2. Safe and effective interferon-beta gene therapy for multiple sclerosis by designing interferon-beta-galectin-9 fusion proteins

In Chapter III Section 2, I designed a series of novel IFN-β fusion proteins containing gal-9, which exerts immunosuppressive effects through the binding to its receptor on activated T_h1 cells. I hypothesized that these fusion proteins would improve the therapeutic effects and reduce the side effects of IFN-β. The IFN-β-gal-9 fusion proteins showed less IFN-β biological activity on non-T cells than IFN-β alone. *In vitro* experiments using re-stimulated T cells isolated from mice with EAE showed that the IFN-β-gal-9 fusion proteins suppressed activated T cells more effectively than IFN-β. Moreover, in my *in vivo* experiments, the gene transfer of IFN-β-gal-9 fusion protein-expressing plasmid DNA into EAE mice showed beneficial therapeutic effects without cytopenia, a known side effect of IFN-β. In contrast, the gene transfer of IFN-β-expressing plasmid DNA induced a rapid decrease in the WBC count, despite its therapeutic effect. These results indicate that gene therapy using IFN-β-gal-9 fusion proteins is expected to be safe and effective for the treatment of MS.

Acknowledgements

I would like to express my sincere gratitude and thanks to Dr. Yoshinobu Takakura, Professor of Department of Biopharmaceutics and Drug Metabolism, Graduate School of Pharmaceutical Sciences, Kyoto University for giving me wonderful opportunities and their support with his patience, motivation, enthusiasm, and immense knowledge. His guidance helped me in all the time of research and writing of this thesis.

I am extremely grateful to my research guides, Dr. Yuki Takahashi, Associate Professor of Department of Biopharmaceutics and Drug Metabolism. It was a great opportunity to do my doctoral program under their guidance and to learn from their research expertise. All of their encouragement, insightful comments, and hard questions are fully helpful and essential for my Ph.D. course.

I wish to express my deepest appreciation to Dr. Makiya Nishikawa, Professor of Laboratory of Biopharmaceutics, Faculty of Pharmaceutical Sciences, Tokyo University of Science for his patient supervision, insightful comments, suggestions, guidance and direction, valuable discussions and supports facilitating the successful completion of this study throughout the whole this study.

I highly appreciate the supports received through the collaborative work provided from Dr. Kazuaki Chayama, Professor of Department of Gastroenterology and Metabolism, Programs for Biomedical Research, Graduate School of Biomedical Science, Hiroshima University, Dr. Michio Imamura, Lecturer of Department of Gastroenterology and Metabolism, and Dr. Takuro Uchida. They kindly supported on data collection by using NS3- and NS5A-mutated HCV-infected chimeric mice in Chapter II.

I would like to express sincere gratitude to Ms. Akane Tanioka and Ms. Misako Takenaka for their great achievement and contribution as a co-author for Chapter III, and their advice and warm support for this study.

I am greatly indebted to all members of Department of Biopharmaceutics and Drug metabolism and of Drug Delivery Research, Graduate School of Pharmaceutics Sciences, Kyoto University for their experimental assistance.

Finally, I would like to express my deepest gratitude to my family for their support, encouragements, and understanding throughout the doctoral course of this study.

List of Publications

Interferon-inducible Mx promoter-driven, long-term transgene expression system of interferon-β for cancer gene therapy.

Atsushi Hamana, Yuki Takahashi, Makiya Nishikawa, Yoshinobu Takakura

Human Gene Ther. 2016. 27, 936-945

Evaluation of antiviral effect of type I, II, and III interferons on direct-acting antiviral-resistant hepatitis C virus.

Atsushi Hamana, Yuki Takahashi, Takuro Uchida, Makiya Nishikawa, Michio Imamura, Kazuaki Chayama, Yoshinobu Takakura

Antiviral Res. 2017. 146, 130-138

Amelioration of experimental autoimmune encephalomyelitis in mice by interferon-beta gene therapy using long-term expression plasmid vector.

Atsushi Hamana, Yuki Takahashi, Akane Tanioka, Makiya Nishikawa, Yoshinobu Takakura

Mol Pharm. 2017. 14, 1212-1217.

Safe and effective interferon-beta gene therapy for the treatment of multiple sclerosis by regulating biological activity through the design of interferon-beta-galectin-9 fusion proteins

Atsushi Hamana, Yuki Takahashi, Akane Tanioka, Makiya Nishikawa, Yoshinobu Takakura

Int J Pharm. 2017. 536, 310-317.

Other Publications

Effects of transgene expression level per cell in mice livers on induction of transgene-specific immune responses after hydrodynamic gene transfer.

Yalei Yin, Yuki Takahashi, Atsushi Hamana, Makiya Nishikawa, Yoshinobu Takakura

Gene Ther. 2016. 23, 565-71

Targeted delivery of interferon gamma using a recombinant fusion protein of a fibrin-clot binding peptide with interferon gamma for cancer gene therapy

Mitsuru Ando, Mai Fujimoto, Yuki Takahashi, Makiya Nishikawa, Atsushi Hamana, Yoshinobu Takakura

J Pharm Sci. 2017. 106, 892-897

References

1. George. P.M, Badiger. R, Alazawi. W, Foster G.R, Mitchell. J.A. Pharmacology and therapeutic potential of interferons. *Pharmacol Ther*. 2012. 135, 44-53.
2. Chiang. J, Gloff. C.A, Yoshizawa. C.N, Williams. G.J. Pharmacokinetics of recombinant human interferon-β ser in healthy volunteers and its effect on serum neopterin. *Pharm Res*. 1993. 10, 567-72.
3. Wirth. T, Parker. N, Ylä-Herttuala. S. History of gene therapy. *Gene*. 2013. 525, 162-9.
4. Mitsui. M, Nishikawa. M, Zang. L, Ando. M, Hattori. K, Takahashi. Y, Watanabe. Y, Takakura. Y. Effect of the content of unmethylated CpG dinucleotides in plasmid DNA on the sustainability of transgene expression. *J Gene Med*. 2009. 11, 435-43.
5. Yoshida. J, Mizuno. M, Wakabayashi. T. Interferon-β gene therapy for cancer: basic research to clinical application. *Cancer Sci*. 2004. 95, 858-65.
6. Hong. Y.K, Chung. D.S, Joe. Y.A, Yang. Y.J, Kim. K.M, Park. Y.S, Yung. W.K, Kang. J.K. Efficient inhibition of *in vivo* human malignant glioma growth and angiogenesis by interferon-β treatment at early stage of tumor development. *Clin Cancer Res*. 2000. 6, 3354-60.
7. Hegen. H, Auer. M, Deisenhammer. F. Pharmacokinetic considerations in the treatment of multiple sclerosis with interferon-β. *Expert Opin Drug Metab Toxicol*. 2015. 30, 1-17.
8. Mager. D.E, Neuteboom. B, Jusko. W.J. Pharmacokinetics and pharmacodynamics of PEGylated IFN-β 1a following subcutaneous administration in monkeys. *Pharm Res*. 2005. 22, 58-61.
9. Baker. D.P, Lin. E.Y, Lin. K, Pellegrini. M, Petter. R.C, Chen. L.L, Arduini. R.M, Brickelmaier. M, Wen. D, Hess. D.M, Chen. L, Grant. D, Whitty. A, Gill. A, Lindner. D.J, Pepinsky. R.B. N-terminally PEGylated human interferon-β-1a with improved pharmacokinetic properties and *in vivo* efficacy in a melanoma angiogenesis model. *Bioconjug Chem*. 2006. 17, 179-88.
10. Pisal. D.S, Kosloski. M.P, Balu-Iyer. S.V. Delivery of therapeutic proteins. *J Pharm Sci*. 2010. 99, 2557-75.
11. Chiocca. E.A, Smith. K.M, McKinney. B, Palmer. C.A, Rosenfeld. S, Lillehei. K, Hamilton. A, DeMasters. B.K, Judy. K, Kirn. D. A phase I trial of Ad.hIFN-β gene therapy for glioma. *Mol Ther*. 2008. 16, 618-26.
12. Sterman. D.H, Recio. A, Carroll. R.G, Gillespie. C.T, Haas. A, Vachani. A, Kapoor. V, Sun. J, Hodinka. R, Brown. J.L, Corbley. M.J, Parr. M, Ho. M, Pastan. I, Machuzak. M, Benedict. W, Zhang. X.Q, Lord. E.M, Litzky. L.A, Heitjan. D.F, June. C.H, Kaiser. L.R, Vonderheide. R.H, Albelda. S.M, Kanther. M. A phase I clinical trial of single-dose intrapleural IFN-β gene transfer for malignant pleural mesothelioma and metastatic pleural effusions: high rate of antitumor immune responses. *Clin Cancer Res*. 2007. 13, 4456-66.
13. Kawano. H, Nishikawa. M, Mitsui. M, Takahashi. Y, Kako. K, Yamaoka. K, Watanabe. Y, Takakura. Y. Improved anti-cancer effect of interferon gene transfer by sustained expression using CpG-reduced plasmid DNA. *Int J Cancer*. 2007. 121, 401-6.

14. Donnelly. R.P, Dickensheets. H, O'Brien. T.R. Interferon-lambda and therapy for chronic hepatitis C virus infection. *Trends Immunol*. 2011. 32, 443-50.
15. Schneider. W.M, Chevillotte. M.D, Rice. C.M. Interferon-stimulated genes: a complex web of host defenses. *Annu Rev Immunol*. 2014. 32, 513-45.
16. Sellins. K, Fradkin. L, Liggitt. D, Dow. S. Type I interferons potently suppress gene expression following gene delivery using liposome(-)DNA complexes. *Mol Ther*. 2005. 12, 451-9.
17. Takahashi. Y, Vikman. E, Nishikawa. M, Ando. M, Watanabe. Y, Takakura. Y. Persistent interferon transgene expression by RNA interference-mediated silencing of interferon receptors. *J Gene Med*. 2010. 12, 739-46.
18. Hug. H, Costas. M, Staeheli. P, Aebi. M, Weissmann. C. Organization of the murine Mx gene and characterization of its interferon- and virus-inducible promoter. *Mol Cell Biol*. 1988. 8, 3065-79.
19. Asano. A, Jin. H.K, Watanabe. T. Mouse Mx2 gene: organization, mRNA expression and the role of the interferon-response promoter in its regulation. *Gene*. 2003. 306, 105-13.
20. Nakamura. K, Yoshikawa. N, Yamaguchi. Y, Kagota. S, Shinozuka. K, Kunitomo. M. Characterization of mouse melanoma cell lines by their mortal malignancy using an experimental metastatic model. *Life Sci*. 2002. 70, 791-8.
21. Kawabata. K, Kondo. M, Watanabe. Y, Takakura. Y, Hashida. M. Non-polarized secretion of mouse interferon-β from gene-transferred human intestinal Caco-2 cells. *Pharm Res*. 1997. 14, 483-5.
22. Yin. Y, Takahashi. Y, Ebisuura. N, Nishikawa. M, Takakura. Y. Removal of transgene-expressing cells by a specific immune response induced by sustained transgene expression. *J Gene Med*. 2014. 16, 97-106.
23. Yin. Y, Takahashi. Y, Hamana. A, Nishikawa. M, Takakura. Y. Effects of transgene expression level per cell in mice livers on induction of transgene-specific immune responses after hydrodynamic gene transfer. *Gene Ther*. 2016. 23, 565-71
24. Liu. F, Song. Y, Liu. D. Hydrodynamics-based transfection in animals by systemic administration of plasmid DNA. *Gene Ther*. 1999. 6, 1258-66.
25. Hemmi. H, Takeuchi. O, Kawai. T, Kaisho. T, Sato. S, Sanjo. H, Matsumoto. M, Hoshino. K, Wagner. H, Takeda. K, Akira. S. A Toll-like receptor recognizes bacterial DNA. *Nature*. 2000. 408, 740-5.
26. Ahmad-Nejad. P, Häcker. H, Rutz. M, Bauer. S, Vabulas. R.M, Wagner. H. Bacterial CpG-DNA and lipopolysaccharides activate Toll-like receptors at distinct cellular compartments. *Eur J Immunol*. 2002. 32, 1958-68.
27. Tan. Y, Li. S, Pitt. B.R, Huang. L.The inhibitory role of CpG immunostimulatory motifs in cationic lipid vector-mediated transgene expression *in vivo*. *Hum Gene Ther*. 1999. 10, 2153-61.
28. Kako. K, Nishikawa. M, Yoshida. H, Takakura. Y. Effects of Inflammatory Response on *In Vivo* Transgene Expression by Plasmid DNA in Mice. *J Pharm Sci*. 2008. 97, 3074-83.
29. Jørgensen. J.B, Johansen. A, Hegseth. M.N, Zou. J, Robertsen. B, Collet. B, Secombes. C.J. A recombinant CHSE-214 cell line expressing an Mx1 promoter-reporter system responds to both interferon type I and type II

from salmonids and represents a versatile tool to study the IFN-system in teleost fish. *Fish Shellfish Immunol*. 2007. 23, 1294-303.

30. Schumacher. B, Bernasconi. D, Schultz. U, Staeheli. P. The chicken Mx promoter contains an ISRE motif and confers interferon inducibility to a reporter gene in chick and monkey cells. *Virology* 1994. 203, 144-8.
31. Dempsey. A, Bowie. A.G. Innate immune recognition of DNA: A recent history. *Virology*. 2015. 479-480, 146-52.
32. Mohd. H.K, Groeger. J, Flaxman. A.D, Wiersma. S.T. Global epidemiology of hepatitis C virus infection: new estimates of age-specific antibody to HCV seroprevalence. *Hepatology*. 2013. 57, 1333-42.
33. Chayama. K, Hayes. C.N. Hepatitis C virus: How genetic variability affects pathobiology of disease. *J Gastroenterol Hepatol*. 2011. 26, 83-95.
34. Puig-Basagoiti. F, Forns. X, Furcić. I, Ampurdanés. S, Giménez-Barcons. M, Franco. S, Sánchez-Tapias. J.M, Saiz. J.C. Dynamics of hepatitis C virus NS5A quasispecies during interferon and ribavirin therapy in responder and non-responder patients with genotype 1b chronic hepatitis C. *J Gen Virol*. 2005. 86, 1067-75.
35. Majumdar. A, Kitson. M.T, Roberts. S.K. Systematic review: current concepts and challenges for the direct-acting antiviral era in hepatitis C cirrhosis. *Aliment Pharmacol Ther*. 2016. 43, 1276-92.
36. Wyles. D, Pockros. P, Morelli. G, Younes. Z, Svarovskaia. E, Yang. J.C, Pang. P.S, Zhu. Y, McHutchison. J.G, Flamm. S, Lawitz. E. Ledipasvir-sofosbuvir plus ribavirin for patients with genotype 1 hepatitis C virus previously treated in clinical trials of sofosbuvir regimens. *Hepatology*. 2015. 61, 1793-7.
37. Kohli. A, Kapoor. R, Sims. Z, Nelson. A, Sidharthan. S, Lam. B, Silk. R, Kotb. C, Gross. C, Teferi. G, Sugarman. K, Pang. P.S, Osinusi. A, Polis. M.A, Rustgi. V, Masur. H, Kottilil. S. Ledipasvir and sofosbuvir for hepatitis C genotype 4: a proof-of-concept, single-centre, open-label phase 2a cohort study. *Lancet Infect Dis*. 2015. 15, 1049-54.
38. Lawitz. E, Reau. N, Hinestrosa. F, Rabinovitz. M, Schiff. E, Sheikh. A, Younes. Z, Herring. R. Jr, Reddy. K.R, Tran. T, Bennett. M, Nahass. R, Yang. J.C, Lu. S, Dvory-Sobol. H, Stamm. L.M, Brainard. D.M, McHutchison. J.G, Pearlman. B, Shiffman. M, Hawkins. T, Curry. M, Jacobson. I. Efficacy of Sofosbuvir, Velpatasvir, and GS-9857 in Patients With Genotype 1 Hepatitis C Virus Infection in an Open-Label, Phase 2 Trial. *Gastroenterology*. 2016. 151, 893-901.e1.
39. Kevin. Tin, Eiei. Soe, James. Park. Management of Direct-Acting Antiviral Failures in Chronic Hepatitis C Infection. *Curr Hepatology Rep*. 2016. 15, 296–306.
40. Chayama. K, Hayes. C.N. HCV Drug Resistance Challenges in Japan: The Role of Pre-Existing Variants and Emerging Resistant Strains in Direct Acting Antiviral Therapy. *Viruses*. 2015. 7, 5328-42.
41. Cento. V, Chevaliez. S, Perno. C.F. Resistance to direct-acting antiviral agents: clinical utility and significance. *Curr Opin HIV AIDS*. 2015. 10, 381-9.
42. Pawlotsky. J.M. Hepatitis C Virus Resistance to Direct-Acting Antiviral Drugs in Interferon-Free Regimens. *Gastroenterology*. 2016. 151, 70-86.

43. Itakura. J, Kurosaki. M, Takada. H, Nakakuki. N, Matsuda. S, Gondou. K, Asano. Y, Hattori. N, Itakura. Y, Tamaki. N, Yasui. Y, Suzuki. S, Hosokawa. T, Tsuchiya. K, Nakanishi. H, Takahashi. Y, Maekawa. S, Enomoto. N, Izumi. N. Naturally occurring, resistance-associated hepatitis C virus NS5A variants are linked to interleukin-28B genotype and are sensitive to interferon-based therapy. *Hepatol Res*. 2015. 45, E115-21.
44. Zhang. Y, Cao. Y, Zhang. R, Zhang. X, Lu. H, Wu. C, Huo. N, Xu. X. Pre-Existing HCV Variants Resistant to DAAs and Their Sensitivity to PegIFN/RBV in Chinese HCV Genotype 1b Patients. *PLoS One*. 2016. 11, e0165658.
45. Sadler. A.J, Williams. B.R. Interferon-inducible antiviral effectors. *Nat Rev Immunol*. 2008. 8, 559-68.
46. Qashqari. H, Al-Mars. A, Chaudhary. A, Abuzenadah. A, Damanhouri. G, Alqahtani. M, Mahmoud. M, El Sayed Zaki. M, Fatima. K, Qadri. I. Understanding the molecular mechanism(s) of hepatitis C virus (HCV) induced interferon resistance. *Infect Genet Evol*. 2013. 19, 113-9.
47. Oshiumi. H, Funami. K, Aly. H.H, Matsumoto. M, Seya. T. Multi-step regulation of interferon induction by hepatitis C virus. *Arch Immunol Ther Exp (Warsz)*. 2013. 61, 127-38.
48. Scagnolari. C, Antonelli. G. Antiviral activity of the interferon α family: biological and pharmacological aspects of the treatment of chronic hepatitis C. *Expert Opin Biol Ther*. 2013. 13, 693-711.
49. Tan. H, Derrick. J, Hong. J, Sanda. C, Grosse. W.M, Edenberg. H.J, Taylor. M, Seiwert. S, Blatt. L.M. Global transcriptional profiling demonstrates the combination of type I and type II interferon enhances antiviral and immune responses at clinically relevant doses. *J Interferon Cytokine Res*. 2005. 25, 632-49.
50. Panigrahi. R, Hazari. S, Chandra. S, Chandra. P.K, Datta. S, Kurt. R, Cameron. C.E, Huang. Z, Zhang. H, Garry. R.F, Balart. L.A, Dash. S. Interferon and ribavirin combination treatment synergistically inhibit HCV internal ribosome entry site mediated translation at the level of polyribosome formation. *PLoS One*. 2013. 8, e72791.
51. Chayama. K, Hayes. C.N, Hiraga. N, Abe. H, Tsuge. M, Imamura. M. Animal model for study of human hepatitis viruses. *J Gastroenterol Hepatol*. 2011. 26, 13-8.
52. Takahashi. Y, Ando. M, Nishikawa. M, Hiraga. N, Imamura. M, Chayama. K, Takakura. Y. Long-term elimination of hepatitis C virus from human hepatocyte chimeric mice after interferon-γ gene transfer. *Hum Gene Ther Clin Dev*. 2014. 25, 28-39.
53. Hamana. A, Takahashi. Y, Nishikawa. M, Takakura. Y. Interferon-Inducible Mx Promoter-Driven, Long-Term Transgene Expression System of Interferon-β for Cancer Gene Therapy. *Hum Gene Ther*. 2016. 27, 936-45.
54. Goto. K, Watashi. K, Murata. T, Hishiki. T, Hijikata. M, Shimotohno. K. Evaluation of the anti-hepatitis C virus effects of cyclophilin inhibitors, cyclosporin A, and NIM811. *Biochem Biophys Res Commun*. 2006. 343, 879-84.

55. Uno. S, Nishikawa. M, Mohri. K, Umeki. Y, Matsuzaki. N, Takahashi. Y, Fujita. H, Kadowaki. N, Takakura. Y. Efficient delivery of immunostimulatory DNA to mouse and human immune cells through the construction of polypod-like structured DNA. *Nanomedicine*. 2014. 10, 765-74.
56. Tateno. C, Yoshizane. Y, Saito. N, Kataoka. M, Utoh. R, Yamasaki. C, Tachibana. A, Soeno. Y, Asahina. K, Hino. H, Asahara. T, Yokoi. T, Furukawa. T, Yoshizato. K. Near completely humanized liver in mice shows human-type metabolic responses to drugs. *Am J Pathol*. 2004. 165, 901-12.
57. Kan. H, Imamura. M, Uchida. T, Hiraga. N, Hayes. C.N, Tsuge. M, Abe. H, Aikata. H, Makokha. G.N, Chowdhury. S, Miki. D, Ochi. H, Ishida. Y, Tateno. C, Chayama. K. Protease Inhibitor Resistance Remains Even After Mutant Strains Become Undetectable by Deep Sequencing. *J Infect Dis*. 2016. 214, 1687-94.
58. Yoshimi. S, Ochi. H, Murakami. E, Uchida. T, Kan. H, Akamatsu. S, Hayes. C.N, Abe. H, Miki. D, Hiraga. N, Imamura. M, Aikata. H, Chayama. K. Rapid, Sensitive, and Accurate Evaluation of Drug Resistant Mutant (NS5A-Y93H) Strain Frequency in Genotype 1b HCV by Invader Assay. *PLoS One*. 2015. 10, e0130022.
59. Kimura. T, Imamura. M, Hiraga. N, Hatakeyama. T, Miki. D, Noguchi. C, Mori. N, Tsuge. M, Takahashi. S, Fujimoto. Y, Iwao. E, Ochi. H, Abe. H, Maekawa. T, Arataki. K, Tateno. C, Yoshizato. K, Wakita. T, Okamoto. T, Matsuura. Y, Chayama. K. Establishment of an infectious genotype 1b hepatitis C virus clone in human hepatocyte chimeric mice. *J Gen Virol*. 2008. 89, 2108-13.
60. Hiraga. N, Imamura. M, Tsuge. M, Noguchi. C, Takahashi. S, Iwao. E, Fujimoto. Y, Abe. H, Maekawa. T, Ochi. H, Tateno. C, Yoshizato. K, Sakai. A, Sakai. Y, Honda. M, Kaneko. S, Wakita. T, Chayama. K. Infection of human hepatocyte chimeric mouse with genetically engineered hepatitis C virus and its susceptibility to interferon. *FEBS Lett*. 2007. 581, 1983-7.
61. Hiraga. N, Abe. H, Imamura. M, Tsuge. M, Takahashi. S, Hayes. C.N, Ochi. H, Tateno. C, Yoshizato. K, Nakamura. Y, Kamatani. N, Chayama. K. Impact of viral amino acid substitutions and host interleukin-28b polymorphism on replication and susceptibility to interferon of hepatitis C virus. *Hepatology*. 2011. 54, 764-71.
62. Hiraga. N, Imamura. M, Abe. H, Hayes. C.N, Kono. T, Onishi. M, Tsuge. M, Takahashi. S, Ochi. H, Iwao. E, Kamiya. N, Yamada. I, Tateno. C, Yoshizato. K, Matsui. H, Kanai. A, Inaba. T, Tanaka. S, Chayama. K. Rapid emergence of telaprevir resistant hepatitis C virus strain from wildtype clone *in vivo*. *Hepatology*. 2011. 54, 781-8.
63. Dalgard. O, Mangia. A, Short-term therapy for patients with hepatitis C virus genotype 2 or 3 infection. *Drugs*. 2006. 66, 1807-15.
64. Kohli. A, Shaffer. A, Sherman. A, Kottilil. S. Treatment of hepatitis C: a systematic review. *JAMA*. 2014. 312, 631-40.
65. Nishikawa. M, Nakayama. A, Takahashi. Y, Fukuhara. Y, Takakura. Y. Reactivation of silenced transgene expression in mouse liver by rapid, large-volume injection of isotonic solution. *Hum Gene Ther*. 2008. 19, 1009-20.

66. Lasfar. A, Abushahba. W, Balan. M, Cohen-Solal. K.A. Interferon lambda: a new sword in cancer immunotherapy. *Clin Dev Immunol*. 2011. 2011, 349575.
67. Doyle. S.E, Schreckhise. H, Khuu-Duong. K, Henderson. K, Rosler. R, Storey. H, Yao. L, Liu. H, Barahmand-pour. F, Sivakumar. P, Chan. C, Birks. C, Foster. D, Clegg. C.H, Wietzke-Braun. P, Mihm. S, Klucher. K.M. Interleukin-29 uses a type 1 interferon-like program to promote antiviral responses in human hepatocytes. *Hepatology*. 2006. 44, 896-906.
68. Muir. A.J, Arora. S, Everson. G, Flisiak. R, George. J, Ghalib. R, Gordon. S.C, Gray. T, Greenbloom. S, Hassanein. T, Hillson. J, Horga. M.A, Jacobson. I.M, Jeffers. L, Kowdley. K.V, Lawitz. E, Lueth. S, Rodriguez-Torres. M, Rustgi. V, Shemanski. L, Shiffman. M.L, Srinivasan. S, Vargas. H.E, Vierling. J.M, Xu. D, Lopez-Talavera. J.C, Zeuzem. S.; EMERGE study group. A randomized phase 2b study of peginterferon lambda-1a for the treatment of chronic HCV infection. *J Hepatol*. 2014. 61, 1238-46.
69. Stromnes. I. M, Goverman. J. M. Active induction of experimental allergic encephalomyelitis. *Nat Protoc*. 2006. 1, 1810-9.
70. Koritschoner. R.S, Schweinburg. F. Induktion von Paralyse und Ruckenmarksentzundung durch Immunisierung von Kaninchen mit menschlichem Ruckenmarksgewebe. *Z. Immunitatsf. Exp. Ther*. 1925. 42, 217–83.
71. Yong. V. W, Zabad. R. K, Agrawal. S, Goncalves. D. A, Metz. L. M. Elevation of matrix metalloproteinases (MMPs) in multiple sclerosis and impact of immunomodulators. *J Neurol Sci*. 2007. 259, 79-84.
72. Arima. Y, Kamimura. D, Sabharwal. L, Yamada. M, Bando. H, Ogura. H, Atsumi. T, Murakami. M. Regulation of immune cell infiltration into the CNS by regional neural inputs explained by the gate theory. *Mediators Inflamm*. 2013. 2013, 898165.
73. Merrill. J. E, Kono. D. H, Clayton. J, Ando. D. G, Hinton. D. R, Hofman. F. M. Inflammatory leukocytes and cytokines in the peptide-induced disease of experimental allergic encephalomyelitis in SJL and B10.PL mice. *Proc Natl Acad Sci U S A*. 1992. 89, 574-8.
74. Sriramoju. B, Kanwar. R. K, Kanwar. J. R. Neurobehavioral burden of multiple sclerosis with nanotheranostics. *Neuropsychiatr Dis Treat*. 2015. 11, 2675-89.
75. Lutterotti. A, Berger. T. Advanced in multiple sclerosis therapy: New oral disease-modifying agents. *CML Mult Scler*. 2010. 2, 1-10.
76. Harkins. R. N, Szymanski. P, Petry. H, Brooks. A, Qian. H. S, Schaefer. C, Kretschmer. P. J, Orme. A, Wang. P, Rubanyi. G. M, Hermiston. T. W. Regulated expression of the interferon-β gene in mice. *Gene Ther*. 2008. 15, 1-11.
77. Triantaphyllopoulos. K, Croxford. J, Baker. D, Chernajovsky. Y. Cloning and expression of murine IFN β and a TNF antagonist for gene therapy of experimental allergic encephalomyelitis. *Gene Ther*. 1998. 5, 253-63.

78. Moreno. B, Fernandez-Diez. B, Di. P. A, Villoslada. P. Preclinical studies of methylthioadenosine for the treatment of multiple sclerosis. *Mult Scler*. 2010. 16, 1102-8.
79. Kobayashi. N, Nishikawa. M, Takakura. Y. The hydrodynamics-based procedure for controlling the pharmacokinetics of gene medicines at whole body, organ and cellular levels. *Adv Drug Deliv Rev*. 2005. 57, 713-31.
80. Boivin. N, Baillargeon. J, Doss. P. M, Roy. A. P, Rangachari. M. Interferon-β suppresses murine Th1 cell function in the absence of antigen-presenting cells. *PLoS One*. 2015. 10, e0124802.
81. Axtell. R. C, de Jong. B. A, Boniface. K, van der Voort. L. F, Bhat. R, De Sarno. P, Naves. R, Han. M, Zhong. F, Castellanos. J. G, Mair. R, Christakos. A, Kolkowitz. I, Katz. L, Killestein. J, Polman. C. H, de Waal Malefyt. R, Steinman. L, Raman. C. T helper type 1 and 17 cells determine efficacy of interferon-β in multiple sclerosis and experimental encephalomyelitis. *Nat Med*. 2010. 16, 406-12.
82. Kalinke. U, Prinz. M. Endogenous, or therapeutically induced, type I interferon responses differentially modulate Th1/Th17-mediated autoimmunity in the CNS. *Immunol Cell Biol*. 2012. 90, 505-9.
83. Pan. W, Banks. W. A, Kennedy. M. K, Gutierrez. E. G, Kastin. A. J. Differential permeability of the BBB in acute EAE: enhanced transport of TNT-alpha. *Am J Physiol*. 1996. 271, E636-42.
84. Martino. G, Poliani. P. L, Furlan. R, Marconi. P, Glorioso. J. C, Adorini. L, Comi. G. Cytokine therapy in immune-mediated demyelinating diseases of the central nervous system: a novel gene therapy approach. *J Neuroimmunol*. 2000. 107, 184-90.
85. Qin. L, Ding. Y, Pahud. D. R, Chang. E, Imperiale. M. J, Bromberg, J. S. Promoter attenuation in gene therapy: interferon-gamma and tumor necrosis factor-alpha inhibit transgene expression. *Hum Gene Ther*. 1997. 8, 2019-29.
86. Correale. J, Gaitán. M.I. Multiple sclerosis and environmental factors: the role of vitamin D, parasites, and Epstein-Barr virus infection. *Acta Neurol Scand*. 2015. 132, 46-55.
87. Patejdl. R, Zettl. U.K. Spasticity in multiple sclerosis: Contribution of inflammation, autoimmune mediated neuronal damage and therapeutic interventions. *Autoimmun Rev*. 2017. 16, 925-36.
88. Rangachari. M, Kuchroo. V.K. Using EAE to better understand principles of immune function and autoimmune pathology. *J Autoimmun*. 2013. 45, 31-9.
89. Monney. L, Sabatos. C.A, Gaglia. J.L, Ryu. A, Waldner. H, Chernova. T, Manning. S, Greenfield. E.A, Coyle. A.J, Sobel. R.A, Freeman. G.J, Kuchroo. V.K. Th1-specific cell surface protein Tim-3 regulates macrophage activation and severity of an autoimmune disease. *Nature*. 2002. 415, 536-41.
90. Zhu. C, Anderson. A.C, Schubart. A, Xiong. H, Imitola. J, Khoury S.J, Zheng. X.X, Strom. T.B, Kuchroo. V.K. The Tim-3 ligand galectin-9 negatively regulates T helper type 1 immunity. *Nat Immunol*. 2005. 6, 1245-52.
91. Meyers. J.H, Sabatos. C.A, Chakravarti. S, Kuchroo. V.K. The TIM gene family regulates autoimmune and allergic diseases. *Trends Mol Med*. 2005. 11, 362-9.

92. Anderson. A.C, Anderson. D.E. TIM-3 in autoimmunity. *Curr Opin Immunol*. 2006. 18, 665-9.
93. Burman. J, Svenningsson. A. Cerebrospinal fluid concentration of Galectin-9 is increased in secondary progressive multiple sclerosis. *J Neuroimmunol*. 2016. 292, 40-4.
94. Hamana. A, Takahashi. Y, Tanioka. A, Nishikawa. M, Takakura. Y. Amelioration of Experimental Autoimmune Encephalomyelitis in Mice by Interferon-β Gene Therapy, Using a Long-Term Expression Plasmid Vector. *Mol Pharm*. 2017. 14, 1212-7.
95. Zhao. H.L, Xue. C, Wang. Y, Li. X.Y, Xiong. X.H, Yao. X.Q, Liu. Z.M. Circumventing the heterogeneity and instability of human serum albumin-interferon-α2b fusion protein by altering its orientation. *J Biotechnol*. 2007. 131, 245-52.
96. Lee. S.Y, Goverman. J.M. The influence of T cell Ig mucin-3 signaling on central nervous system autoimmune disease is determined by the effector function of the pathogenic T cells. *J Immunol*. 2013. 190, 4991-9.
97. Haining. W.N. Thinking inside the box: how T cell inhibitory receptors signal. *Nat Med*. 2012. 18, 1338-9.
98. Neilley. L.K, Goodin. D.S, Goodkin. D.E, Hauser. S.L. Side effect profile of interferon β-1b in MS: results of an open label trial. *Neurology*. 1996. 46, 552-4.